TAMPEREEN TEKNILLINEN YLIOPISTO
TAMPERE UNIVERSITY OF TECHNOLOGY

JON ANDER BEITIA

URBAN, SUBURBAN AND RURAL CHANNEL MODELS BASED ON CELLULAR AND WIRELESS AREA NETWORK SIGNALS FOR POSITIONING PURPOSES

Master of Science Thesis

Examiners:

Associate Professor Elena-Simona Lohan
Jukka Talvitie

Examiners and topic approved
by the Council of the Faculty of
Computing and Electrical Engineering on
5th of March 2014

ABSTRACT

TAMPERE UNIVERSITY OF TECHNOLOGY
BEITIA MENDAZA, JON ANDER: Urban, suburban and rural channel models based on cellular and wireless area network signals for positioning purposes.
Master of Science Thesis, 98 pages, 7 Appendix pages
July 2014
Major: Communication Engineering
Examiner: Associate Professor Elena-Simona Lohan and Jukka Talvitie

Keywords: Received signal strength (RSS), cellular networks, wireless local area networks (WLANs), Path-loss models, Positioning

Location information is becoming more and more useful in everyday life. The cellular-based and wireless area network based positioning are being used to predict the location of users in environments such as indoors and densely urban, where the Global Navigation Satellite Systems often fail. The Received Signal Strength (RSS) is used more and more due to its wide availability on any mobile device and based on various signals. However, studies about the availability of signal measurements in various urban and sub-urban scenarios and about the RSS fluctuations in various terrain types are still lacking in the current literature. The main objective of this thesis is to analyze method wide range of measurement-based RSS in urban, suburban and rural environments.

The thesis is divided in two parts. In the literature study part, issues related to cellular and wireless local area networks (WLANs) such as frequency bands, system architectures, radio interfaces and RSS measurements are described. Also the propagation channel characteristics and the different path-loss models existing in the literature are exposed. The information explained in this part was useful in order to be able to process the available data measurements. In the measurements and analysis part, the collected results were evaluated. The different parameters of cellular and WLAN signals were studied and compared. Availability of signals in various scenarios, density of the transmitters and path loss coefficients were deeply analyzed, by dividing the measured scenarios into seven distinct environments: airport areas, Seaside or beach areas, Mountain or forest areas, suburban areas, densely urban areas, lake areas, and other urban areas.

The obtained results provide more insight into the availability of RSS signal measurements on mobile devices nowadays and into the possibility of creating generic and unified RSS-based positioning algorithms (based on the similarities between different types of signals and different types of environments).

PREFACE

This Master of Science Thesis has been carried out in the Department of Electronics and Communication Engineering at Tampere University of Technology (TUT), Tampere, Finland between Fall 2013 and Summer 2014.

I am pleased to express my gratitude to my thesis supervisor Associate Professor Dr. Elena-Simona Lohan for her guidance and advise during the realization of this thesis. I would like also to thank Jukka Talvitie for sharing the Matlab code when I got stack in the extraction of data.

Finally, I would like to thank my family and friends for their continued support throughout my life.

Tampere, 21st of July 2014.
Jon Ander Beitia Mendaza

TABLE OF CONTENTS

LIST OF ABBREVIATIONS

2G	Second Generation
3G	Third Generation
4G	Fourth Generation
AGCH	Access Grant Channel
AOA	Angle of Arrival
AP	Access Points
ARFCN	Absolute Radio Frequency Channel Number
AuC	Authentication Centre
AWGN	Additive White Gaussian Noise
BCCH	Broadcast Control Channel
BMPL	Basic Median Path Loss
BSC	Base Station Controller
BSS	Basic Service Set
BTS	Base Transceiver Station
CCA	Clear Channel Assessment
CCCH	Common Control Channel
CCH	Control Channels
CDMA	Code Division Multiple Access
CN	Core Network
CPICH RSCP	Common Pilot Channel Received Signal Code Power

CRC	Redundancy Check
CS	Circuit Switched
dB	Decibel
dBm	Decibel Milliwatt
dBw	Decibel Watt
DCCH	Dedicated Control Channel
DPCCH	Dedicated Physical Control Channel
DPCH	Dedicated Physical Channel
DPCH RSCP	Dedicated Physical Channel Received Signal Code Power
DPDCH	Dedicated Physical Data Channel
DSSS	Direct Sequence Spread Spectrum
E-GSM	Extender GSM
EIR	Equipment Identity
EN	External Networks
ESS	Extended Service Set
ESSID	Extended Service Set Identifier
ETSI	European Telecommunications standard Institute
EU	European Union
FACCH	Fast Associated Dedicated Control Channel
FBI	Feedback Information Field
FCCH	Frequency Correction Channel

FDD	Frequency Division Duplex
FDMA	Frequency Division Multiple Access
FHSS	Frequency Hopping Spread Spectrum
FSPL	Free Space Path Loss
GGSN	Gateway GPRS Support Node
GMSC	Gateway MSC
GNSS	Global Navigation Satellite System
GPRS	General Packet Radio Service
GPS	Global Positioning System
GSM	Global System for Mobile Communication
HEC	Header Error Check
HLR	Home Location Registers
IBSS	Independent BSSs
ID	Identifier
IEEE	Institute of Electrical and Electronics Engineers
IMT	International Mobile Telecommunications
ISCP	Interference Signal Code Power
ISDN	Integrated Services Digital Network
LAN	Local Area Network
LOS	Line-of-Sight
LS	Least Square

LTE	Long-term Evolution
LTP	Local Tangent Plane
ME	Mobile Equipment
MIMO	Multiple-Input Multiple-Output
MIMO-OFDM	Multiple-Input Multiple-Output OFDM
MMS	Multimedia Message Service
MS	Mobile Stations
MSC	Mobile Services Switching Centre
MSC	Mobile Switching Centre
MU-MIMO	Multi User Multiple-Input Multiple-Output
MWF	Multi Floor and Wall
N/A	Not Available
NLOS	Non Line-of-Sight
NSS	Network and Switching Subsystem
OFDM	Orthogonal Frequency Division Multiplexing
OSS	Operation Subsystem
OTDOA-IPDL	Observed Time Difference of Arrival – Idle Period Downlink
OVSF	Orthogonal Variable Spreading Factor
P-GSM	Primary GSM
PCCPCH RSCP	Primary Physical Common control channel Received Signal Code Power
PCH	Paging Channel

PDSCH RSCP	Physical Downlink Shared Channel Received Signal Code Power
PHY	Physical
PL	Path loss
PLCP	Physical Layer Convergence Procedure
PLW	PLCP PDU Length Word
PRACH	Physical Random Access Channel
PSF	PLCP Signaling Field
PSTN	Public Switched Telephone Network
R-GSM	Railways GSM
RACH	Random Access Channel
RF	Radio Frequency
RMS	Root Mean Square
RNC	Radio Network Controller
RNS	Radio Network Subsystems
RSCP	Received Signal Code Power
RSS	Radio Subsystem
RSS	Received Signal Strength
RSSI	Received Signal Strength Indicator
RTT	Round Trip Time
RXLEV	Received Level
SACCH	Slow Associated Dedicated Control Channel

SAP	Service Access Point
SCH	Synchronization Channels
SD	Secure Digital
SDCCH	Stand-alone Dedicated Control Channel
SDMA	Space Division Multiple Access
SFD	Start Frame Delimiter
SGSN	GPRS Support Node
SIM	Subscriber Identity Module
SMS	Short Message Service
STA	Station
SUI	Stanford University Interim
STD	Standard Deviation
TA	Timing Advance
TCH	Traffic Channels
TDD	Time Division Duplex
TDMA	Time Division Multiple Access
TDOA	Time Difference of Arrival
TFCI	Transport Format Combination Identifier
TOA	Time of Arrival
TPC	Transmit Power Control
TRAU	Transcoder and Rate Adaption Unit

TUT	Tampere University if Technology
TV	Television
UAB	Universitat Autònoma de Barcelona
UE	User Equipment
UMTS	Universal Mobile Telecommunications System
USIM	UMTS Subscriber Identity Module
UTRA	Universal Terrestrial Radio Access
UTRAN	UTRA network
VLR	Visitor Location Register
WCDMA	Wideband Direct-Sequence Code Division Multiple Access DS-CDMA
WLAN	Wireless Local Area Network
XML	Extensive Markup Language

LIST OF SYMBOLS

T	Temperature
B	Bandwidth
F	Noise Factor
ϕ	Road orientation with respect to the direct radio path
w	Street width
λ	Wavelength
γ	Path loss exponent
d	Distance
f	Frequency
L_0	Path loss in a distance of one meter
n	Slope factor
h_b	Transmission antenna height
h_r	Receiver antenna height
G_r	Receiver antenna gain factor
h_{roof}	Height of buildings
B	Building to building distance
G_m	Gain of the receiver antenna relative to half-wave dipole
s	Correction for shadowing
π	Pi
K	Clutter Factor

TABLE OF TABLES

TABLE OF FIGURES

1. INTRODUCTION

1.1 Problem formulation and state of art

In the last decades, the location information has been becoming very useful and important for life. At the beginnings of location technologies, the location of a mobile device was predicted using satellites. With the expansion of the wireless networks, now, at least in theory, we can use any of the available wireless signals at a receiver for positioning purposes. The satellite signals may be not available many times, for example when there is no Line Of Sight (LOS) path between the transmitter and the receiver, such as in indoor conditions [1]. In such cases, we can use the signals provided by the cellular systems and other wireless networks to locate the device. The location information is nowadays always employed in wireless communications for mobility and radio resource management functions [2]. The location information was first used in safety and emergency applications, such as calling to the nearest public safety answering point. In the last years, many other applications appeared, such as pet and fleet tracking, location-based advertising, location-based billing and tolling, and so on [2]. Some of these new applications belong to the category of the information services and tracking. Examples are: finding a museum in a city map or the current location of a bus. Mobile phone manufacturers and software companies have realized about the value of this location information and they use it to improve their services or to customize the shared data. Important companies, such as Google or Facebook, use location information to provide information around your current position and to add the place of an uploaded picture. Positioning information is very helpful and gives many advantages that make our life easier and more confortable so the companies and services that use it are increasing. There is also significant effort in research and industrial world to develop new location techniques in order to get more accurate information.

The acquisition of the location of a mobile unit is divided in two parts: the data collection and the data processing [2].

Nowadays there are many wireless communication systems with different characteristics. The most developed non-GNSS systems used for location services are GSM, 3G and WLAN standards. Most of the data used in positioning are related to time and receiver power levels, but there are also other indicators that can be used for this purpose. Some of the used parameters are cell ID, received signal strength (RSS), time of arrival (TOA), time difference of arrival (TDOA), angle of arrival (AOA), observed

time difference of arrival – idle period downlink (OTDOA-IPDL), timing advance (TA) in GSM system and round trip time (RTT) in 3G standard [2; 3; 4].

The location is obtained using one or several of the previous indicators and a positioning algorithm. The accuracy of the location will depend on the type and number of indicators used in the algorithm and how it processes the different data. The positioning algorithm should be adjustable and it should choose the criterion that suits better to the communication channel´s characteristics where we are estimating the location. The algorithm´s quality and versatility will be critical for the truthfulness of the results [2; 5; 6].

This location acquisition process is shown in a simplified manner in Figure 1.1.

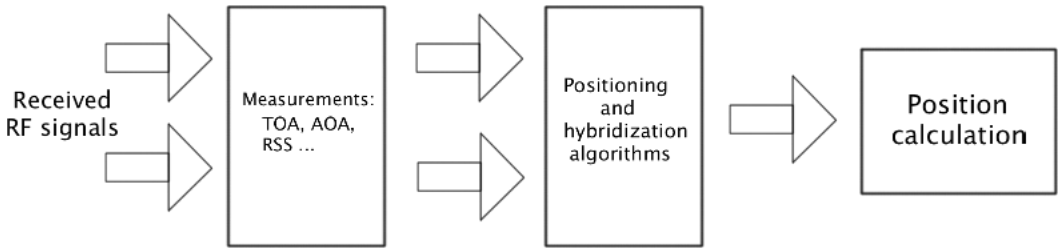

Figure 1.1 Location acquisition process

The received signals used for localization of the mobile unit are affected and disturbed by the environment, due to different objects or obstacles in the path of the communication [7]. In any wireless communication, there will be reflections, diffractions and shadowing situations that will produce multipath propagation. More about the channel impairments will be discussed in Chapter 3 of this thesis.

There are three types of environments to characterize wireless communications known as urban, suburban and rural. A terrain is classified taking into account the density, dimension and average height of buildings or the area coverage by vegetation [8; 9].

In an **urban environment,** the height and the density of buildings will be high.

In **rural areas,** the dimensions of the constructions will be smaller and most of the terrain will be covered by vegetation [8].

Suburban areas are in between the two cases above.

Depending on the environment the propagation of signal will be different and we will need to use the correct equations and approaches to get an accurate location of the user

[10]. This thesis however focuses on the initial stage in any RSS-based positioning estimation, that is on the training phase, where the available signals are analyzed and compared and path-loss models parameters are derived. The scope of the thesis has been two-folds: first to implement a Matlab-based software to process the available measurement data and secondly, to analyze the following characteristics based on the measurement data:

- The availability of various signals (GPS, 2G, 3G and WLAN) in various environments
- The statistical characterization of the RSS coming from various signals and in various scenarios
- The path-loss parameters, such as path-loss slope and shadowing variance for cellular and WLAN signals in various environments
- The estimated transmitter location and network density based on the RSS measurements
- A comparative analysis between cellular 2G, cellular 3G and WLAN RSS values.

1.2 Author contribution

The main objective of this thesis has been to create a Matlab program to analyze xml measurements of 2G, 3G and WLAN networks. This analysis included the estimation of the emitter location of 2G, 3G and WLAN networks from the available RSS measurements, the estimation of the path loss parameters and the shadowing statistics and the comparison between different terrain types in terms of signal propagation. The author has contributed to the followings:

- Literature review of 2G, 3G and WLAN systems
- Description of urban and rural channel characteristics
- Definition of different path-loss models
- Implementation of a Matlab simulator to analyze the measurement data available in xml format
- Implementation of a Matlab program for localization of emitters using one-slope path-loss model in different terrains
- Analysis of real-field measurements of 2G, 3G and WLAN signal parameters in the different environments
- Analyzing the shadowing statistics of the cellular and WLAN signals in various terrain types
- Comparative analysis of the results obtained in the different terrains

2. PRINCIPLES OF WIRELESS POSITIONING VIA RECEIVED SIGNAL STRENGTH

The Received Signal Strength (RSS) based location methods use the received power value of the transmitted signal in order to predict the position of a mobile device [3; 4]. These power values can be taken from several cellular and wireless networks that have different indicators. For GSM systems, the received power is given by the reception level (RXLEV) [11], in 3G or UMTS networks, the signal strength is measured using the Common Pilot Channel Received Signal Code Power (CPICH RSCP) value [12] and for WLAN standard the received power is given by the Received Signal Strength Indicator (RSSI) value [13].

There are different methods to obtain the RSS values at the mobile device and to use them in localization. The three most important methods can be classified as:

1. fingerprinting [14],
2. path loss model [2] and
3. methods based on probabilistic approaches [14].

In the fingerprinting methods, a device stores the RSS values and possibly other receiver parameters, measured for example by sensors, such as gyroscopes, accelerometers, barometers, etc. With the saved data, we can know the received signal strength values or the ‘fingerprints’ of each potential mobile location and we can see how the values vary when the receiver is moving along the area and during different time instants [14; 15]. The positioning is based on comparing the new receiver measurements with the measurements or fingerprints stored in a database [16]. This method is very reliable because it uses real samples. It also requires large storage spaces and high data transfers between the mobile and the network.

Another method is to use the path loss models. If we know the operating frequency of the system, the distance between the transmitter and the receiver, the transmitted power by the base station or the terrain type, we can use several equations (or path-loss models) to calculate the propagation losses and to get the RSS value received in the mobile unit. The correctness of the location depends on how the selected path loss model matches to the terrain type [2; 17; 18].

The third method works using probabilistic approaches. This method is based on how the RSS values are distributed on a sample of different RSS measurements collected at several known locations [14; 19]. These data can be extrapolated to estimate the RSS values and their distribution for a new location using probability [20]. This method is very common in indoor positioning using WLAN networks.

Once we have collected all the RSS data, we may use trilateration to predict the location of the receiver. Trilateration is the process of determining the location of a mobile station by measurement of distances, using the geometry of circles or triangles for 2D and spheres for 3D spaces [2; 21]. In cellular and wireless based positioning, the geometry of circles is used most times. The centres of the circles are the location of the transmitters and the radius of the circles are the distances obtained with the path loss model [22]. Depending on the distances between the transmitters and the receiver we will have bigger or smaller radius and circles of different sizes. The intersection of the circles will define the location of the mobile unit [23; 24].

Figure 2.1 shows the trilateration method.

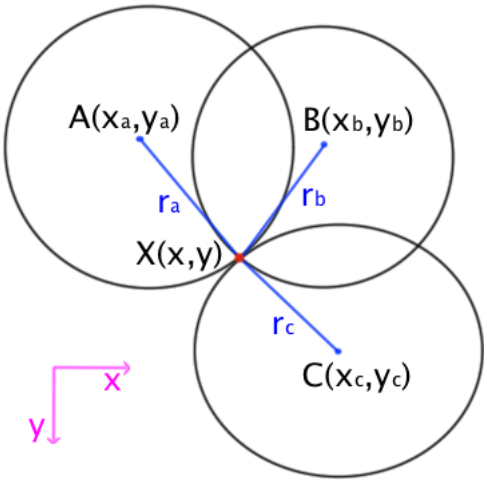

Figure 2.1 Trilateration

If we use the Cartesian coordinates system to specify the locations of the transmitters and a 2D model, the location of the receiver can be calculated using the following expressions:

$$\begin{aligned} x^2 + y^2 &= r_a^2 \\ (x - x_b)^2 + y^2 &= r_b^2 \\ (x - x_c)^2 + (y - y_c)^2 &= r_c^2 \end{aligned} \tag{2.1}$$

where r_a, r_b and r_c are the radius of the circles, x_b, x_c and y_c are the location of the transmitters and x and y are the coordinates of the receiver.

And the receiver position is given by.

$$x = \frac{x_b^2 + r_a^2 - r_b^2}{2x_b}$$
$$y = \frac{x_c^2 + y_c^2 + r_a^2 - r_c^2 - 2xx_c}{2y_c} \quad (2.2)$$

In fact, in the presence of noises the trilateration methods do not work very well and that is why probabilistic approaches may be preferred.

Nowadays there are many cellular and wireless area network systems coexisting together, such as GSM, 3G, WLAN and the newest 4G or LTE. All of these systems have different network architecture, frequency bands and a different way to transmit the data but all of them can be used to get the location of a user with RSS-based method [25]. In what follows we give a brief overview of these systems, because this thesis is based on processing RSS measurements coming from cellular and WLAN systems.

2.1 GSM-based RSS

The Global System for Mobile Communication or GSM was developed by the European Telecommunications standard Institute (ETSI) in 1982. It is the global standard for mobile communications and it is the most extended system with 70% market share in 2012 and it is available in more than 200 countries and territories in the world [26; 27]. GSM offers many different services such as the emergency number, short message service (SMS), multimedia message service (MMS), user identification, call redirection and call forwarding [27].

2.1.1 GSM frequency bands

The GSM systems have different frequency bands. GSM frequencies vary depending on the countries [28]. The most common frequency bands of the GSM system are shown in the Table 2.1.

Table 2.1 GSM frequency bands**.**

System	Number of channels	Uplink frequency band (MHz)	Downlink frequency band (MHz)
GSM-850	128-251	824.2-849.2	869.2-894.2
P-GSM-900	1-124	890.0-915.0	935.0-960.0
E-GSM-900	0-124, 975-1023	880.0-915.0	925.0-960.0
R-GSM-900	0-124, 955-1023	876.0-915.0	921.0-960.0

DCS-1800	512-885	1710.2-1784.8	1805.2-1879.8
PCS-1900	512-810	1850.2-1909.8	1930.2-1989.8

The P-GSM system is the standard or primary GSM-900 band. The E-GSM system is known as extended GSM 900 band because it includes the P-GSM band and the Railways GSM 900 band or R-GSM 900 band comprises both P-GSM and E-GSM bands. [28]

GSM-900 and DCS-1800 are used in most parts of the world such as Europe, Middle East, Africa, Australia, Oceania and many countries of Asia while GSM-850 and PCS-1900 are used in the United States and many other countries of the Americas [28].

Due to technical reasons the lower and upper channels of a frequency band are not used.

2.1.2 GSM system architecture

In all GSM networks, we can find the system architecture simplified in Figure 2.2. The system architecture is divided in three subsystems, the radio subsystem (RSS), the network and switching subsystem (NSS) and the operation subsystem (OSS)[27].

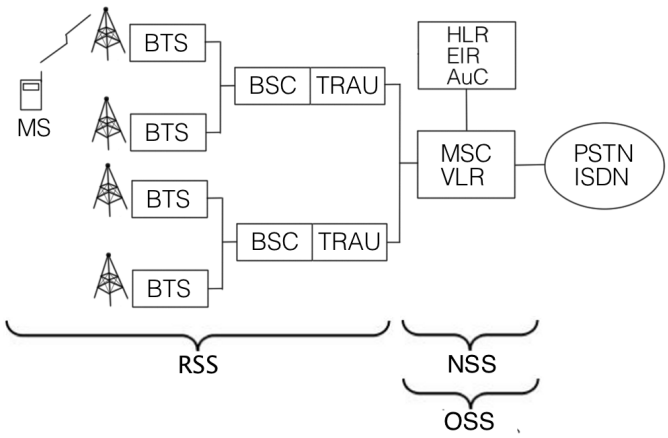

Figure 2.2 GSM system architecture.

Radio subsystem

The RSS is the radio infrastructure needed to connect the mobile stations (MS) to the base station subsystem. The mobile station is a wireless device, such a telephone that includes radio transceiver, digital processors and a subscriber identity module (SIM) card that is used to authenticate the user in the network. [27]

The base transceiver station (BTS) contains all the equipment needed for transmitting and receiving the wireless signals such as signal processing, amplification and

encrypting or decrypting devices. A BTS can divide the coverage area in smaller cells using sectorized antennas [27].

The base station controller (BSC) is the part of the RSS network that controls several BTSs at the same time and manages the radio channels, the authentication of the MSs, location registries and the handovers [27].

The transcoder and rate adaption unit (TRAU) is the responsible for transcoding function for speech channels and rate adaptation for data channels that is required between the BSC and the mobile services switching centre (MSC) [27].

Network and switching subsystem

The MSC performs the changing of BSC and the communication´s data when the MS moves from the current BTS to another BTS of a neighbor BSC [27].

The home location register (HLR) is a database used to store the information about each subscriber that belongs to it. The HLR saves the subscribed services such as call forwarding or roaming restrictions [27].

The visitor location register (VLR) contains information about subscribers that are currently in the region covered by the MSC [27].

Operation subsystem

The equipment identity (EIR) register is a database where MSs information and user rights are stored. It also gives the chance to lock the stolen MSs and sometimes the stolen MSs can be even localized [27].

The authentication centre (AuC) is used to generate user specific authentication parameters on request of a VLR for authentication of MSs and encryption of user data [27].

With all the elements explained above the GSM system is connected to the Public switched telephone network (PSTN) and to the integrated services digital network (ISDN).

2.1.3 GSM radio interface

GSM uses three different types of multiplexing and media access techniques: Space Division Multiple Access (SDMA), Frequency Division Multiple Access (FDMA) and Time Division Multiple Access (TDMA) [27].

The SDMA is implemented using cells and assigning a BTS to a MS inside the BTS´s covered area. These cells will have different sizes depending on the maximum output power emitted by the BTS and they do not have a specific shape but they are typically modeled via hexagonal shapes, as shown in Figure 2.3. [27]

Figure 2.3 Hexagonal cell.

The GSM system also uses a combination of FDMA and TDMA techniques. FDMA works dividing the frequency band in different channels of 200 KHz in order to separate uplink and downlink transmissions. The number of channels will change if we are using one GSM band or another. For the case of GSM-900 band, 32 channels of the 124 are reserved for organizational data and the remaining 90 are used for customers. [27]

Each of the frequency channels are subdivided in frames known as GSM TDMA frames that are repeated continuously and each of these frame of 4.615 ms is again subdivided into 8 GSM time slots [27].

Figure 2.4 shows the allocation of one TDMA frame.

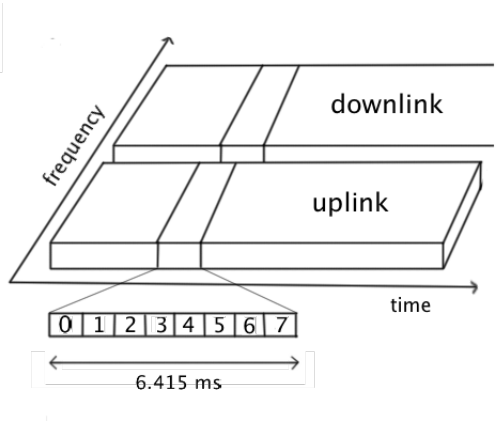

Figure 2.4 TDMA frame.

Each time slot of the TDMA frame is transmitted in 125.25 bits within 577 μs [29]. The information within the time slot is illustrated in Figure 2.5.

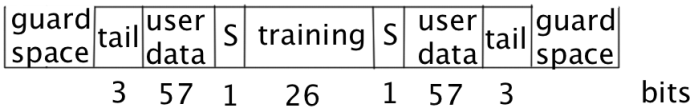

Figure 2.5 GSM time slot.

The guard space is to avoid the overlapping with the other bursts. Each guard space has duration of 30.5 μs. The first and last 3 bits, known as tail, are used to improve the receiver performance. The flags (S) are two bits that alert if the GSM time slot contents user data or network control data. The 26 bits of training are used to adapt the receiver´s parameters to the current radio propagation characteristics [27].

There are four more burst types for data transmission: the frequency correction burst, the synchronization burst, the access burst and the dummy burst. The frequency correction burst is used to correct the local oscillator of the MS to avoid interferences with adjacent channels. The synchronization burst synchronizes the MS and BTS in time. The access burst is used for the setup in the initial connection between the MS and BTS and finally the dummy burst is used when there are no available data for a slot [27].

Physical and logical channels

A physical channel is a slot that is repeated every TDMA frame or 4.615 ms. The physical channel can be divided in two logical channels, one is obtained reading every fourth slot and another logical channel that reads the rest of slots. The use of the time slots is regulated by a frame hierarchy and channels can not take a time slot arbitrarily [27].

There are two main groups of logical channels: traffic channels (TCH) and control channels (CCH), each group of channel is divided again in subchannels [27].

GSM uses a TCH to transmit data as user voice. There are two basic options for this TCH: full-rate TCH (TCH/F) and half-rate TCH (TCH/H). The transmission data rate for TCH/F is 22.8 kbit/s whereas for TCH/H is 11.4 kbit/s [27].

In GSM system there are many CCH channels used to control medium access, allocation of traffic and mobility management. A BTS use the broadcast control channel (BCCH) to transmit information about cell identifier, available frequencies and options within the cell. The frequency corrections are sent using frequency correction subchannel (FCCH) and the time synchronizations are done using synchronization subchannels (SCH) [27].

Another CCH type is the common control channel (CCCH) that is used to transmit all the information required for connection setup. There are three subchannels used for connection setup. If a BTS needs to transmit a call toward a MS the BTS will send a paging channel (PCH) to paging the correct MS. If a MS wants to set up a call it will send data using the random access channel (RACH) and the BTS will respond via the access grant channel (AGCH) [27].

The last group of the control channel is the dedicated control channel (DCCH). The stand-alone dedicated control channel (SDCCH) has low data rate and it is used for signaling and to send authentication, registration and other data needed for setting up a TCH. Each of the SDCCH channel has a slow associated dedicated control channel (SACCH) to exchange information such as the channel quality and the signal power level. The fast associated dedicated control channel (FACCH) is used to transmit large amount of data in handovers [27].

2.1.4 RSS measurements in GSM systems

In GSM system, the RSS is obtained from the received signal level. The received signal level is measured on the CCH channels of the TDMA frame. In order to get the received signal levels, the values of two parameters have to be considered: the physical parameter and the statistical parameter [11, 30].

Physical parameter

The received signal level in GSM system, measured on CCH channels, will vary from -110 dBm to -48 dBm and it is measured at the receiver input. The absolute accuracy of the measured Root Mean Square (RMS) of the received signal level shall be of the order of ± 4 dB from -110 dBm to -70 dBm under normal conditions and ± 6 dB under both normal and extreme conditions over the full range [11].

It may occur that the MS could not measure the signal levels below the reference sensitivity level. In case the received signal level falls below the MS´s reference sensitivity level, the MS will report a level within a range allowing for the accuracy described above. If the upper limit of the received signal level range is lower than the reference sensitivity of the MS, the upper limit will be considered as equal to the reference sensitivity level [11].

The relative accuracy is measured as follows:

If the receiver hears two signal levels with x_1 and x_2 dBm (where $x_1 \leq x_2$) and levels y_1 and y_2 dBm respectively are measured, if $x_2 - x_1 < 20$ dB and x_1 is not below the

reference sensitivity level, the measured levels y_1 and y_2 will be as given in the equations 2.3 and 2.4 [11].

If the measurements are on the same or on different RF channel within the same GSM band

$$(x_2 - x_1) - a \leq y_2 - y_1 \leq (x_2 - x_1 + b) \tag{2.3}$$

and if the measurement are on different GSM bands.

$$(x_2 - x_1) - c \leq y_2 - y_1 \leq (x_2 - x_1 + d) \tag{2.4}$$

where a, b, c and d are in dB units and depend on the value of x_1 as shown in Table 2.2 [11].

Table 2.2 a, b, c and d parameters values.

	a	**b**	**c**	**d**
$x_1 \geq s+14$	2	2	4	4
$s+14 > x_1 \geq s+1$	3	2	5	4
$s+1 > x_1$	4	2	6	4

At extreme temperature conditions, 2 dB have to be added to c and d values.

For single-band MS, meaning that the measurements between absolute radio frequency channel number (ARFCN) in the same GSM band, the reference sensitivity level is [11]:

s = reference sensitivity level of the used GSM system, MS and BTS.

For measurements between ARFCN in different bands, the reference sensitivity level is:

s = reference sensitivity level of the used GSM system, MS and BTS including x_1 signal level.

where the value of s for GSM-900 MS and normal BTS is -104 dBm.

Statistical parameters

The reported received level values are the average of the received signal level measurement samples in dBm that are taken within the reporting period of length one SACCH multiframe. By this averaging, the measurements done during the previous reporting periods will be discarded [11].

The MS will start measuring the received level when it has an assigned TCH or SDCCH. The measurement can be done in every TDMA frame on at least one of the BCCH channels or on all bursts of the associated physical channel such as SACCH channels [11].

The RSS values are stored in the MS using 6 bits so there will be 64 different values of received levels from 0 to 63 [11].

The mapping between the measured signal level and the received level value is shown in the next table.

Table 2.3 Mapping of received signal level.

Received level value	Received power	Description
00	RXLEV< -110 dBm	Minimum reception
01	-110 dBm ≤ RXLEV < -109 dBm	
02	-109 dBm ≤ RXLEV < -108 dBm	
03	-108 dBm ≤ RXLEV < -107 dBm	
…	…	…
62	-49 dBm ≤ RXLEV < -48 dBm	Maximum reception
63	-48 dBm ≤ RXLEV	Not known or not detectable

2.2 UMTS-based RSS

The universal mobile telecommunications system (UMTS) or third generation (3G) networks was proposed by the international mobile telecommunications (IMT) 2000 program to create a common worldwide communication system. Another aim of this project was to allow the mobiles to work in different environments, such as indoor use, vehicles, satellites and pedestrians. An additional goal in designing the 3G systems was to have a smooth transition from GSM system to UMTS, saving money by extending the current system instead of introducing a new system. In addition, the aim was to improve the spectral efficiency, to increase the supported data rates and to support the multimedia applications. The backward compatibility was achieved creating a new network architecture that allows the mobility between GSM and UMTS systems [27].

2.2.1 UMTS frequency bands

The most common 3G frequency bands are shown in Table 2.4. The used frequency band varies from one country to another. The United States, Canada, Mexico and most countries in the Americas use 850 MHz, 1900 MHz, 1700 MHz or 2100 MHz frequency bands while all the countries of Europe, Asia, Middle East, Africa and Australia use 900

MHz and 2100 MHz. The 2100 MHz frequency band is also used for international 3G coverage because this band is supported in all the countries [27].

Table 2.4 UMTS frequency bands

System	Frequency band	Uplink (MHz)	Downlink (MHz)	UARFCN UL channel number	UARFCN UL channel number	DL to UL frequency separation (MHz)
IMT	2100	1920-1980	2110-2170	9612-9888	10562-10838	190
PCS A-F	1900	1850-1910	1930-1990	9262-9538 additional 12, 37, 62, 87, 112, 137, 162, 187, 212, 237, 262, 287	9662- 9938 additional 412, 417, 462, 487, 512, 537, 562, 587, 612, 637, 662, 687	80
AWS A-F	1700	1710-1755	2110-2155	1312-1513 additional 1662, 1687, 1712, 1737, 1762, 1787, 1812, 1837, 1862	1537- 1738 additional 1887, 1912, 1937, 1962, 1987, 2012, 2037, 2062, 2087	400
E-GSM	900	880-915	925-960	2712-2863	2937-3088	45
CLR	850	824-849	869-894	4132-4233 additional 782, 787, 807, 812, 837, 862	4357-4458 additional 1007, 1012, 1032, 1037, 1062, 1087	45

2.2.2 UMTS system architecture

The UMTS system architecture is based in the elements shown in Figure 2.6.

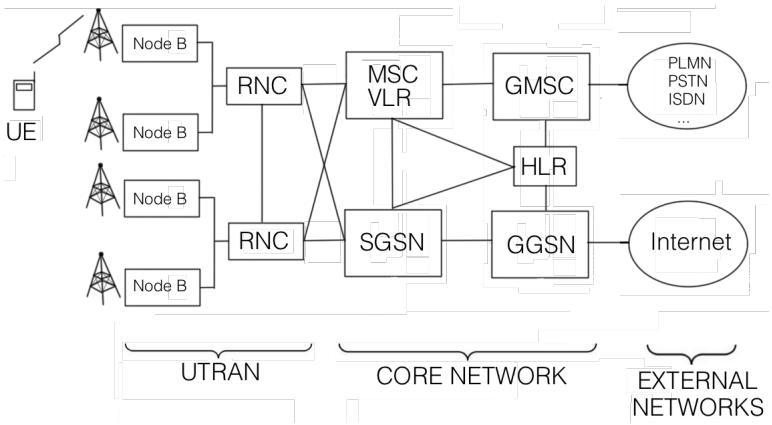

Figure 2.6 UMTS system architecture.

The UMTS system architecture is divided in three parts: The UTRA network (UTRAN) the core network (CN) and the external networks (EN) [31].

UTRAN

The UTRAN is the part of the architecture that contains several user equipment (UE), Node Bs and radio network subsystems (RNS) [32].

The user equipment consists in two main parts: the mobile equipment (ME) and UMTS subscriber identity module (USIM). The ME is the device that allows the radio communication between the transmitter and the receiver and the USIM is a chip used for authentication and encryption functions.

The Node B is the equivalent of the BTS in GSM system´s architecture. It is used to control the inner loop power, to measure the signal quality and received signal strength and for handover management [31; 32].

The radio network controller (RNC) has a lot of different functions. Some of the tasks that the RNC do are the radio resource control, the code allocation and the handover management. It also does the data conversion between the UTRAN and the CN [31].

Core network

The mobile switching centre (MSC) is used to switch the circuit switched (CS) services inside the CN. The MSC can hold GSM and UMTS connections at the same time. In most of the cases the MSC has the visitor location register (VLR) incorporated. The VLR is a database that stores the subscriber data of all MSs in its area. The information of the active subscriber is stored temporally and when a MS is connected to another network with other VLR, the data of the first VLR are removed. The subscriber's information is permanently stored in the home location registers (HLR) [31].

The gateway MSC (GMSC) is the used to route the calls coming form the EN to the correct MSC. The serving GPRS support node (SGSN) is the element of the CN used for packet-switched network. It is linked to the Gateway GPRS support node (GGSN) and this is connected to the Internet [31].

The UMTS network also has the AuC and the EIR databases like in GSM system but in UMTS system architecture this elements are implemented in the same unit of the HLR [31].

External networks

Using this structure the UMTS network is connected to the EN. The EN comprises the PLMN, the PSTN, the ISDN and the Internet.

2.2.3 UMTS radio interface

UMTS uses WCDMA to transmit the data from the Node B to the UE. WCDMA is a Wideband Direct-Sequence Code Division Multiple Access (DS-CDMA) system that works spreading the user information bits over a wide bandwidth by multiplying those with a sequence of bits called chips. The number of bits used in the spreading sequence is known as spreading factor. The chipping sequence is unique for each user of the cell and the codes used for the spreading should be (quasi) orthogonal [27].

UMTS uses a constant chipping rate of 3.84 Mchip/s. Different user data rates are achieved using different spreading factors. The UMTS systems use orthogonal variable spreading factor (OVSF) codes. The orthogonal codes are generated doubling the chipping sequence. First a spreading sequence is applied and all the data are summed. After that another bit sequence is used known as scrambling code. The scrambling code does not spread the bit sequence but XORs the chips based on a code. After the scrambling procedure, the transmitted signals are quasi orthogonal. The WCDMA systems support two duplexing techniques: Frequency Division Duplex (FDD) and Time Division Duplex (TDD). In FDD mode, all the users of the cell have different scrambling code, whereas in TDD mode, the scrambling code is the same for al UEs of the cell [27].

The spreading and the scrambling of the data is shown in a simplified manner in the Figure 2.7.

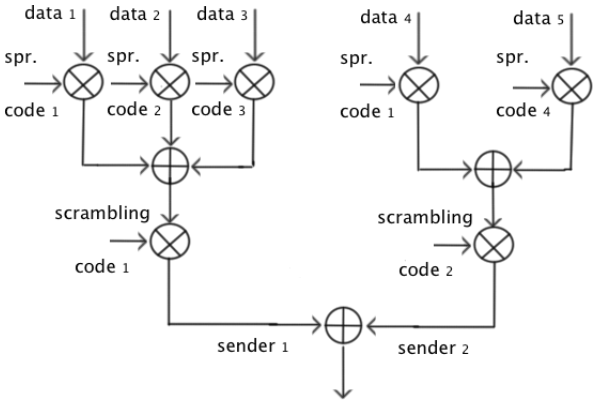

Figure 2.7 Spreading and scrambling of the data.

UTRA FDD (WCDMA)

In the FDD mode, the system uses separate 5 MHz carrier frequencies for uplink and downlink transmissions. [31].

The allocation of bandwidth in WCDMA systems is explained in Figure 2.8 [31].

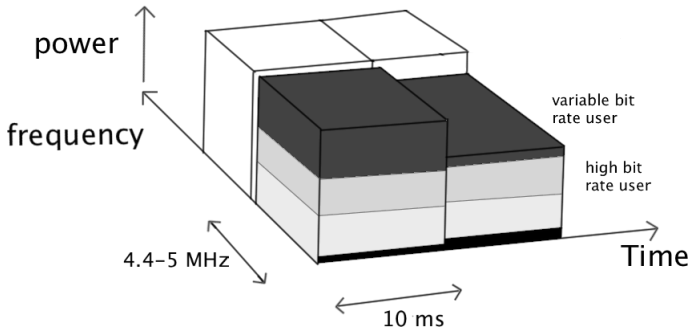

Figure 2.8 Allocation of bandwidth in WCDMA systems.

The FDD mode for UTRA uses different frequencies for uplink and downlink channels. The FDD frequencies depend on the system is used as is explained in 2.2.1 [31].

A UTRA FDD radio frame uses 38,400 chips and it is transmitted during 10 ms frame. The frame is divided in 15 time slot of 2,560 chips. The occupied bandwidth of a WCDMA channel is 4.4-5 MHz. but sometimes the width of the channel is reduced to avoid interference between channels of different network operators [27; 31].

WCDMA employs coherent detection using pilot symbols or common pilot and asynchronous synchronization, so there is no need for a global time reference [31].

The structure of a UTRA FDD frame is shown is the figure below.

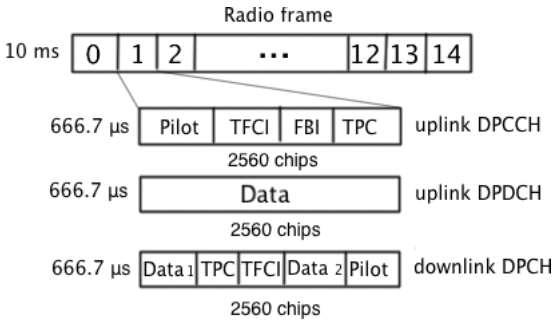

Figure 2.9 UTRA FDD (WCDMA) frame.

In UMTS, similar with GSM, there are many physical and logical channels. The different channels are shown in Figure 2.9.

There are two main physical channels for uplink, called dedicated physical data channel (DPDCH) and the dedicated physical control channel (DPCCH) [27].

The DPDCH transfers user and signaling data. The data rate of the DPDCH channel depends on the used spreading factor [27].

The DPCCH transmits control data for the physical layer using a constant spreading factor of 256. The DPCCH is divided in four subchannels: the pilot, the transport format combination identifier (TFCI), the feedback information field (FBI) and the transmit power control (TPC). The pilot is used for channel estimation. The TFCI transmits information about the channels inside the DPDCH. The FBI is used for signaling during handovers. The TPC informs about the transmission power of the UE [27].

The dedicated physical channel (DPCH) multiplexes the user and control data. The multiplexing of the data varies with the downlink time. The utilized spreading factors are between 2 and 512 providing a data rates from 6 to 1872 kbit/s [27].

There is also another channel known physical random access channel (PRACH) used to avoid the collision between downlink and uplink connections.

UTRA TDD (TD-CDMA)

In the TDD mode, one 5 MHz is time-shared between the uplink and downlink channels. The TDD mode for UTRA divides the radio frame in 15 different slots of 2,560 chips. The used chipping rate is the same as in FDD mode, 3.84 Mchips/s. The different user data rates are obtained using symmetrical or asymmetrical TDD frames [27].

A symmetrical frame is when there are the same number of uplink and downlink slot in the frame and if the number of uplink and downlink is no equal the frame is called asymmetrical. In UTRA TDD the system changes the spreading factor to get the desired data rate.

The next figure shows the example of a UTRA TDD frame and a time slot [27].

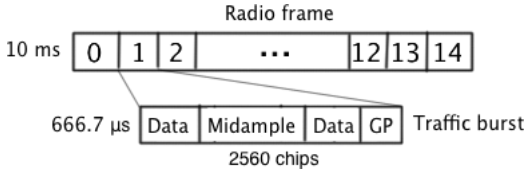

Figure 2.10 UTRA TDD (TD-CDMA) time slot.

The traffic burst of the UTRA TDD is divided in two data fields of 1,104 chips, a midample used for training and channel estimation and a guard band (GP) in the end of the slot that facilitates the synchronization [27].

2.2.4 RSS measurements in UMTS systems

The received signal strength measurements are done using the physical layer values on downlink DPCH channels. These data are measured using the received signal code power (RSCP) in different physical layers. The most used RSS indicator are PCCPCH RSCP, CPICH RSCP and DPCH /PDSCH RSCP [12].

PCCPCH RSCP

The PCCPCH RSCP is the received power on a PCCPCH of own or neighbor cell after despreading. The reference point of RSCP measurements is the antenna connector at the UE. This value can be measured in idle and connected modes. In the connected mode the RSCP value can be taken in intra frequency and inter frequency options [12].

CPICH RSCP

The CPICH RSCP is the received power on the CPICH code after despreading. The reference point of the obtained value is the antenna connector of the ME. This data can be also obtained in idle mode and on the inter frequency connected mode [12].

DPCH / PDSCH RSCP

DPCH / PDSCH RSCP is the received power of a specified DPCH or PDSCH after despreading. The reference point for the measured data is the antenna connector of the UE and this data are only available in connected mode in intra frequency domain [12].

The mapping between the measured power and the saved level for the previous channels is shown in the next table.

Table 2.5 RSCP mapping values.

Signal level	Received power	Description
00	RSCP < -115 dBm	Minimum reception
01	-115 dBm ≤ RSCP <-114 dBm	
02	-114 dBm ≤ RSCP < -113 dBm	
03	-113 dBm ≤ RSCP < -112 dBm	
…	…	…
89	-27 dBm ≤ RSCP < -26 dBm	
90	-26 dBm ≤ RSCP < -25 dBm	Maximum reception
91	-25 dBm ≤ RSCP	Not known or not detectable

There are many other physical layers that can be used for RSS measuring such as UTRA carrier RSSI or ISCP [12].

In this thesis we used the values of CPICH RSCP levels for RSS measuring.

2.3 WLAN-based RSS

The wireless local area networks (WLAN) have become very popular in the last years. The first wireless network was developed in the University of Hawaii using seven computers deployed over four Hawaiian islands. In 1991, the IEEE 802 executive committee started creating a WLAN standard and in 1997 the first WLAN 802.11 standard was approved. In the next years, other new 802.11 standard appeared such as the 802.11g, the 802.11n and the newest 802.11ac [27].

2.3.1 WLAN frequencies and characteristics

The main differences and similarities between different 802.11 standards are shown in Table 2.6. [33; 34]

Table 2.6 802.11 standards.

Standard	**802.11**	**802.11b**	**802.11a**	**802.11g**	**802.11n**	**802.11ac**
Release date	1997	1999	1999	2003	2009	2013
Frequency band (GHz)	2.4	2.4	5	2.4	2.4, 5	5
Bandwidth (MHz)	20	20	20	20	20, 40	40, 80, 160
Modulation	DSSS FHSS	DSSS	OFDM	DSSS OFDM	OFDM	OFDM
Advanced antenna technologies	N/A	N/A	N/A	N/A	MIMO	MIMO MU-MIMO
Maximum data rate	2 Mbit/s	11 Mbit/s	54 Mbit/s	54 Mbit/s	600 Mbit/s	6.93 Gbit/s

Nowadays, the most used standards are the 802.11b and 802.11g. The 802.11g is backward compatible with 802.11b and both use 2.4 GHz frequency band [27].

The 2.4 GHz frequency band is divided in fourteen non-overlapping channels. The occupied bandwidth of each of these channels is 22 MHz and the separation between the centre frequencies of the channels should be at least 25 MHz. The number of

available channels varies along the world. For example, in United States and Canada, the first eleven channels are used, in Europe there are thirteen channels and in Japan all frequencies are used [27].

2.3.2 WLAN system architecture

The WLAN system architecture can be implemented in two different ways: infrastructure based or ad-hoc [27].

The infrastructure based IEEE 802.11 architecture is shown in a simplified form in the next figure.

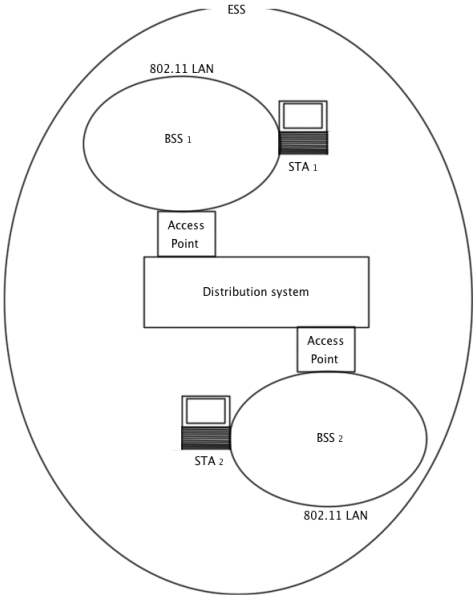

Figure 2.11 WLAN infrastructure based system architecture.

The architecture consists on several nodes called stations (STA), connected to different access points (AP). The station can be any wireless device that contacts the AP. All the stations and APs in the same coverage area are considered as basic service set (BSS). The different BSS may be connected to each other using a distribution system. The distribution system creates a network of different BSS using APs. This bigger network is called extended service set (ESS) and has its own identifier (ESSID) used to differentiate the networks. The wireless network is connected to the other LANs using gateway [27].

IEEE 802.11 also supports the building of ad-hoc networks between stations creating one or more independent BSSs (IBSS). In one IBSS all the stations use the same frequency for data transmission. Different IBSSs can be created using the distance between the IBSSs or using different carrier frequencies [27].

Figure 2.12 shows the ad hoc architecture.

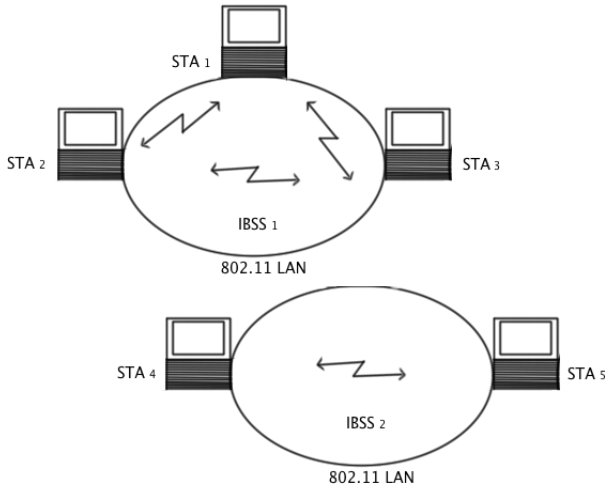

Figure 2.12 WLAN ad hoc based system architecture.

2.3.3 WLAN radio interface/ Physical layer

There are three main types of physical (PHY) layers in 802.11: one layer is for infrared communication and two layers for radio communication. All PHY layers have the clear channel assessment (CCA) signal that is used for controlling medium access [27]. In this thesis we will focus on the radio communications channels.

The different PHY layers provide a service access point (SAP). There are several versions of a PHY layer for radio communication [27]:

1. the frequency hopping spread spectrum (FHSS)
2. the direct sequence spread spectrum (DSSS)
3. orthogonal frequency-division multiplexing (OFDM)
4. multiple input, multiple output OFDM (MIMO-OFDM)

In this thesis we will explain the FHSS PHY layer because this is the most widely used to the best of our knowledge [27].

The frequency hopping spread spectrum (FHSS)

The FHSS technique divides the total available bandwidth into many channels of smaller bandwidth and with guard spaces between them. In FHSS the stations and the APs transmit the data in one of these channels and after a certain time they hop to another channel. The pattern of channel utilization is called hopping sequence and the duration of a station transmitting on a certain frequency is known as dwell time. There are two types of FHSS: slow hopping and fast hopping [27].

The slow hopping the data are transmitted using one frequency for several bit periods. The slow hopping is a cheap system that supports relaxed tolerances but it is affected by narrowband interference [27].

In fast hopping systems the transmitter changes the used channel several times for each bit. The fast hopping systems are more expensive because they require synchronization between the transmitter and receiver. Due to the short duration on a frequency the fast hopping systems respond better to narrowband interference and frequency selective fading (as it will be explained in chapter 3) [27].

Figure 2.13 shows the difference between slow and fast hopping.

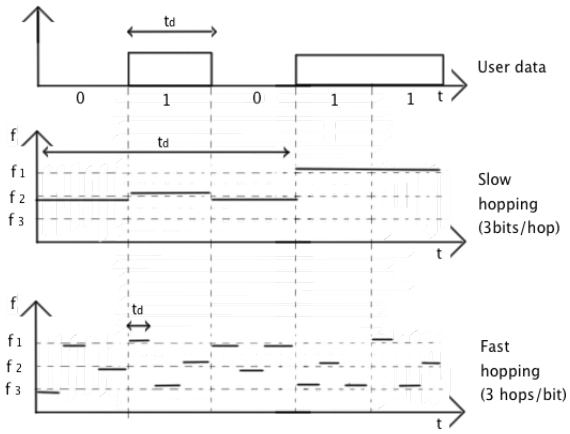

Figure 2.13 Frequency hopping types.

In 802.11 standard the bandwidth is divided in 79 hopping channels for United States and Europe and 23 hopping channels for Japan. Each of these channels has a bandwidth of 1 MHz in the 2.4 GHz frequency band [27].

One FHSS frame is divided in two main parts: The physical layer convergence procedure (PLCP) preamble and PLCP header, as well as the payload [27].

The structure of a FHSS frame is shown in the next figure.

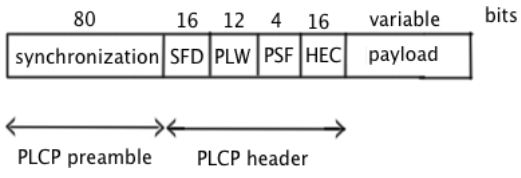

Figure 2.14 FHSS frame.

The PLCP preamble contains information about synchronization and start frame delimiter (SFD) [27]. The synchronization part uses 80 bits for synchronization of

potential receivers and the signal detection done by the CCA. The 16 bits of the SFD defines the frame timing and helps frame synchronization [13; 27].

The PLCP header´s data are divided in three parts: the PLCP PDU length word (PLW) and PLCP signaling field (PSF) and the header error check (HEC) [27].

The PLW indicates the length of the payload including the 32 bits of the cyclic redundancy check (CRC). The PLW is a sequence of 12 bits with 4096 different values [27].

The 4 bits of the PSF are used to express the data rate of the attached payload. When all bits are set to zero (0000) the lowest data rate (1 Mbps) is used for transmission and when all bits are set to one (1111) the maximum data rate is provided (4.5 Mbps) [12; 27].

The FHSS frame also has a HEC field which protects the PLCP header using a CRC of 16-bit checksum [12; 27].

2.3.4 RSS measurements in WLAN systems

In 802.11 standard the received signal strength is measured using RSSI parameter.

For FHSS the RSSI value should be measured between the beginning of the SFD and the end of HEC. RSSI should be used in a relative mode as in GSM. The 802.11 standard does not specify an absolute accuracy. The RSSI parameter should me measured using no more than 16 bits and taking the antenna connector as reference point. [12; 35; 36]

Depending on the chipset manufacturer the RSSI value is measured using different values and granularity. For all vendors the RSSI value will be between 0 and RSSImax. Cisco chipsets provide 101 different RSSI values between 0 and 100 while Qualcomm Atheros chipsets use 61 different values in a range between 0 and 60. Chipsets with more RSSI values will measure the signal strength with more precision than chipset of low values [37; 38].

In the first case, in Cisco chipsets the RSSI signal level is mapped as in Table 2.7.

Table 2.7 RSSI mapping in Cisco chipsets.

Signal level	Received power	Description
00	RSSI < -113 dBm	
01	-113 dBm≤ RSSI < -112 dBm	

02	-112 dBm ≤ RSSI < -111 dBm	
03	-111 dBm ≤ RSSI < -110 dBm	
…	…	…
16	-97 dBm ≤ RSSI < -96 dBm	Minimum reception
…	…	…
92	-14 dBm ≤ RSSI < -13 dBm	
93	-13 dBm ≤ RSSI < -12 dBm	
94	-11 dBm ≤ RSSI < -10 dBm	Maximum reception
…	…	
100	-10 dBm ≤ RSSI	

Notice that the sensitivity of Cisco devices is -96 dBm and there are more signal levels below this value so all these will be saved as not detectable signals. For signals above signal level 94 all of them will have the same received power and thus the maximum received signal will be 94 or -10 dBm.

Another example is shown here, for Qualcomm Atheros chipsets, where the power translation of these signals can be seen in Table 2.8.

Table 2.8 RSSI mapping in Qualcomm Atheros chipsets.

Signal level	**Received power**	**Description**
00	RSSI < -95 dBm	Minimum reception
01	-95 dBm ≤ RSSI < -94 dBm	
02	-94 dBm ≤ RSSI < -93 dBm	
03	-93 dBm ≤ RSSI < -92 dBm	
…	…	…
57	-39 dBm ≤ RSSI < -38 dbm	
58	-38 dBm ≤ RSSI < -37 dBm	
59	-37 dBm ≤ RSSI < -36 dBm	
60	-35 dBm ≤ RSSI	Maximum reception

As seen by comparing Table 2.7 and Table 2.8, different manufacturers use different mappings, and this is an issue to be always considered when analyzing the measurement data. In our available xml files, a mapping between 0 and 63 was used, but we are not sure about the manufacturer of the chipset used in our measurement devices.

3. URBAN AND RURAL CHANNEL CHARACTERISTICS

We define an urban environment as an environment where the buildings cover most of the terrain and where there are not many areas with vegetation. The height of the building is large in most of the cases and they could hinder the propagation of the radio signal. This environment is completely different from the rural environment where the area covered by buildings is smaller than in urban case, the dimensions of the buildings are smaller and the vegetation coverage is higher than in urban case [8]. In urban areas we will find more transmitters of different communication systems producing a stronger wireless traffic and many unwanted signals or situations.

The following sub-sections describe the different types of noises and interferences that may affect the wireless signal propagation in urban, suburban and rural areas.

3.1 Noise

In a radio link communication we can find several noises that can perturb the signal. Some of them are generated by the electronic components of a circuit and some other ones are due to the overlap of signals produced by different appliances in the environment. The most important noises are the thermal noise and the man-made noise.

Thermal noise

The thermal noise or also known as Johnson-Nyquist noise is the noise caused by the thermal agitation of charges (usually electrons) in a conducting media. It is generated in all electronic devices and is a function of temperature. The thermal noise is uniformly distributed across the bandwidth so we can refer to it as white noise [39]. The effective thermal noise power is expressed as

$$P_N(W) = kTB \cdot F \tag{3.1}$$

where k is the Boltzmann´s constant with a value of $k = 1.3805 \times 10^{-23}$ [J/K], T is the temperature in K, B is the bandwidth in Hz and F is the noise factor.

The previous expression can be written in dBm units as

$$P_N(dBm) = 10\log_{10}\left(\frac{kT}{1mW}\right) + 10\log_{10}(B) + 10\log_{10}(F) \tag{3.2}$$

The typical model for the thermal noise, from the point of view of analysis, is the additive white Gaussian noise (AWGN) [39].

Man-made noise

Man-made noise is caused due to all types of electronic devices that are in an urban environment. This noise is strongly dependent on the distance from the sources and it can vary on frequency and emitted power. These noise signals could come from different technologies, such as TV and radio communication installations, cellular or other wireless networks and from other sources as ignition systems, frequency inhibitors, remote controls, satellite communications or power lines. The important characteristics of these noise signals are the type of emitted waves, continuous or impulsive, the used modulation and the wave polarization [40].

3.2 Interference

Interference is anything that alters, modifies or disrupts a signal when it travels along a channel between a source and a receiver. It can be also considered as including all types of unwanted signals that are added to the useful signal. There are two main categories of interference, namely the unintentional interference and the intentional interference [41].

The unintentional interferences are those that may be caused by radio waves, other type of electronic or electric equipment and atmospheric conditions. These could happen when someone is keying on the wrong frequency or when there is any equipment malfunction that creates spurious emissions. Unintentional interference can be easily rectified once the source of the interference is identified. It normally travels only a short distance and a search in the immediate area will reveal the source of this type of interference [41].

The intentional interference, also known as harmful interference, occurs when a transmitter emits frequencies out of the frequency band of the signal of interest. It may also occur when the emissions of nearby transmitters have more than the permitted power. These interferences can be solved reporting a form to the administration of the country where the infringement occurred and it will decide the penalty according to the law. There is also research work dedicated to the mitigation of various sources of intentional and unintentional interferences at the receiver side.

Depending on the frequency spectrum of the interference we could have two types of interferences: narrowband interference or wideband interference [27].

The narrowband interference is the interference that has a small bandwidth or which is narrower than the wanted signal. This type of interference could be very prejudicial for signals which are transmitted in a narrow bandwidth because it can destroy completely the desired signal [42; 43].

The wideband interference or broadband interference is the interference that has an ample bandwidth or is wider than the useful signal.

The narrowband interference for a single channel can be sometimes reduced when using spread spectrum techniques, such as those used in CDMAone, CDMA2000 or WCDMA systems (e.g., 3G). To deal with the broadband interference the receiver may use a bandpass filter that cuts off the frequencies outside the signal or the useful band.

3.3 Multipath causing sources

In urban and rural environments, it is very common to have some objects or obstacles that may affect the normal propagation of the signal. Due to these obstacles, the transmitted signal could suffer shadowing, reflection, refraction, scattering or diffraction and as a result we will have multipath propagation.

Shadowing

Shadowing occur when there is an obstacle that hinder the signal in the LOS path between the transmitter and the receiver. The signal can be completely attenuated by the object or can be received from a different path [12].

An example of shadowing is shown in Figure 3.1.

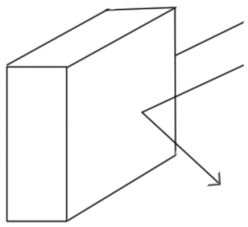

Figure 3.1 Shadowing

Reflection

Reflection happens when a signal hits an object and the wave changes its direction and its power [12]. The direction of the reflected wave will depend on the angle of incidence and the power will vary according to the material of the object. Some materials will absorb more power than others and in some cases the power of the reflected wave will be considerably reduced [23; 44].

The next figure shows the reflection of a signal.

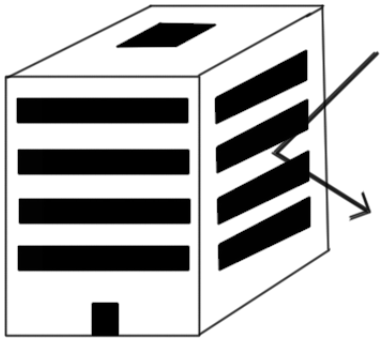

Figure 3.2 Reflection

Refraction

Refraction happens when the transmission medium changes [27]. The wave will suffer a change in its direction and power depending on the material of the mediums as is shown in the following figure.

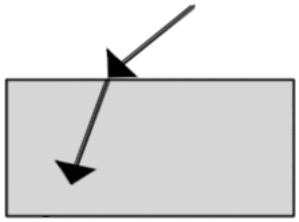

Figure 3.3 Refraction

Scattering

Scattering is a random change in the directions and powers of a group of waves caused by physical interactions. It occurs when the size of the obstacle is on the order of the wavelength of the transmitted signal or less [27, 45].

A scattering situation is illustrated in Figure 3.4.

Figure 3.4 Scattering

Diffraction

Finally, diffraction is also a random change in the directions and powers of a group of waves [27]. It occurs at the edge of an impenetrable body that is large compared to the wavelength of the transmitted signal. After passing by the edge a group of weaker waves that have different directions of the original wave will propagate.

An example of diffraction is shown in Figure 3.5.

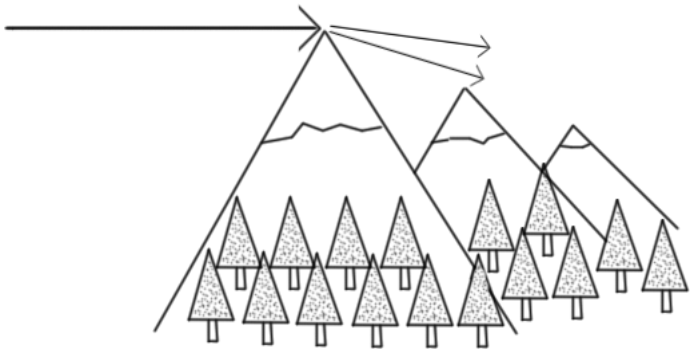

Figure 3.5 Diffraction

Because all these effects, there will be multipath propagation in most of the communication. Multipath means that a receiver will hear the direct signal and multiple copies of the signal coming from different paths [27]. These copies of the original signal will have different phases and depending on the addition of the signals they will be constructive or destructive signals.

3.4 Fading and shadowing

Fading effects occur due to the variations of the environment of a wireless communication and the movement of the receiver [27]. These variations can be caused by the changes in the reflecting surfaces or the scattering obstacles and they will give rise to random variations of the received power. Statistical models have to be considered to predict the fading effects. There are two main types of fading known as fast fading and slow fading [27; 46; 47].

Fast fading is the quick changes in the instantaneous received power. These changes occur in a short period of time and the amplitude could vary as much as 20 or 30 dB.

Slow fading is the variation of the average received power. This change in the received power appears when the mobile unit travels long distances.

Fading effects can also be classified as flat or selective depending on how these variations appear according to frequency.

The flat fading or nonselective fading is the type of fading in which all frequency components of the received signal fluctuate in the same proportions simultaneously [27].

The selective fading is the fading that affects unequally the different spectral components of the signal [27].

3.5 Differences between urban and rural environments

The propagation of waves in an urban environment and a rural environment is typically different.

In an urban environment, there will be many objects such as buildings, traffic signals or cars that will create many reflections, scatterings and shadowing. Multipath propagation is very usual in cities or urban areas.

In rural environment, there will be different signal propagation problems due to the geography of the land. In a rural area, we may find a high tree density, valleys or mountains that will disturb the signal. In these circumstances the signal will suffer shadowing, diffraction or reflections producing hindered areas and poor signal quality zones.

The ability of defining the environment is important in order to get accurate location results. Depending on the environment, the analysis of the measurements to predict the location could be fine-tined to the different causes explained above. For example, an appropriate path loss model that fit better to the terrain could be choose or different interference sources could be identified. In this thesis however, the focus is on the signal propagation characteristics and emitters density in various urban and rural areas. We will investigate which are the typical deployments (e.g., in terms of number of emitters and average coverage areas) in urban and rural situations for 2G, 3G and WLAN systems. We will also look at the similarities and differences of different path-loss models in different environments. The shadowing effects in each of those different environments will be also analyzed.

4. PATH-LOSS MODELS

There are many different path-loss models in the literature. Some of them are more appropriated for outdoor conditions such as urban, suburban or rural whereas others are more appropriate for indoors. Here most important path loss models are explained.

4.1 Free space path loss model

The free space path loss (FSPL) models the attenuation of the signal strength due to the broadening of the wave front. It is measured in dB and it depends on the frequency and the distance between the transmitter and the receiver [12]. It is formally expressed as

$$PL = 32.44 + 20\log_{10}(d) + 20\log_{10}(f) \tag{4.1}$$

where d is the distance given in Km and f is the frequency in MHz. The above expression is in dB scale.

The FSPL is typically not an accurate model because it is limited to LOS and there are no other parameters to adjust the terrain model.

4.2 One-slope model

This empirical path loss model is used for the large-scale attenuation for the indoor radio channel or densely populated areas. In here we model the loss exhibited over the channel, measured in dB. The path loss is given by [39]:

$$PL = L_0 + 10n\log_{10}(d) \tag{4.2}$$

The variable L_0 denotes the path loss in a distance of one meter and n is the path loss slope factor or power decay index, while d is the distance between the emitter and the receiver.

The slope factor n can have different values depending on the environment. Table 4.1 shows some examples according to [40], but usually n is environment-dependent and should be estimated. We will show based on the measurement data, that the expected n in several environments is below the free space loss coefficient of 2. In our thesis we will adopt this one-slope path loss model, as being one of the most used in the literature,

and we will describe its parameters in the various measured environments (see Chapter 6).

Table 4.1 Slope factor values according to [40]

Environment	*n*
Free space	2
Flat rural, home	3
Rolling rural	3.5
Suburban	4
Dense urban	4.5
Office building (same floor)	1.6 – 3.5
Office building (multiple floors)	2 - 6

4.3 Ericsson path loss model

The Ericsson model is path-loss model developed by Ericsson company in order to predict the path loss of a network [48]. The path loss can be calculated using the following equation

$$PL = a_0 + a_1 \log_{10}(d) + a_2 \log_{10}(h_b) + a_3 \log_{10}(h_b) \log_{10}(d) - 3.3(\log_{10}(11.78h_r)^2) + g(f) \quad (4.3)$$

where $g(f)$ is defined as

$$g(f) = 44.51 \log_{10}(f) - 4.79(\log_{10}(f))^2 \quad (4.4)$$

Here h_b is transmission antenna height in m, h_r is receiver antenna height in m and a_0, a_1, a_2 and a_3 are parameters for different terrain. The values of these parameters are given in the next table:

Table 4.2 a_0, a_1, a_2 and a_3 parameters

Environment	a_0	a_1	a_2	a_3
Urban	36.2	30.02	12.0	0.1
Suburban	43.20	68.93	12.0	0.1
Rural	45.95	100.6	12.0	0.1

4.4 Okumura-Hata

This empirical path loss model was created by Okumura Hata using the data collected in the city of Tokyo in Japan [48] and its equation is written as

$$PL = FSPL + BMPL + G_b + G_r \quad (4.5)$$

where *BMPL* is basic median path loss and G_r is receiver antenna gain factor.

These factors can be described as

$$BMPL = 21.41 + 9.83\log_{10}(d) + 8.782\log_{10}(f) + 9.58[\log_{10}(f)]^2 \quad (4.6)$$

$$G_b = \log_{10}\left(\frac{h_b}{200}\right) + 14.865 + 6.1[\log_{10}(d)]^2 \quad (4.7)$$

When dealing with gain for urban areas, the G_r will be expressed in terms of the following

$$G_r = [42.58 + 13.7\log_{10}(f)][\log_{10}(h_r) - 0.586] \quad (4.8)$$

for quite large urban areas,

$$G_r = 0.860h_r - 1.960 \quad (4.9)$$

where *f* is frequency range in GHz.

4.5 Cost 231 Walfich-Ikegami model

This model is an extension of the Okumura Hata model for medium to small cities and to cover a frequency range from 800 MHz to 2000 MHz. This path loss model is used in GSM frequency bands [49].

The expressions for proposed model are:

a) For LOS condition

$$PL_{LOS} = 42.6 + 26\log_{10}(d) + 20\log_{10}(f) \quad (4.10)$$

b) For NLOS condition

$$PL_{NLOS} = \begin{cases} L_{FSL} + L_{rts} + L_{msd} & for\ urban\ and\ suburban \\ L_{FS} & L_{rts} + L_{msd} > 0 \end{cases} \quad (4.11)$$

where

L_{FSL} is the free space loss
L_{rts} is the roof top to street diffraction
L_{msd} is the multi-screen diffraction loss

The roof top to street diffraction is

$$L_{rts} = \begin{cases} -16.9 - 10\log_{10}(w) + 10\log_{10}(f) + 20\log_{10}(\Delta h_r) + L_{ori} & , for\ h_{roof} > h_r \\ 0 \end{cases} \quad (4.12)$$

where

$$L_{ori} = \begin{cases} -10 + 0.354\phi & for\ 0 \leq \phi < 35 \\ 2.5 + 0.075(\phi - 35) & for\ 35 \leq \phi < 55 \\ 4 - 0.114(\phi - 55) & for\ 55 \leq \phi \leq 90 \end{cases} \quad (4.13)$$

and ϕ is the road orientation with respect to the direct radio path in degrees.

We note that

$$\begin{aligned} \Delta h_r &= h_{roof} - h_r \\ \Delta h_b &= h_b - h_{roof} \end{aligned} \quad (4.14)$$

where h_{roof} is the height of buildings.

The multi-screen diffraction loss is

$$L_{msd} = \begin{cases} L_{bsh} + k_a + k_d\log_{10}(d) + k_f\log_{10}(f) - 9\log_{10}(f) - 9\log_{10}(B) & , L_{msd} > 0 \\ 0 & , L_{msd} < 0 \end{cases} \quad (4.15)$$

The values of L_{bsh}, k_a, k_d, and k_f are

$$L_{bsh} = \begin{cases} -18\log_{10}(1 + \Delta h_b) & , h_b > h_{roof} \\ 0 & , h_b \leq h_{roof} \end{cases} \quad (4.16)$$

$$k_a = \begin{cases} 54 & , for\ h_b > h_{roof} \\ 54 - 0.8\Delta h_b & , for\ d \geq 0.5\ km\ and\ h_b \leq h_{roof} \\ 54 - 0.8\Delta h_b\left(\frac{d}{0.5}\right) & , for\ d < 0.5\ km\ and\ h_b \leq h_{roof} \end{cases} \quad (4.17)$$

$$k_d = \begin{cases} 18 & , for\ h_b > h_{roof} \\ 18 - 15\left(\frac{\Delta h_b}{h_{roof}}\right) & , for\ h_b \leq h_{roof} \end{cases} \quad (4.18)$$

For suburban or medium size cities with moderate tree density

$$k_f = -4 + 0.7\left(\frac{f}{925} - 1\right) \tag{4.19}$$

and for metropolitan-urban

$$k_f = -4 + 1.5\left(\frac{f}{925} - 1\right) \tag{4.20}$$

where d is the distance in m, f is the frequency in GHz, B is the building to building distance in m and w is the street width in m.

4.6 Stanford University Interim (SUI) channel model

The basic path loss expression of SUI model [50] with correction factors are presented as

$$PL = A + 10y\log_{10}\left(\frac{d}{d_0}\right) + X_f + X_h + s \qquad ,for\ d > d_0 \tag{4.21}$$

The variable d is the distance between the BS and the receiver antenna (m), d_0 is 100 m, X_f is the correction for frequency 940 MHz, X_h correction for receiving antenna height, s correction for shadowing and y is the path loss exponent.

The parameter A is defined as

$$A = 20\log_{10}\left(\frac{4\pi d_0}{\lambda}\right) \tag{4.22}$$

where λ is the wave length in m.

By statistical method, the random variables are taken as the path loss exponent y and the weak fading standard s is derived. The path loss exponent y is given as follows

$$y = a - bh_b + \left(\frac{c}{h_b}\right) \tag{4.23}$$

The constants a, b and c depend upon the types of terrain. The value of these parameters is shown in the Table 4.3.

Table 4.3 a, b, c and s parameters

Model parameters	Terrain A	Terrain B	Terrain C
a	4.6	4.0	3.6
b (m^{-1})	0.0075	0.0065	0.0050
c (m)	12.6	17.1	20.0
s	10.6	9.6	8.2

There is no description of any particular environment. Terrain A is characterized for hilly areas with moderate or very dense vegetation. Terrain B can be used for hilly terrains with rare vegetation or flat terrains with moderate or heavy tree densities. This terrain is also considered for suburban environment. Terrain C is suitable for flat areas or rural with light vegetation.

The correction factors X_f and X_h are expressed as follows

$$X_f = 6.0 \log_{10}\left(\frac{f}{2000}\right) \tag{4.24}$$

For terrain type A and B

$$X_h = -10.8 \log_{10}\left(\frac{h_r}{2000}\right) \tag{4.25}$$

for terrain type C

$$X_h = -20.0 \log_{10}\left(\frac{h_r}{2000}\right) \tag{4.26}$$

where f is the operating frequency in MHz.

4.7 Lee path-loss model

Lee´s model is used to predict the local-mean of a received signal along a mobile path where the mobile unit travels [51]. The path loss curve according to Lee´s model for area-to-area mode can be expressed as:

$$PL = L_0 + \gamma \log_{10}(d) - 10 \log_{10}(F_0) \tag{4.27}$$

The adjustment factor F_0 can be expressed as

$$F_0 = F_1 F_2 F_3 F_4 F_5 \tag{4.28}$$

where F_1, F_2, F_3, F_4 and F_5 are

$$F_1 = \left(\frac{h_b}{30.48}\right)^2 \tag{4.29}$$

$$F_2 = \frac{G_b}{4} \tag{4.30}$$

$$F_3 = \begin{cases} \left(\frac{h_r}{3}\right)^2 & if\ h_r > 3 \\ \left(\frac{h_r}{3}\right) & if\ h_r < 3 \end{cases} \tag{4.31}$$

$$F_4 = \left(\frac{f}{900}\right)^{-n} \qquad , for\ 2 < n < 3 \tag{4.32}$$

$$F_5 = \frac{1}{G_m} \tag{4.33}$$

where f is the operating frequency in MHz and G_m is the gain of the receiver antenna relative to half-wave dipole.

4.8 Clutter factor and plane-earth model

In these deterministic models, the path loss expression for plane-earth model is given by

$$PL = 40\log_{10}(d) - 20\log_{10}(h_r) - 20\log_{10}(h_b) \qquad h_r, h_b \ll d \tag{4.34}$$

For the Clutter factor model the expression is defined as

$$PL = 40\log_{10}(d) - 20\log_{10}(h_r) - 20\log_{10}(h_b) + K \tag{4.35}$$

where K is the clutter factor in dB [49].

4.9 Multi floor and wall model

Motley and Kennan developed the Floor and wall model that takes into account all penetrated walls and floors by individual penetration looses depending on their thickness and material [52]. The expression for this model can be written as

$$PL = L_0 + 10n\log_{10}(d) + \sum_{i=1}^{I}\sum_{k=1}^{K_{wi}} L_{wik} + \sum_{j=1}^{J}\sum_{k=1}^{K_{fj}} L_{fjk} \tag{4.36}$$

where L_0 is the path loss at a distance of 1 m, n is the power decay index, L_{wik} is the attenuation due to wall type i and k-th traversed wall, L_{fjk} is the attenuation due to floor type j and k-th traversed floor, I is the number of wall types, J is the number of floor types, K_{wi} is the number of traversed walls of category i, and K_{fj} is the number of traversed floors of category j.

The penetration loss values for MWF model are given in the next table.

Table 4.4 Penetration loss values

Wall material	Thickness	k=1	k=2
Concrete	10 cm	L_{w11}= 16 dB	L_{w12}= 14 dB
Concrete	20 cm	L_{w21}= 29 dB	L_{w22}= 24 dB

4.10 Classification of path-loss models depending on the environment

Some of the path loss models explained above have different parameters to fix the equation to the environment of the propagation. The accuracy of the obtained location will depend on the used path loss model. The free-space path loss only can be used for outdoor conditions and its results will be imprecise due to the simplicity of the equation. The one-slope path loss model is used in all environments and terrains modeling the slope factor. The accuracy of this model will depend on the slope factor parameter. The Ericsson path loss model works in different outdoor situations but it can not be used in indoor conditions. The Okumura-Hata model is designed for outdoor environment but only for urban terrain. Cost 231 Walfich-Ikegami model only can be used in outdoor conditions for urban and suburban environments. The SUI path loss model has different constant values to adjust the equation for urban, suburban and rural environments. The Lee, Clutter factor and Plane-earth models only work in outdoor environments because all their parameters are fixed. Otherwise, the multi floor and wall model is designed to predict the path losses in indoor conditions.

In this thesis the one-slope path loss model is adopted to predict the location of the transmitters because it fits both indoor and outdoor situations. This model can be modeled for urban, suburban and rural terrains where the measurements were collected.

The classification of the path loss models according to the environment is shown in the Table 4.5.

Table 4.5 Classification of path loss models

Path Loss Model	Outdoor	Indoor	Outdoor and Indoor
Free Space Path Loss	X		
One-slope			X
Ericsson	X		
Okumura-Hata	X		
Cost Hata 231	X		
SUI	X		
Lee	X		
Clutter factor and Plane Earth	X		
Multi Floor and Wall model		X	

5. MEASUREMENT UNITS, FORMAT AND CAMPAIGNS

The measurements were collected using a Nokia C7-00 smartphone. The users taking the data were several employees at TUT, Department of Electronics and Communications Engineering. The measurement campaigns were done during 2011-2012. The data were collected in various environments (urban, sub-urban, rural), in various EU cities, and with various speeds (e.g., pedestrian, by bike, by train, by bus, by car, by boat, etc.). The data were saved in a SD memory card in Extensive Markup Language (xml) format. The code of the .xml files stores information about many parameters of GPS, GSM, 3G and WLAN signals.

From the GPS part of the code we used 5 variables:

- Starting time
- Ending time
- Latitude
- Longitude
- Altitude

The GPS information also stored additional information about speed, vertical speed or course, etc.

From the GSM part of the .xml code we saved the next data:

- Base station identifier code
- Received level
- Network operator´s name
- Cell ID

If the MS hears more than one BS in the same area the .xml code will store base station identifier code and received level information of the other BSs.

From the 3G information of the code we used the following data:

- Starting time
- Ending time
- Primary scrambling code

- Downlink code in FDD
- Cell ID
- Received energy per chip divided by the power density in the band measured in the CPICH
- CPICH RSCP
- Path loss
- Primary CPICH
- Mobile country code
- Network ID
- Location area code

If the UE hears more than one Node B the .xml code will store the values of cell ID, primary scrambling code, received energy per chip divided by the power density in the band measured in the CPICH, CPICH RSCP and path loss of the other Node Bs.

The WLAN data that we used from the .xml files are:

- MAC address
- Received signal strength level

If the station receives signals from several APs, all the values of MAC address and received signal strength level are stored.

5.1 RSS measurement units

The stored RSS values can be given in two main units.

5.1.1 Decibel milliwatts

Decibel milliwatts or also known as dBm is an abbreviation for the power expressed in decibels relative to one milliwatt [15]. The power in dBm is given by

$$Power\ [dBm] = 10 \log_{10} \frac{P\ [mW]}{1mW} \tag{5.1}$$

5.1.2 Decibel watt

The decibel watt or dBw is the measurement for the power expressed in decibels relative to one watt [15]. The power in dBw is expressed as follows

$$Power\ [dBw] = 10 \log_{10} \frac{P[W]}{1W} \tag{5.2}$$

In our measurements the data are given in dBm.

5.2 Measurement format

The .xml files were processed using MATLAB numerical computation software developed by MathWorks. The Matlab simulator was created during this thesis. With this program we saved the data mentioned above in a readable format, as explained in what follows. These data were saved in fourteen different variables. The variables are named as shown in Figure 5.1.

Name ▲	Value
DURATION	*3x1 cell*
EtelFileSet	*2x7 cell*
GPS	*27512x1 cell*
GPSinLTP	*27512x1 cell*
GSMBSandRX	*27512x1 cell*
GSMSERVINGCELL	*27512x1 cell*
ID_register_wcdma	*7x15 double*
ROAMING	*27512x1 cell*
TIME	*27512x6 cell*
TNMEAS	27512
WCDMANBandRX	*27512x1 cell*
WCDMASERVINGCELL	*27512x1 cell*
WLANAPandRX	*27512x1 cell*
ref_point	[50.8487 4.3531 0]

Figure 5.1 Matlab processed data based on xml files

The information stored in these variables is:

DURATION

It is the duration of the measurements taking into account the starting time of consecutive measurement. If there is a difference of more than one minute between one value and the next one, another measurement is considered.

The next figure shows an example of this variable.

	1
1	0hour54min53sec
2	0hour26min46sec
3	6hour35min8sec

Figure 5.2 Example of the DURATION variable

EtelFileSet

It saves the names and the directories of the processed etelreader files.

	1	2
1	etelreader_20121107_182227.xml	etelreader_20121107_191606.xml
2	/Users/Jonan/Cosas/MSc Thesis/...	/Users/Jonan/Cosas/MSc Thesis/...

Figure 5.3 Example of EtelFileSet variable

GPS

This variable stores the GPS coordinates in latitude, longitude and altitude format.

An example of these values is given in Figure 5.4.

702	[50.8499 4.3509 75.5000]
703	[50.8500 4.3510 75.5000]

Figure 5.4 Example of GPS variable

GPSinLTP

These values are the GPS coordinates in local tangent plane (LTP) format.

Figure 5.5 shows an example of GPSinLTP data.

702	[-158.2460 138.4567 75.5035]
703	[-150.9217 143.5742 75.5034]

Figure 5.5 Example of GPSinLTP variable

GSMBSandRX

The GSMBSandRX variable contains the identification numbers of the GSM BSs and the received levels in dBm.

The figure below shows an example of the content of GSMBSandRX variable, where three BS were heard (indexed 44, 40 and 43) at the RSS levels -83 dBm, -64 dBm and, respectively, -67 dBm.

	1	2	3
1	44	40	43
2	-83	-64	-67

Figure 5.6 Example of GSMBSandRX variable

GSMSERVINGCELL

These numbers refers to the cell ID of the GSM BSs.

ID_register_wcdma

It is a register of all 3G Node Bs. Each column has information about a different Node B. This information contains: the mobile country code, the network ID, location area code, the cell ID, the primary scrambling code and the downlink code in FDD of each Node B.

ROAMING

It is the name of the network operator of each country, such as Elisa or Saunalahti in Finland, or Yoigo or Vodaphone in Spain, etc.

TIME

The time information is divided in six columns. The first column is the starting time, the second column is the ending time, the third column is the starting time in seconds and the fourth column is ending time in seconds. The last two columns are the subtraction of the current starting time and the previous starting time and the difference between the current starting time and the current ending time.

An example of TIME variable is shown in the next figure.

27	'12.10.2012 11.5.7.56000'	'12.10.2012 11.5.8.54000'	6.3517e+10	6.3517e+10	1	0.9800
28	'12.10.2012 11.5.9.54000'	'12.10.2012 11.5.10.49250'	6.3517e+10	6.3517e+10	1.9800	0.9525

Figure 5.7 Example of TIME variable

TNMEAS

It is the total number of measurements of all the processed etelreader files.

WCDMANBandRX

This is the identification number of 3G Node Bs and the received level of each Node B in dBm units.

An example of WCDMANBandRX is given in Figure 5.8. In this example three Node B were heard (indexed 1, 2 and 4) at the RSS levels -89 dBm, -93 dBm and -88 dBm, respectively.

	1	2	3
1	1	2	4
2	-89	-93	-88

Figure 5.8 Example of WCDMANBandRX variable

WCDMASERVINGCELL

This variable is the cell ID of the 3G Node Bs.

WLANAPandRX

The columns of WLANAPandRX variable contain the number of the WLAN AP and the received level in dBm for each AP.

Figure 5.9 gives an example of WLANAPandRX variable.

	1	2	3
1	1	2	5
2	-74	-74	-93

Figure 5.9 Example of WLANAPandRX variable

ref_point

It is the reference point for GPSinLTP variable. The reference point is the ***mean*** of all the latitudes and the ***mean*** of all the longitudes in the analyzed .xml files.

5.3 Measurement campaigns

All the data were collected in different cities and towns of Europe in 2011 and 2012. We grouped our measurements in seven different terrain types, with different characteristics. The different terrain types defined by us are:

- airport areas,
- seaside or beach areas,
- mountain or forest areas,
- suburban areas,
- densely urban areas or downtowns,
- lake areas and
- urban areas.

We will describe the measurements taken in each of these areas and we remark that this classification may not be the best possible, since there are overlapping factors in some of them (e.g., beach areas can also contain the downtown part of a small town, lake areas may be close to some residential buildings, etc.). However, for lack of better classification in the existing literature, we will adopt our own classification, described in more details in what follows.

5.3.1 Airport areas

In this type of terrain the data were taken in five different airport of Europe. The selected airports are Tampere-Pirkkala and Helsinki airports in Finland, Paris Charles de Gaulle airport in France, Munich Franz Josef Strauss airport in Germany and

Budapest Ferenc Liszt airport in Hungary. In most of the cases the measurements were collected within the terminal or in the surroundings of the airport terminal areas.

In general, airports consist in one or two buildings of few floors, surrounded by a large flat area. Most of the area is asphalt and there is no very much vegetation.

The next figure shows the location of the measurements in the airport terminal of Munich, when those measurements were taken outdoors. For the indoor measurements, we did not have any GPS or local coordinates, thus the indoor measurements were saved without a reference x,y,z coordinate and are not included in this plot.

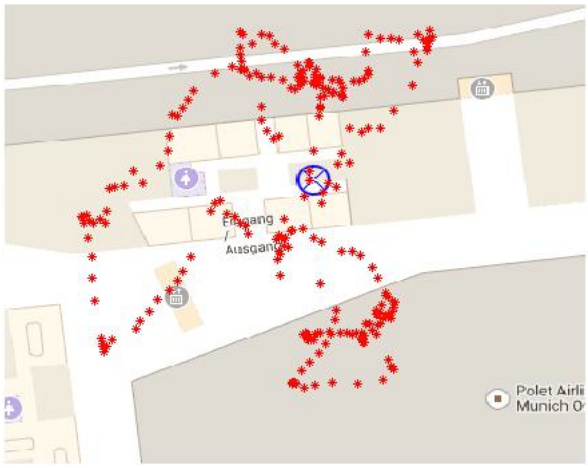

Figure 5.10 Munich airport

5.3.2 Seaside or beach areas

Another environment are seven different seaside towns. The first measurements were taken in four towns of Denmark called Sletterstrand, Skagen, Lønstrup and Fjerrislev. Other seaside towns where measurements were done are: Argeles sur mer, Cerbere and Collioure in the south-east of France and Caldes d´Estrac, Castelldefelts and Montgat in the north-east of Spain.

In most of the towns, the measurements were collected walking in the seafront, on the sandy beaches. The main characteristics of this type of terrain are small buildings on one side, a promenade in the middle and beach or sea on the other side.

Figure 5.11 shows the path of the measurements in the beach of Argeles sur mer, France.

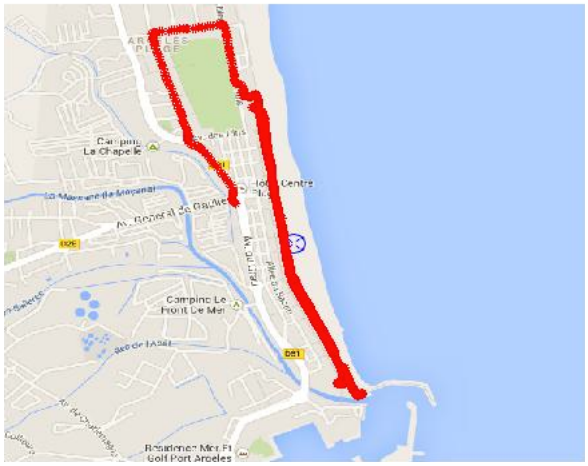

Figure 5.11 Argeles sur mer beach area

5.3.3 Mountain or forest areas

The third type of terrain is mountain or forest areas. The results of this type of terrain were collected in mountains of France near Boissiere, Palau-del-Vidre and Valmy. Other measurements were taken in forest areas and natural reservations of Spain known as Collserola, Can Coll in Cerdanyola del Vallès, Garraf and Montseny as well as a mountain area near Busteni in Romania.

In mountain or forest areas most of the surface is covered by vegetation. In this type of environment there could be lawns, trees, rivers and rocks around the pathway and there will be a few number of small buildings such as refuges and hermitages.

The next figure shows the walk in Montseny mountain area.

Figure 5.12 Montseny mountain area

5.3.4 Suburban (various areas)

We considered suburban terrain the measurements we got traveling by train in Rovaniemi and the data collected walking in Kaukajärvi in Finland. Other suburban measurements were taken in towns of France called Elne, Carcassone, Limours, the Disneyland amusement park in Paris and around the university campus of the Universitat Autònoma de Barcelona (UAB) in Spain.

A suburban area is usually a residential area around a major city. The suburban terrain is characterized by a lower building density than urban areas, a lower height of the constructions and a considerable part of the environment covered by vegetation.

Figure 5.13 shows the measurements collected in the suburban area of Tampere.

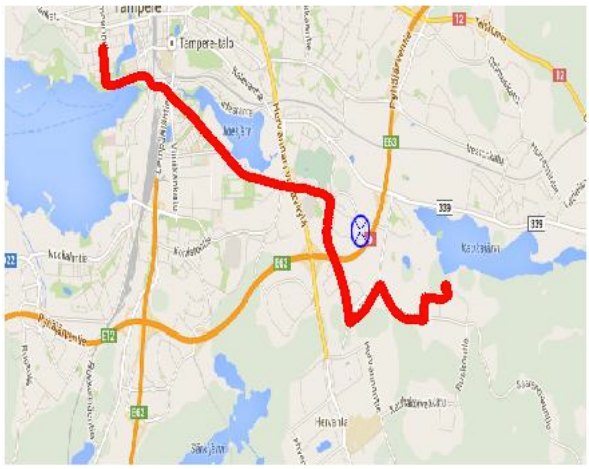

Figure 5.13 Tampere suburban area

5.3.5 Densely urban areas or downtowns

The data of urban or downtown areas were taken in some important cities of Europe such as Belgium in Brussels, Bucharest in Romania and Barcelona in Spain.

Urban area is a terrain with a high density of buildings and a low density of vegetation. Most of the area is covered by height constructions or roads and in some cases there could be some river or small parks with trees and gardens.

Figure 5.14 shows the measurements in the city centre of Brussels.

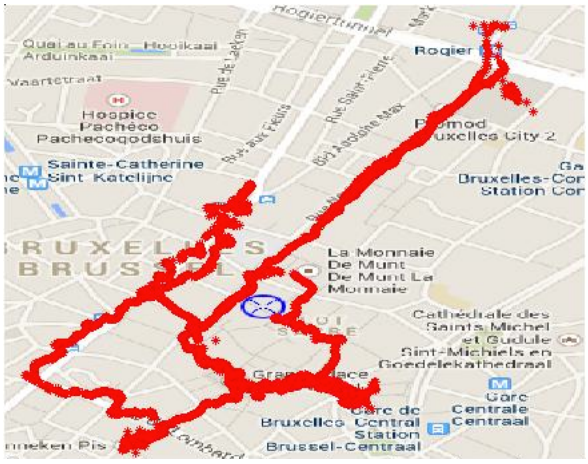

Figure 5.14 Brussels downtown

5.3.6 Lake areas

The data of lake areas were measured around the lake of Starnberg in Germany and the different lakes in Tampere, Finland.

The most important characteristic of this terrain is the lake and the edges of the lake usually surrounded by small houses or forest.

The next figure shows the measurements taken around the lakes in Tampere.

Figure 5.15 Lakes of Tampere

5.3.7 Urban various other scenarios

The measurements in urban environment were collected in the cities of Tampere in Finland, Montpellier, Narbonne and Perpignan in the south-east of France, a residential area of Bucharest in Romania and the city of Sant Cugat in the north east of Spain.

The main difference of this terrain with the densely urban terrain is that the cities are smaller.

The next figure shows the measurements of Perpignan.

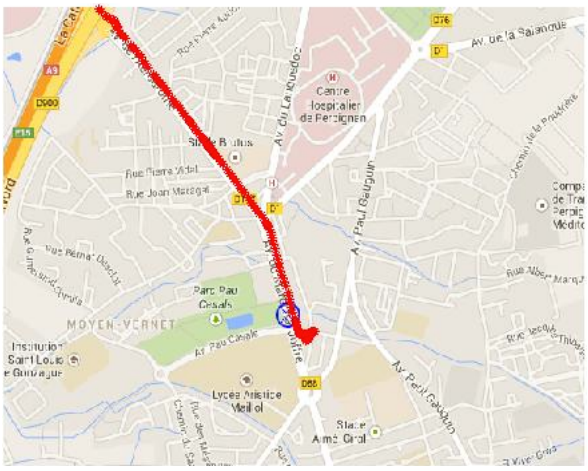

Figure 5.16 Perpignan urban area

We remark that a detailed overview of all maps and measurement points from the available data is given in Appendix A.

6. MEASUREMENT ANALYSIS AND RESULTS

This chapter focuses on the processing and analysis of the measurement data. Mainly, the RSS is the parameter of interest, but we will look also at other parameters, such as the GPS coordinates, the time duration of the measurements and the number of available or heard emitters. The emitters will be referred to as: BS (for cellular 2G), Node Bs (for cellular 3G) and AP (for WLAN), respectively. The fluctuations of RSS and other studied parameters will be presented for each studied environment. We will show that these parameters vary depending on the terrain due to the different propagation conditions of signals.

The first parameter that we will analyze is the percentage availability of GPS, 2G, 3G and WLAN signals, respectively. The availability is computed as the number of measurements where a signal of a certain type was present divided by the total number of measurements. For example, let's say that in a certain environment we took 1000 measurements and in 900 of them a GPS fix was available. Then, the GPS availability for this example will be computed as 900/1000=0.9 (factor wise) or 90% (percent wise). In the tables, the percentage notation will be used, as it is more informative. The translation into positioning performance is as follows: the higher the availability of a signal type is, the more accurate locations of the emitters and of the users are expected.

The second studied parameter is the number of emitters, namely BSs, Node Bs and APs per studied region (e.g., town, district, etc.). With a bigger amount of emitters, we will have more diversity in the received data and thus, it may be expected that more positioning accuracy could be obtained. We emphasize however that this thesis is not about studying the positioning accuracy, but rather about focusing on signal characteristics and on RSS statistics.

The third set of parameters refers to the path loss parameters: the apparent transmit power from the emitters and the path-loss slope. A single-slope path loss model (as given in section 4.2) is used and Least Square (LS) fitting is employed to compute these parameters, similar with [20].

The fourth studied parameter is the shadowing variance of the collected data. The shadowing parameter is computed based on the differences between the measurement data and a simple path-loss model fitting. We will analyze shadowing variance, because the positioning precision is likely to depend on the amount of shadowing (higher

shadowing variance, more noisy measurements, and thus less accuracy expected in the positioning results).

Afterwards, we will also use the received power values to create power maps and to predict the locations of BSs, Node Bs and APs.

Finally in the last section, we will create plots of Voronoi tesselation areas with the collected results in order to study the density of the emitters in various environments.

6.1 Percentage availability of GPS, 2G, 3G and WLAN signals

Tables 6.1, 6.2, 6.3, 6.4, 6.5, 6.6 and 6.7 show the percentage availability of the GPS, 2G, 3G and WLAN signals in seven different terrains.

6.1.1 Airport areas

The percentage availability of the different signals measured in airport areas are shown in Table 6.1.

Table 6.1 Signal percentage availability in airport areas

Scenario	Signal percentage availability [%]			
	GPS	2G	3G	WLAN
Finland, Helsinki airport	9.33	52.75	N/A	96.91
France, Paris airport	45.94	100	N/A	100
Germany, Munich airport	46.92	N/A	100	99.83
Hungary, Budapest airport	N/A	N/A	99.85	98.13
Finland, Tampere airport	96.65	100	N/A	44.42
Mean	**49.71**	**84.25**	**99.93**	**87.86**

The N/A values stand for Not Available and it means that no measurements were taken for that particular signal in that particular scenario. In our measurements, it is not possible to do simultaneous measurements on both 2G and 3G, only one network type was available at a time. In some scenarios, the measurements were repeated for both 2G and 3G, but for most cases, we only have one of the two cellular signal types. In Table 6.1 we can see that the average availability of GPS signal is low in airport areas. Nearly half of the measurements do not have information about GPS signal. This low value of availability is because most of the measurements were collected within the terminal of the different airports, indoor. With this result we could deduct that GPS signals is not much available in indoor conditions. According to Table 6.1 we could say that 2G signal is available in most of the measurements collected in airport areas. In some cases such as Paris airport and Tampere airport the 2G signal was always available. The 3G

signal was only available in Munich and Budapest airports but we could say that in these two locations the availability of this signal was 100%. Regarding WLAN signal, it was available over the 90% of the measurements except of Tampere where the availability of this signals was 44.42%. This low value of availability is due to the low number of APs within the airport terminal, as it will be shown later in Table 6.8.

6.1.2 Seaside or beach areas

Table 6.2 shows thee percentage availability of GPS, 2G, 3G and WLAN in beach areas.

Table 6.2 Signal percentage availability in beach areas

Scenario	Signal percentage availability [%]			
	GPS	2G	3G	WLAN
Denmark, Sletterstrand (sea region)	95.00	N/A	98.53	3.05
France, Argeles sur Mer, downtown	95.97	N/A	99.82	34.98
France, Cerbere sea resort	95.97	N/A	99.46	28.17
France, Collioure sea resort	97.07	N/A	97.68	27.60
Spain, Montgat beach area	100	N/A	99.77	87.33
Spain, Castelldefelts, beach area	89.51	N/A	98.31	7.62
Spain, Caldes d'Estrac, beach area	96.80	N/A	100	53.33
Mean	**95.76**	**N/A**	**99.08**	**34.58**

For this particular type of environment, no 2G measurements were done. The availability of GPS and 3G signals in beach areas were near the 100% because this terrain in most of the cases is an open area and there are not obstacles that disturb the propagation of signals. The WLAN signal availability was low because typically there are no nearby buildings to the sea regions, thus very few APs are likely to be heard. WLAN networks have a small coverage area so the availability of this signal will depend on the distance between the buildings and the beach and the distribution of the constructions around the sea.

6.1.3 Mountain or forest areas

The results for mountain and forest areas are shown in Table 6.3.

Table 6.3 Signal percentage availability in forest areas

Scenario	Signal percentage availability [%]			
	GPS	2G	3G	WLAN
France, Boissiere forest	92.50	N/A	26.78	N/A
France, forest area	95.35	N/A	99.50	0.83
France, Valmy	97.56	N/A	99.54	28.99
Romania, Busteni mountain area	96.87	N/A	98.85	9.60
Spain, Collserola (hilly/mountain area)	95.24	N/A	99.94	N/A
Spain, Can Coll hilly area	90.08	N/A	95.90	68.18

Spain, Garraf natural reservation (mountain area)	97.47	N/A	96.09	46.11
Spain, Montseny natural reservation (mountain area)	87.98	0.69	28.02	1.20
Mean	**94.13**	**0.69**	**80.58**	**25.82**

The GPS signal in this terrain was also highly available in all the different mountain locations. Despite the presence of dense forests, we are in outdoor environments, where Line Of Sight is easy to achieve. Also, on the top of the mountains, the vegetation was much reduced, thus even better clear sky conditions. The 2G signal was only measured in Montseny natural reservation and it had a very low availability, similarly in fact with 3G (whose availability was higher than for 2G, but still pretty low). This low value could be due to a very low number of BSs in the area and high distances to the closest BSs and Node Bs. The 3G signals had nearly 100% of availability in most of the locations, excepting in a French forest (Boissiere) and in a Catalunian natural reservation with high mountains (Montseny), where the availability of this types of signal was around 30%. The WLAN signal had low availability, as expected and similarly with seaside areas, for most of the locations except at Can Coll hilly area where the WLAN signal is available the 68.18% of the measurements. Can Coll hilly area is in fact surrounded by villages and there I also a nearby town, Cerdanyola del Vallès, where the measurements were starting. Thus, the highest percentage of WLAN signals can be due to the measurements done in the village and town areas.

6.1.4 Suburban (various areas)

Table 6.4 shows the results for sub-urban areas.

Table 6.4 Signal percentage availability in suburban areas

Scenario	**Signal percentage availability [%]**			
	GPS	2G	3G	WLAN
Finland, Rovaniemi (railways station area plus via train)	32.73	N/A	99.57	17.03
Finland, Kaukajärvi district	60.85	N/A	52.92	39.28
France, Elne town	74.56	N/A	99.65	100
France, Carcassone castle area	50.06	N/A	87.92	28.86
France, Disneyland park area	81.92	99.64	N/A	16.70
Spain, UAB university campus between hills	71.37	35.39	63.57	84.19
France, Limours	97.51	100	N/A	84.58
Mean	**67**	**78.34**	**80.73**	**52.95**

The availability of the GPS signal varies in each location. For example, in Rovaniemi the availability of the signal was low (32.73%), while in Limours was available the 97.51% of the measurements. The measurements from Rovaniemi were partly taken in the Rovaniemi railway station and partly inside a moving train towards south, passing through forest isolated areas. The 2G signal was highly available in all the locations,

with the exception of the UAB campus, which is located around 30 Km north from Barcelona and within forests and hills. In there, the availability was only 35.39% of the measurements. The 3G signal was highly available in Rovaniemi, Elne, and Carcassone, but in Kaukajärvi and UAB the availability was lower. The WLAN signal availability varies depending on the location. When we have low WLAN percentage, it is typically an indicator that most of the measurements were taken outdoors, where WLAN APs were weakly heard or not heard at all. There are however exceptions, such as in Elne town, where WLAN availability as 100%, despite the fact that most measurements were taken outdoor in there.

These variations of the data are due to the different characteristics of the suburban terrains where the measurements were collected. Some terrains are similar to an urban area unlike other terrains are more comparable with a rural area. Basically, for suburban areas we see that it is more difficult to draw unified conclusions.

6.1.5 Densely urban areas or downtowns

The results for densely urban areas are shown in Table 6.5.

Table 6.5 Signal percentage availability in densely urban areas

Scenario	Signal percentage availability [%]			
	GPS	2G	3G	WLAN
Belgium, Brussels	17.34	N/A	42.57	92.28
Germany, Munich downtown	63.52	N/A	99.71	76.02
Romania, Bucharest downtown	65.50	57.07	42.39	83.91
Spain, Barcelona downtown	74.31	0.36	92.00	82.99
Mean	**55.17**	**28.72**	**69.17**	**83.80**

The availability of the GPS signal was rather low in the four cities especially in Brussels (17.34%). This occurs due to the height and density of buildings which shadow the receiver. The 2G signal is available the 57.07% of the measurements of Bucharest downtown and only the 0.36% of the measurements of Barcelona. The 3G signal was received around the 42% of the measurements in Brussels and Bucharest and more than the 90% in Munich and Barcelona downtowns. These differences in 3G signal availability between the cities could be due to the deployment of 3G networks by the network operators of each county. The density of the 3G emitters (Node Bs) is later shown in Section 6.7. The availability of the WLAN signals is high in the four downtowns because all the terrain is built-up and there we will find a lot of APs.

6.1.6 Lake areas

The results for lake area cases are shown in Table 6.6.

Table 6.6 Signal percentage availability in lake areas

Scenario	Signal percentage availability [%]			
	GPS	2G	3G	WLAN
Finland, Tampere around a lake	98.62	75.76	24.01	6.15
Germany, Starnberg lake area	91.03	N/A	98.83	8.01
Mean	**94.83**	**75.76**	**61.42**	**7.08**

In lake areas the GPS signal was available most of the measurements. Again, this is expected, as we are in outdoor and clear sky conditions. The 2G signal was available only in Tampere, with a percentage of 75.76%. The availability of 3G signal was low for measurements in Tampere (24.01%) and high for Starnberg lake area (98.83%). This difference in the 3G signals is due to the number of Node Bs in the lake area or due to the low deployment of 3G networks. The availability of WLAN signal was extremely small for both Tampere and Starnberg lakes. The reason of this low availability is the small number of buildings surrounding the lakes.

6.1.7 Urban various other scenarios

The results for other urban cases (than those already shown in Section 6.1.5) are shown in Table 6.7.

Table 6.7 Signal percentage availability in urban areas

Scenario	Signal percentage availability [%]			
	GPS	2G	3G	WLAN
Finland, Tampere	81.25	36.68	47.78	76.49
France, Montpellier	63.02	N/A	96.57	84.06
France, Narbonne	80.04	N/A	89.24	83.24
France, Perpignan	33.38	N/A	99.93	93.29
Romania, Bucharest residential area	60.91	85.65	13.05	67.66
Spain, Sant Cugat	64.00	99.98	N/A	55.50
Mean	**63.77**	**74.10**	**69.31**	**76.71**

The percentage availability of GPS signals varies from 33% of the measurements in Perpignan to 81.25% of the measurements in Tampere. This will depend on the building and vegetation density of each location. The percentage availability of 2G signal was high in Bucharest residential areas (85.65%) or Sant Cugat (99.98%) and low in Tampere. Regarding 3G signal, it was highly available in Perpignan with 99.93% of availability but it had very low availability in Bucharest (13.05%). The availability of WLAN signal was high in Perpignan (93.29%) but in towns such as Sant Cugat (55.50%) the WLAN signal only was available nearly on half of the measurements

These big differences between cities are due to the various deployments of the 2G, 3G and WLAN networks in each city and the followed path where the measurements were done.

6.1.8 Comparison between the different terrains

As seen so far, the terrains where the GPS the terrains where the GPS signal was most available were beach areas (95.76%), forest areas (94.13%) and lake areas (94.83%), which are clear sky areas. The common characteristic of these three terrains is that in all of them the receiver is moving in an open area where there are no thick obstacles that could disturb the propagation of signal. In the rest of environments, the GPS signal was less available than in the previous terrains due to the higher density of buildings. The terrain with the lowest GPS signal availability was airport areas because most of the measurements were collected within the airport terminals, indoors.

The terrains where the 2G signal was most available were airport areas (84.25%), suburban areas (75.34%), lake areas (75.76%) and urban areas (74.10%). On the other hand, the terrains with lowest availability of 2G signal were densely urban areas (28.72%) and forest areas (0.69%). These values will depend on the number of BSs in the terrain and the propagation conditions.

The 3G signal is highly available in all the terrains. The minimum value of 3G signal availability was found in densely urban areas (69.17%) and the maximum was in airport areas (99.93%). The followed path and the number of measurements during the saving of data is critical to compare the different terrains. In our measurements in the airport areas the receiver was moving in a small area while in other terrains the receiver was moving along big distances.

The highest WLAN signal availability was in densely urban areas (83.80%) and airport areas (87.86%) and the lowest WLAN signal availability was in lake areas (7.08%). This is as expected, because in densely urban areas we will find many APs while in lake areas, as in forest or beach areas, the number of APs is much smaller, since the nearby buildings are typically at distances higher than the coverage areas of an AP. In the rest of the terrains, the availability varies according to the terrain where the measurements were collected.

6.2 Number of emitters per region and per system

Tables 6.8, 6.9, 6.10, 6.11, 6.12, 6.13 and 6.14 show the number of measurements done for each signal type and the number of heard BSs, Node Bs and APs in each region. We also show the average of the number of emitters for each terrain to do a comparison between the different environments.

6.2.1 Airport areas

The results for airport areas are shown in Table 6.8. We remark that in some cases, we have a higher number of measurements for WLAN than for the cellular data; this is due to the fact that in indoor cases, the collection of 2G and 3G data was sometimes disactivated, and we only focused on WLAN data collection. In other cases, such as Tampere airport, the reverse was true: 2G data was collected, but no WLAN was heard. The number of measurements count only the situations where at least one transmitter was heard.

Table 6.8 Number of heard BS, Node Bs and APs per region in airport areas

Scenario	Number of heard BS, Node Bs and APs per region					
	2G		3G		WLAN	
	No. of meas.	Nr BSs	No. of meas.	Nr Node Bs	No. of meas.	Nr APs
Finland, Helsinki airport	3239	31	0	N/A	5950	341
France, Paris airport	1798	60	0	N/A	1798	84
Germany, Munich airport	0	N/A	584	2	583	84
Hungary, Budapest airport	0	N/A	5297	6	5206	85
Finland, Tampere airport	538	24	0	N/A	239	10
Mean of heard emitters	**38**		**4**		**120**	

In Table 6.8 we see that the number of heard emitters is rather low for 3G signals (2 to 6), moderate for 2G signals (24 to 60) and rather large for WLAN signals (10 to 341). The number of emitters also depend on the area where the measurements were done and on the number of measurements,

6.2.2 Seaside or beach areas

The results for beach areas are shown in Table 6.9.

Table 6.9 Number of heard BSs, Node Bs and APs per region in beach areas

Scenario	Number of heard BS, Node Bs and APs per region					
	2G		3G		WLAN	
	No. of meas.	Nr BSs	No. of meas.	Nr Node Bs	No. of meas.	Nr APs
Denmark, Sletterstrand (sea region)	0	N/A	32216	22	996	20
France, Argeles sur Mer, downtown	0	N/A	4380	5	1535	89
France, Cerbere sea resort	0	N/A	7597	2	2152	84
France, Collioure sea resort	0	N/A	8740	10	2470	183
Spain, Montgat beach area	0	N/A	4253	12	3723	304

Spain, Castelldefelts, beach area	0	N/A	3018	6	234	17
Spain, Caldes d'Estrac, beach area	0	N/A	3660	1	1952	32
Mean of heard emitters	**N/A**		**8**		**104**	

The maximum number of Node Bs found in beach areas were in Sletterstrand (22) and the minimum in Caldes d´Estrac (1). We remark that the number of measurements done in Sletterstrand (32216) is much bigger than in the other towns. Montgat and Collioure beach areas are the locations with the highest number of heard APs with 304 and 183, respectively. Casteldefelts is the town with lowest number of heard APs. The average number of heard APs is comparable with the case of airport areas.

6.2.3 Mountain or forest areas

The results for mountain areas are shown in Table 6.10.

Table 6.10 Number of heard BSs, Node Bs and APs per region in forest areas

Scenario	**Number of heard BS, Node Bs and APs per region**					
	2G		3G		WLAN	
	No. of meas.	Nr BSs	No. of meas.	Nr Node Bs	No. of meas.	Nr APs
France, Boissiere forest	0	N/A	900	4	0	N/A
France, forest area	0	N/A	8345	3	70	1
France, Valmy	0	N/A	5875	6	1711	12
Romania, Busteni mountain area	0	N/A	8978	6	872	26
Spain, Collserola (hilly/mountain area)	0	N/A	12847	3	0	N/A
Spain, Can Coll hilly area	0	N/A	2224	19	1581	229
Spain, Garraf natural reservation (mountain area)	0	N/A	2851	15	1368	113
Spain, Montseny natural reservation (mountain area)	192	46	7829	55	336	64
Mean of heard emitters	**46**		**13**		**74**	

The only location where 2G BSs were measured was Montseny natural reservation where there were 46 BSs heard in total. The maximum number of Node Bs corresponded to Montseny with a total number of 55. In the rest of the locations the number of heard Node Bs was much more smaller, e.g. only 3 in Collserola mountain area. The highest number of heard WLAN APs was found in Can Coll hilly area and in the Garraf natural reservation with a number of 229 and 113 APs respectively. On the other hand the forest area near Palau-del-Vidre there was just 1 AP detected. The big values of Can Coll hilly area and Garraf natural reservation are because part of the measurements were collected in urban area (as can be seen in Figure A.17 and Figure

A18) The number of WLAN emitters is typically lower in these areas than for airport and seaside areas.

6.2.4 Suburban (various areas)

The Number of heard BSs, Node Bs and APs per region in suburban areas are shown in the Table 6.11.

Table 6.11 Number of heard BSs, Node Bs and APs per region in suburban areas

Scenario	Number of heard BS, Node Bs and APs per region					
	2G		3G		WLAN	
	No. of meas.	Nr BSs	No. of meas.	Nr Node Bs	No. of meas.	Nr APs
Finland, Rovaniemi (railways station area plus via train)	0	N/A	29773	130	5093	261
Finland, Kaukajärvi district	0	N/A	3694	22	2742	5
France, Elne town	0	N/A	2248	4	2256	325
France, Carcassone castle area	0	N/A	5861	15	1924	106
France, Disneyland park area	15818	63	0	N/A	2651	202
Spain, UAB university campus between hills	39335	98	70663	66	93540	1482
France, Limours town	8668	61	0	N/A	7331	297
Mean of heard emitters	**74**		**47**		**382**	

In suburban areas the receiver heard 63 BSs in Disneyland park area, 98 BSs in Barcelona university campus and 61 BSs in Limours. The maximum number of detected Node Bs was in Rovaniemi (130) and the minimum in Elne (4). In Rovaniemi case, parts of the measurements where taken in a train of speed above 80km/h, meaning that the measurement area was much larger than in the other studied cases. The number of heard Node Bs will depend on the covered area during the measurements and on the deployment of 3G networks in each town. Regarding the WLAN data, the location where more APs were heard was Barcelona university campus with 1482 APs and the location the lowest number of heard APs was Kaukajärvi with only 5 APs. In most of the cases, the more office buildings there are present around, the more APs are detected.

6.2.5 Densely urban areas or downtowns

Table 6.12 shows the results for densely urban areas.

Table 6.12 Number of heard BSs, Node Bs and APs per region in densely urban areas

Scenario	Number of heard BS, Node Bs and APs per region					
	2G		3G		WLAN	
	No. of meas.	Nr BSs	No. of meas.	Nr Node Bs	No. of meas.	Nr APs
Belgium, Brussels	0	N/A	11711	15	25388	2377
Germany, Munich downtown	0	N/A	28870	63	39179	2374
Romania, Bucharest downtown	28030	47	20820	56	41210	5335
Spain, Barcelona downtown	449	62	115258	539	118427	24433
Mean of heard emitters	**54**		**168**		**8629**	

In these large cities of Europe we found 47 BSs in Bucharest and 62 BSs in Barcelona. The minimum number of heard Node Bs was in Brussels with only 15 Node Bs and the maximum was is Barcelona with 539 Node Bs. Indeed, it appears that Barcelona has a much better 3G coverage than 2G coverage. In Munich and Bucharest downtowns the number of detected Node Bs was around 60. Observe that the number of Node B is significantly higher in Barcelona than in the rest of the cities but also the number of measurements. Barcelona was the city with highest number of heard WLAN APs with 24433 APs. In other cities such as Munich or Bucharest the number of APs were 2374 and 5335, respectively. The reason of this big difference between Barcelona and the other cities is the covered area during the measurements and the number of measurements performed within that area.

6.2.6 Lake areas

The results for lake areas are shown in Table 6.13.

Table 6.13 Number of heard BSs, Node Bs and APs per region in lake areas

Scenario	Number of heard BS, Node Bs and APs per region					
	2G		3G		WLAN	
	No. of meas.	Nr BSs	No. of meas.	Nr Node Bs	No. of meas.	Nr APs
Finland, Tampere around a lake	5270	39	1670	24	428	71
Germany, Starnberg, lake area	0	N/A	22240	40	1802	96
Mean of heard emitters	**39**		**32**		**83**	

The 2G signal was only measured in Tampere and there were 39 BSs detected. Regarding the 3G signal, the number of heard Node Bs were 24 in Tampere and 40 in Starnberg. This difference in Node Bs could be due to the number of measurements collected in each town during the measurement. The number of APs of these two cities

was 71 for Tampere and 96 for Starnberg. The number of APs will depend on the distance between the town and the lake. In Starnberg the town is close to the lake while in Tampere the lake is farther from the urban area.

6.2.7 Urban various other scenarios

Table 6.14 shows the Number of heard BSs, Node Bs and APs per region in urban areas.

Table 6.14 Number of heard BSs, Node Bs and APs per region in urban areas

Scenario	Number of heard BS, Node Bs and APs per region					
	2G		3G		WLAN	
	No. of meas.	Nr BSs	No. of meas.	Nr Node Bs	No. of meas.	Nr APs
Finland, Tampere	79801	50	103941	529	166385	15190
France, Montpellier	0	N/A	12304	70	10710	3159
France, Narbonne	0	N/A	5800	19	5410	1627
France, Perpignan	0	N/A	2994	5	2795	204
Romania, Bucharest residential area	193853	62	29532	73	153129	8013
Spain, Sant Cugat	5772	63	0	N/A	3204	626
Mean of heard emitters	**58**		**139**		**4803**	

Among these six cities of urban environment the number of heard BS was rather constant around 60. The city with highest number of Node Bs was Tampere with 529 emitters. Interesting enough, the number of cellular emitters in Tampere is comparable with the number of cellular emitters in Barcelona downtown (Table 6.12). In the other urban areas there are two cities (Montpellier and Bucharest) which had around 70 Node Bs and cities such as Perpignan that had only 5 Node Bs. The two cities with higher amount of WLAN APs were Tampere (15190) and Bucharest residential areas (8013) whereas the location with lowest number of APs was Perpignan (204). Notice that the number of measurements of Tampere and Bucharest are much more higher than the rest of the towns so we can assume that the covered area during the measurements in these cities was wider than in the other towns.

6.2.8 Comparison between the different terrains

In general the terrains with more 2G, 3G and WLAN emitters are suburban, densely urban and urban areas.

The terrains with the highest number of 2G BSs are, as expected, suburban (74 emitters on average), densely urban (54 emitters on average) and urban areas (58 emitters on average). On the other side, the lowest number of BSs was found in mountain (46

emitters on average) and lake areas (39 emitters on average). The reason of those values is that the mountain and lake areas are typically far from cellular emitters, and the user cannot connect to the network unless the network operator installs more BSs.

The amount of 3G Node Bs is also related to the population or the buildings of a certain area. In terrains such as suburban (47 emitters on average), downtowns (168 emitters on average) or urban (139 emitters on average) the number of Node Bs was higher than rural terrains such as mountain or forest areas (13 emitters on average). This could be due to the shadowing of the 3G signal or the number of users within an area. In rural environment the coverage area is bigger so a lower number of Node Bs will be needed.
The terrains with more WLAN APs are the densely urban and the urban areas with more than 4000 APs. In these environments the number of constructions where we could find an AP is high, while in mountain or lake areas the number of buildings and APs is small.

6.3 Average and standard deviation of transmit power

In this section we will analyze the average and the standard deviation (Std) of the received signal strength from the BS, Node Bs and APs in the different terrains. In order to estimate the parameters of the one-slope path loss model adopted here, namely the apparent transmit power (referred to as 'transmit power in what follows) and the path-loss coefficient or slope, we adopted the following procedure: for each transmitter, the set of available measurements were mapped according to their distance to the estimated transmitter location, as seen in Figure 6.1. The estimation of the transmitter location is done via the weighted centroid approach [15]. The LS curve fitting is done, as shown in the red continuous line of Figure 6.1 and the slope and intersection of this curve with the vertical axis are computed. This will give us the path-loss slope and the apparent transmit power parameters.

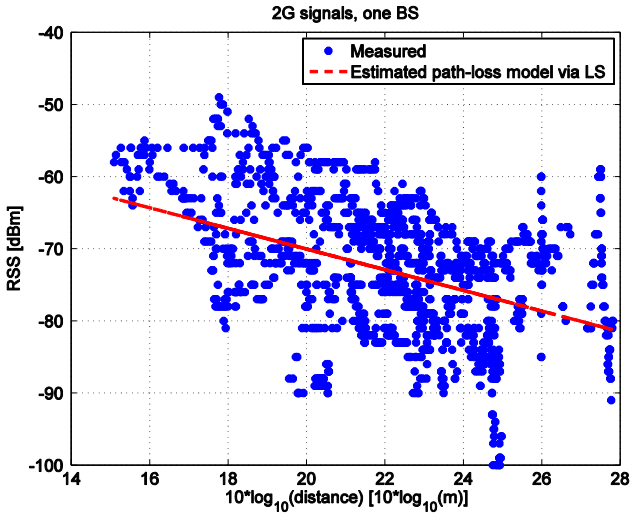

Figure 6.1 Example of path-loss parameter estimation

Figure 6.2 shows histograms of the apparent transmit power and the path loss coefficient of 2G signal.

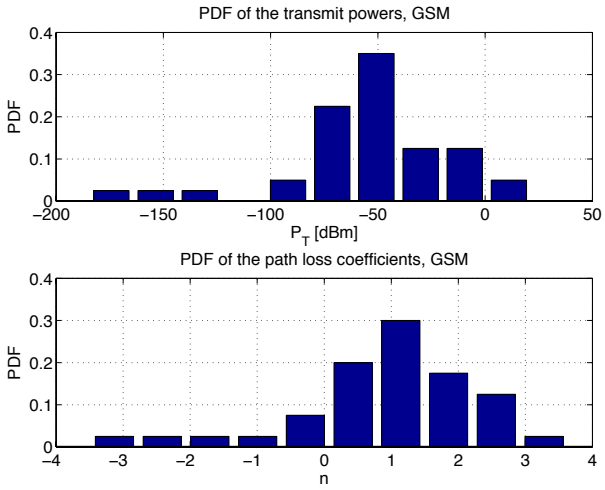

Figure 6.2 Histograms of the apparent transmit power and the path loss coefficient

6.3.1 Airport areas

The estimated transmit powers for airport areas are shown in Table 6.15.

Table 6.15 Average and standard deviation of transmit power in airport areas

Scenario	**Average transmit power [dBm]**			**Std of the transmit power [dB]**		
	2G	3G	WLAN	2G	3G	WLAN
Finland, Helsinki airport	-83.62	N/A	-79.18	17.91	N/A	12.30
France, Paris airport	-68.21	N/A	-75.80	4.66	N/A	12.62
Germany, Munich airport	N/A	-60.20	-76.90	N/A	3.76	8.20
Hungary, Budapest airport	N/A	-56.06	-82.12	N/A	9.37	12.81
Finland, Tampere airport	-83.32	N/A	-75.43	8.82	N/A	10.56
Mean	**-78.38**	**-58.13**	**-77.89**	**10.46**	**6.57**	**11.30**

In Table 6.15 we can see that the highest average transmit power of the 2G signal was measured in Paris airport (-68.21 dBm). In the rest of the airports the average transmit powers were lower than in Paris airport (-83.72 dBm and -83.32 dBm). Regarding 3G signal, the average transmit power was higher than in 2G signal with a value of around -58.13 dBm. The WLAN signal average transmit powers were between -82.12 dBm and -75.43 dBm and the average for all the airports was -77.89 dBm. The highest standard deviation of transmit power of 2G signals was measured in Helsinki airport (17.91 dB) while the minimum was measured in Paris airport (4.66 dB). The standard deviation of the transmit power of 3G signal were 3.76 dB and 9.37 dB in Munich and Bucharest

airport, respectively. The standard deviation of the WLAN transmit power was higher than in cellular signals and it had a value of around 11.30 dB.

Looking to all these values we could say that Helsinki airport had the worse cellular signal because it had the lowest average transmit power and the highest standard deviation. This means that sometime the transmit power will be below the minimum reception level of the receiver. Regarding WLAN signal the worse airport is Bucharest airport because it had an average of transmit power of -82.12 dBm and a standard deviation of 12.81 dB.

6.3.2 Seaside or beach areas

The averages and standard deviations of transmit power in beach areas is shown in Table 6.16.

Table 6.16 Average and standard deviation of transmit power in beach areas

Scenario	**Average transmit power [dBm]**			**Std of the transmit power [dB]**		
	2G	3G	WLAN	2G	3G	WLAN
Denmark, Sletterstrand (sea region)	N/A	-86.54	-87.73	N/A	11.16	9.56
France, Argeles sur Mer, downtown	N/A	-75.04	-92.96	N/A	10.93	5.66
France, Cerbere sea resort	N/A	-65.61	-90.83	N/A	7.76	6.43
France, Collioure sea resort	N/A	-85.48	-89.97	N/A	11.28	6.88
Spain, Montgat beach area	N/A	-82.39	-93.75	N/A	13.50	4.92
Spain, Castelldefelts, beach area	N/A	-86.68	-87.80	N/A	14.78	9.51
Spain, Caldes d'Estrac, beach area	N/A	-57.59	-94.08	N/A	9.93	5.22
Mean	**N/A**	**-77.05**	**-91.02**	**N/A**	**11.33**	**6.88**

In the analyzed seaside regions there was not any 2G signal available. Among all the 3G signals of beach towns the best average transmit power was found in Caldes d´Estrac beach area (-57.59 dBm). In the rest of the locations the average transmit signal was below -80.dBm excepting Cerbere sea resort where the average transmit power was -65.61 dBm. The WLAN signals had an average transmit power lower than the cellular signals and an average of -91.02 dBm. The standard deviation transmited 3G signal was between 7.76 dB and 14.78 dB. In this terrain the WLAN signal had a lower standard deviation than cellular signals with an average of 6.88 dB.

6.3.3 Mountain or forest areas

The results for forest areas are shown in Table 6.17.

Table 6.17 Average and standard deviation of transmit power in forest areas

Scenario	Average transmit power [dBm]			Std of the transmit power [dB]		
	2G	3G	WLAN	2G	3G	WLAN
France, Boissiere forest	N/A	-102.62	N/A	N/A	7.21	N/A
France, forest area	N/A	-95.58	-95.76	N/A	6.00	3.41
France, Valmy	N/A	-91.00	-92.64	N/A	7.29	6.41
Romania, Busteni mountain area	N/A	-93.63	-86.19	N/A	10.90	9.59
Spain, Collserola (hilly/mountain area)	N/A	-81.85	N/A	N/A	12.00	N/A
Spain, Can Coll hilly area	N/A	-97.43	-91.56	N/A	9.29	7.18
Spain, Garraf natural reservation (mountain area)	N/A	-85.54	-93.82	N/A	14.86	4.68
Spain, Montseny natural reservation (mountain area)	-66.52	-89.37	N/A	5.95	11.54	N/A
Mean	**-66.52**	**-92.94**	**-91.99**	**5.95**	**9.65**	**6.25**

In this terrain the 2G signal was only measured in Montseny mountain area and it had an average transmit power of -66.52 dBm and a standard deviation of 5.95 dB. The lowest average transmit power of 3G signal was measured in Boissiere forest area (-102.62 dBm) and the highest average transmit power in Collserola mountain area (-81.85 dBm). The standard deviation of this type of signal had an average of 9.65 dB. Regarding the WLAN signal, the values of the average transmit powers were similar to 3G signal but they had lower standard deviation (6.25 dB).

6.3.4 Suburban (various areas)

Table 6.18 shows the results of suburban areas.

Table 6.18 Average and standard deviation of transmit power in suburban areas

Scenario	Average transmit power [dBm]			Std of the transmit power [dB]		
	2G	3G	WLAN	2G	3G	WLAN
Finland, Rovaniemi (railways station area plus via train)	N/A	-89.95	-88.64	N/A	19.68	9.49
Finland, Kaukajärvi district	N/A	-70.39	-83.15	N/A	10.84	18.37
France, Elne town	N/A	-83.22	-85.82	N/A	14.57	10.17
France, Carcassone castle area	N/A	-91.49	-88.20	N/A	11.04	8.22
France, Disneyland park area	-82.20	N/A	-88.26	11.10	N/A	9.21
Spain, UAB university campus between hills	-84.83	-91.34	-89.76	10.89	13.20	6.79
France, Limours town	-88.56	N/A	-79.81	9.21	N/A	12.25
Mean	**-85.20**	**-85.28**	**-86.23**	**10.4**	**13.87**	**10.64**

The 2G signal in suburban areas was measured in Disneyland park area, UAB university campus and Limours town where it had an average transmit power of -82.20

dBm, -84.83 dBm and -88.20 dBm, respectively. The standard deviation in these suburban areas had an average of 10.4 dB. The average transmit power of 3G signals had an average of -85.28 dBm and 13.87 dB standard deviation. Notice that the standard deviations of transmit powers was higher in suburban areas than in beach and mountain areas. The WLAN average transmit powers had a similar value to cellular signals and a standard deviation around 10.64 dB.

6.3.5 Densely urban areas or downtowns

The results measured in densely urban areas are shown in Table 6.19.

Table 6.19 Average and standard deviation of transmit power in downtowns

Scenario	Average transmit power [dBm]			Std of the transmit power [dB]		
	2G	3G	WLAN	2G	3G	WLAN
Belgium, Brussels	N/A	-87.94	-84.55	N/A	16.04	9.90
Germany, Munich downtown	N/A	-50.42	-86.93	N/A	29.33	6.24
Romania, Bucharest downtown	-76.01	-74.04	-85.12	13.08	11.89	8.88
Spain, Barcelona downtown	-71.51	-49.69	N/A	12.51	41.68	N/A
Mean	**-73.76**	**-65.52**	**-85.53**	**12.80**	**24.74**	**8.34**

The cellular signal had higher average transmit power than the previous terrains with values of -73.76 dBm for 2G signal and -65.52 dBm for 3G signal. The WLAN signal had an average transmit power similar to the suburban areas signal but the standard deviation in this terrain is 2 dB smaller. The most interesting data of densely urban areas is that the standard deviation of transmit power in downtowns is even higher than in suburban terrain. This occurs due to the higher density of buildings and greater height.

6.3.6 Lake areas

Table 6.20 shows the results measured in lake areas.

Table 6.20 Average and standard deviation of transmit power in lake areas

Scenario	Average transmit power [dBm]			Std of the transmit power [dB]		
	2G	3G	WLAN	2G	3G	WLAN
Finland, Tampere around a lake	-90.27	-92.35	-87.70	9.77	13.35	10.13
Germany, Starnberg, lake area	N/A	-90.66	-86.90	N/A	12.55	9.67
Mean	**-90.27**	**-91.51**	**-87.3**	**9.77**	**12.95**	**9.9**

2G signal was only measured in Tampere lake area and it had an average transmit power of -90.27 dBm and 9.77 dB standard deviation. Regarding 3G signal, the average transmit power in lake areas was around -91.51 dBm and it had a standard deviation of

12.95 dB. On the other side, the WLAN signal, had an average transmit power of -87.3 dBm and 9.9 dB standard deviation. Observe that the average transmit power of cellular signals was the lowest transmit power of all the analyzed terrains and the WLAN signal had one of the lowest one.

6.3.7 Urban various other scenarios

The results of urban areas are shown in Table 6.21.

Table 6.21 Average and standard deviation of transmit power in urban areas

Scenario	Average transmit power [dBm]			Std of the transmit power [dB]		
	2G	3G	WLAN	2G	3G	WLAN
Finland, Tampere	-41.46	-44.26	-86.47	34.73	28.41	8.99
France, Montpellier	N/A	-48.66	-84.68	N/A	31.42	16.95
France, Narbonne	N/A	-59.66	-82.69	N/A	29.91	7.37
France, Perpignan	N/A	-78.22	-102.58	N/A	14.74	13.15
Romania, Bucharest residential area	-44.88	-52.11	-82.40	44.41	33.29	20.57
Spain, Sant Cugat	-53.57	N/A	-83.78	25.14	N/A	4.75
Mean	**-46.64**	**-56.58**	**-87.1**	**34.76**	**27.55**	**11.96**

In the Table 6.21 we can observe that urban terrains had the highest 2G and 3G average transmit powers of all the terrains with values around -46.64 dBm for 2G signal and -56.58 dBm for 3G signal. The WLAN signal had similar average transmit power as the analyzed metropolitan areas but the main characteristic of this terrain is that the standard deviation of transmit powers is the highest one of all the terrains. These high values are due to the buildings and objects that we could find in an urban area.

6.3.8 Comparison between the different terrains

As we saw in the previous subsections the highest average of transmit power were in densely urban and urban area. The main disadvantage of these terrains is that the transmit powers suffer a high standard deviation due to the buildings and obstacles within the urban environment.

On the other hand, the beach, mountain and lake areas had low average transmit power but small standard deviation.

Airport areas had great average transmit power but the signals are affected due to the multipath propagation of the indoor condition.

6.4 Average and standard deviation of path-loss coefficient

Tables 6.22, 6.23, 6.24, 6.25, 6.26, 6.27 and 6.28 show the average and standard deviation of the path loss coefficient or slope obtained from the LS fitting of a path-loss model to the data, as explained in Section 6.3.

Figures 6.3 show an example of how the path loss modeling was done via LS curve fitting for WLAN signal.

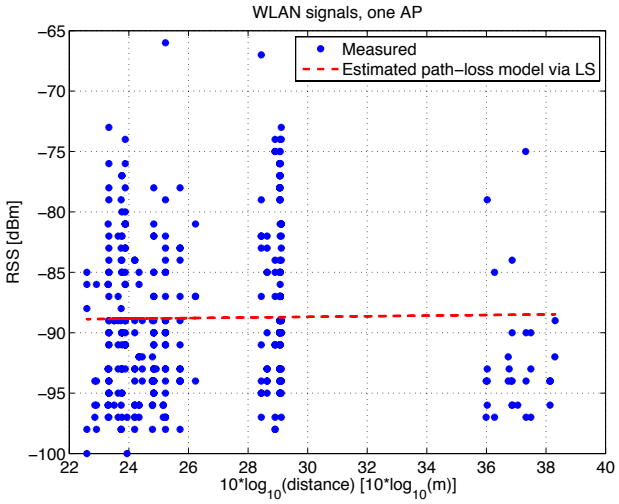

Figure 6.3 Estimated path-loss model via LS for WLAN signal

We observe that in WLAN signal the values are lower and flatter than in 2G signal (Figure 6.1) producing a path-loss coefficient close to 0.

6.4.1 Airport areas

The average and standard deviation of path los coefficients in airport areas are shown in Table 6.22.

Table 6.22 Average and standard deviation of path loss coefficients in airport areas

Scenario	**Average path loss coefficient**			**Std of the path loss coefficient**		
	2G	3G	WLAN	2G	3G	WLAN
Finland, Helsinki airport	0.62	N/A	0.08	0.96	N/A	0.35
France, Paris airport	-0.07	N/A	0.01	0.09	N/A	0.50
Germany, Munich airport	N/A	0.31	1.18	N/A	0.54	3.19
Hungary, Budapest airport	N/A	N/A	N/A	N/A	N/A	N/A
Finland, Tampere airport	0.8	N/A	-0.03	0.51	N/A	0.02
Mean	**0.45**	**0.31**	**0.31**	**0.52**	**0.54**	**1.02**

The average path loss coefficient of 2G signal had values between -0.07 and 0.8 and a standard deviation between 0.09 and 0.96. A negative or close to zero value means in fact that the data was so noisy, that no particular trend with the distance could be noticed, and that the LS fit showed no fluctuation with the distance. In order to get more accurate results, the outliers should be first identified and removed. This analysis was not done, due to the lack of time. 3G signal was only measured in Munich airport and it had an average path loss coefficient of 0.31 and 0.54 standard deviation. The WLAN signal in all the airport areas had an average path loss coefficient of 0.31 and 1.02 standard deviation.

6.4.2 Seaside or beach areas

The results for beach areas are shown in Table 6.23.

Table 6.23 Average and standard deviation of path loss coefficients in beach areas

Scenario	**Average path loss coefficient**			**Std of the path loss coefficient**		
	2G	3G	WLAN	2G	3G	WLAN
Denmark, Sletterstrand (sea region)	N/A	0.72	0.91	N/A	0.88	1.77
France, Argeles sur Mer, downtown	N/A	1.89	0.69	N/A	1.16	2.68
France, Cerbere sea resort	N/A	1.62	0.02	N/A	0.70	0.39
France, Collioure sea resort	N/A	1.03	0.32	N/A	0.73	0.53
Spain, Montgat beach area	N/A	0.69	0.19	N/A	0.99	0.30
Spain, Castelldefelts, beach area	N/A	-2.11	0.76	N/A	1.48	0.60
Spain, Caldes d'Estrac, beach area	N/A	N/A	0.17	N/A	0	0.49
Mean	**N/A**	**0.64**	**0.44**	**N/A**	**0.85**	**0.97**

As can be seen in Table 2.23 there was not 2G signal in beach areas so the average and standard deviation of path loss coefficient could not be calculated. The 3G signal had average path loss coefficient values from -2.11 to 1.89 and an average standard deviation of 0.85. Regarding the WLAN signal, the mean of all the average transmit powers measured in airport areas was 0.44 and its standard deviation 0.97.

6.4.3 Mountain or forest areas

Table 6.24 shows the results that we got in forest areas.

Table 6.24 Average and standard deviation of path loss coefficients in forest areas

Scenario	Average path loss coefficient			Std of the path loss coefficient		
	2G	3G	WLAN	2G	3G	WLAN
France, Boissiere forest	N/A	0.60	0.17	N/A	0	N/A
France, forest area	N/A	0.46	N/A	N/A	0.22	N/A
France, Valmy	N/A	0.07	0.48	N/A	0.93	0.43
Romania, Busteni mountain area	N/A	1.21	0.23	N/A	2.19	0.46
Spain, Collserola (hilly/mountain area)	N/A	2.74	N/A	N/A	0.32	N/A
Spain, Can Coll hilly area	N/A	1.88	0.32	N/A	1.83	0.62
Spain, Garraf natural reservation (mountain area)	N/A	0.96	0.12	N/A	0.61	0.28
Spain, Montseny natural reservation (mountain area)	0.63	0.72	N/A	0.36	0.41	N/A
Mean	**0.63**	**1.08**	**0.26**	**0.36**	**0.81**	**0.45**

Table 6.24 shows that the only measurement of average path loss coefficient of 2G signal was in Montseny mountain areas. This data had an average path loss of 0.63 and 0.36 standard deviation. The 3G signal was measured in all the mountain locations and the average path loss coefficient of all of them was 1.08 and its standard deviation 0.81. The WLAN measurement had a lower average path loss coefficient of 0.26 and a standard deviation of 0.45. These small values average path loss coefficient in WLAN could be due to the indoor propagation condition.

6.4.4 Suburban (various areas)

The results of suburban terrain are collected in Table 6.25.

Table 6.25 Average and standard deviation of path loss coefficients in suburban areas

Scenario	Average path loss coefficient			Std of the path loss coefficient		
	2G	3G	WLAN	2G	3G	WLAN
Finland, Rovaniemi (railways station area plus via train)	N/A	1.61	0.15	N/A	1.33	0.35
Finland, Kaukajärvi district	N/A	1.92	0.33	N/A	1.18	0.70
France, Elne town	N/A	1.55	0.02	N/A	0.17	0.38
France, Carcassone castle area	N/A	0.95	0.36	N/A	0.50	0.57
France, Disneyland park area	0.68	N/A	0.12	0.84	N/A	0.48
Spain, UAB university campus between hills	0.98	1.27	0.02	1.11	1.17	0.44
France, Limours town	0.17	N/A	0.19	0.63	N/A	0.85
Mean	**0.61**	**1.46**	**0.17**	**0.86**	**0.87**	**0.54**

The average path loss coefficient of 2G signal in suburban areas varied from 0.17 to 0.98 and the standard deviation from 0.63 to 1.11. The 3G signal had higher average path loss coefficient than 2G. The value of its average path loss coefficient for all the suburban locations is 1.46 and the standard deviation 0.87. The average path loss coefficient in WLAN signal is smaller than in cellular signals. This smaller value was 0.17 for all the suburban areas and it had a standard deviation of 0.54.

6.4.5 Densely urban areas or downtowns

Table 6.26 shows the results of densely urban areas.

Table 6.26 Average and standard deviation of path loss coefficients in downtowns

Scenario	**Average path loss coefficient**			**Std of the path loss coefficient**		
	2G	3G	WLAN	2G	3G	WLAN
Belgium, Brussels	N/A	1.62	0.12	N/A	0.71	0.46
Germany, Munich downtown	N/A	1.53	0.21	N/A	1.08	0.37
Romania, Bucharest downtown	1.07	1.65	0.21	1.24	1.04	0.36
Spain, Barcelona downtown	0.58	1.29	N/A	0.32	1.49	N/A
Mean	**0.83**	**1.52**	**0.18**	**0.78**	**1.08**	**0.40**

As we can see in Table 6.26 the average path loss coefficient of 2G and 3G signals in downtowns were higher than in the previous terrains. The average path loss coefficient of 2G signal varied between 0.58 and 1.07 and the standard deviation from 0.71 to 1.49. The average path loss coefficient of WLAN signal of all the densely urban areas was 0.18 and it had a standard deviation of 0.40.

6.4.6 Lake areas

The results of average and standard deviation of the path loss coefficient in lake areas are shown in Table 6.27.

Table 6.27 Average and standard deviation of path loss coefficients in lake areas

Scenario	**Average path loss coefficient**			**Std of the path loss coefficient**		
	2G	3G	WLAN	2G	3G	WLAN
Finland, Tampere around a lake	1.55	1.58	0.07	0.82	0.92	0.19
Germany, Starnberg, lake area	N/A	1.24	0.74	N/A	1.03	0.70
Mean	**1.55**	**1.41**	**0.41**	**0.82**	**0.98**	**0.45**

The average path loss coefficient of the only measurement of 2G signal in lake areas had a value of 1.55 and a standard deviation of 0.82. The average path loss coefficient

of 3G signal is between 1.24 and 1.58 and its standard deviation varies from 0.92 to 1.03. The average path loss coefficient of all the measured WLAN signals is 0.41 and the standard deviation 0.45.

6.4.7 Urban various other scenarios

The results of urban areas are shown in Table 6.28.

Table 6.28 Average and standard deviation of path loss coefficients in urban areas

Scenario	Average path loss coefficient			Std of the path loss coefficient		
	2G	3G	WLAN	2G	3G	WLAN
Finland, Tampere	1.18	1.71	0.21	1.00	1.06	0.45
France, Montpellier	N/A	1.56	0.17	N/A	1.17	0.65
France, Narbonne	N/A	1.56	0.35	N/A	1.12	0.32
France, Perpignan	N/A	0.92	1.74	N/A	0.42	3.27
Romania, Bucharest residential area	1.02	1.27	0.25	1.29	1.34	0.68
Spain, Sant Cugat	1.08	N/A	0.22	0.97	N/A	0.30
Mean	**1.09**	**1.40**	**0.49**	**1.09**	**1.02**	**0.95**

The mean of average path loss coefficient values of 2G signal was 1.09 and its standard deviation 1.09. The 3G signal had a higher value than the 2G signal. This average path loss coefficient value is 1.40 and it had a standard deviation of 1.02. The average path loss coefficients of WLAN signal are between 0.17 and 1.74 whereas the standard deviation varies from 0.30 to 3.27. The highest average path loss coefficient was measured in Perpignan and it had also the highest standard deviation value. This means that the signal transmit power was reduced considerably in the propagation.

6.4.8 Comparison between the different terrains

As we saw the highest values of average path loss coefficient were in densely urban, urban and lake areas while the lowest values were in mountain area.

The terrains with highest average path loss coefficient of 2G signal were densely urban (0.83), lake (1.55) and urban (1.09) areas. Moreover, the terrains with lowest average path loss coefficient were airport (0.45), forest (0.63) and suburban (0.61) areas. The standard deviation of the average path loss coefficient is higher in urban (1.09) and suburban (0.86) terrains than in other environments such as forest areas (0.36).

About 3G signal, the highest average path loss coefficient was measured in suburban (1.46), densely urban (1.52) and lake areas (1.41) while the lowest values were in airport (0.31) and beach areas (0.64). We notice that the standard deviation of the

average path loss is higher in terrains such as dense urban (1.08) or lake areas (0.98) than in airport terrain (0.54).

The average path loss coefficient of WLAN signal was high in lake (0.81) and urban areas (0.41) and small in suburban (0.17) or densely urban (0.18) terrains. From the standard deviation information we can deduce that the path los coefficient will vary more in terrains such as airport (1.02) or beach areas (0.97) than in other environments such as densely urban areas (0.40).

In conclusion we could say that average path loss coefficients have big values in terrains with high density of buildings and low values in open areas.

6.5 Shadowing statistics

In this section we will analyze the mean and the standard deviation of shadowing standard deviation in the different terrains. The shadowing was computed as the difference between the blue crosses and the red curve from Figure 6.1. We then computed the standard deviation of the shadowing for each transmitter. The tables in this section show the average of standard deviation and the standard deviation of the shadowing standard deviation, taken over all heard transmitters.

6.5.1 Airport areas

Table 6.29 shows the results of shadowing statistics in airport areas.

Table 6.29 Mean and standard deviation of shadowing std in airport areas

Scenario	Mean of shadowing std [dB]			Std of shadowing std [dB]		
	2G	3G	WLAN	2G	3G	WLAN
Finland, Helsinki airport	4.43	N/A	11.02	2.32	N/A	3.61
France, Paris airport	1.91	N/A	12.51	0.86	N/A	0.22
Germany, Munich airport	N/A	2.36	8.85	N/A	0.02	0.48
Hungary, Budapest airport	N/A	N/A	N/A	N/A	N/A	N/A
Finland, Tampere airport	2.21	N/A	10.48	1.38	N/A	0.07
Mean	**2.85**	**2.36**	**10.72**	**1.52**	**0.02**	**1.10**

As we can see in Table 6.29 the highest mean of shadowing standard deviation of 2G signal was measured in Helsinki airport with a standard deviation of the shadowing std of 2.32 dB. The airport with the lowest mean of shadowing standard deviation value for 2G signal was Paris airport (1.91 dB) and it had a standard deviation of shadowing std of 0.86 dB. The measurements of Tampere airport had a mean of shadowing standard deviation value of 2.21 dB and 1.38 dB standard deviation of shadowing std. The only

location where 3G signal mean of shadowing standard deviation was measured was Munich airport and it had a value of 2.36 dB and 0.02 dB standard deviation of shadowing std. The values of mean of shadowing standard deviation of WLAN signal goes from 8.85 dB in Munich to 12.51 dB in Paris. The mean of shadowing standard deviation of Munich (8.85 dB) had a standard deviation of shadowing std of 0.48 dB and the mean of shadowing standard deviation of Paris (12.51 dB) had 0.22 dB. The mean of shadowing standard deviation measured in Helsinki and Tampere airports had values of 11.02 dB and 10.48 dB with a standard deviation of shadowing std of 3.61 dB and 0.07 dB respectively.

We notice that WLAN signal suffers more mean of shadowing standard deviation than the cellular signals. This occurs because the operating frequency of WLAN is higher than the operating frequencies of cellular signals. Due to the dimensions of the wavelength, high frequencies are more affected by reflections and absorptions than low frequencies.

6.5.2 Seaside or beach areas

The results of beach areas are shown in Table 6.30.

Table 6.30 Mean and standard deviation of shadowing std in beach areas

Scenario	Mean of shadowing std [dB]			Std of shadowing std [dB]		
	2G	3G	WLAN	2G	3G	WLAN
Denmark, Sletterstrand (sea region)	N/A	6.36	6.29	N/A	2.01	1.17
France, Argeles sur Mer, downtown	N/A	7.00	3.66	N/A	1.28	2.14
France, Cerbere sea resort	N/A	5.88	6.24	N/A	0.80	0.40
France, Collioure sea resort	N/A	8.08	6.28	N/A	1.19	1.28
Spain, Montgat beach area	N/A	6.98	4.12	N/A	3.23	1.11
Spain, Castelldefelts, beach area	N/A	10.39	5.27	N/A	1.52	0.78
Spain, Caldes d'Estrac, beach area	N/A	8.56	4.63	N/A	0	1.10
Mean	**N/A**	**7.61**	**5.21**	**N/A**	**1.43**	**1.14**

Among the seven seaside towns of this terrain the highest value of mean of shadowing standard deviation in 3G signal was measured in Castelldefelts beach area (10.39 dB) and the lowest mean of shadowing standard deviation value was in Cerbere sea resort (5.88 dB). The standard deviations of shadowing std of these values are 1.52 dB and 0.80 dB, respectively. The rest of the cities had a value between these two limits and the average mean of shadowing standard deviation and standard deviation of shadowing std was 7.61 dB and 1.43 dB. Regarding WLAN signal, the highest mean of shadowing standard deviation was measured in Sletterstrand (6.29 dB) and the lowest mean of shadowing standard deviation in Argeles sur mer (3.66 dB). The standard deviation of

shadowing std of these measurements was 1.17 dB and 2.4 dB. The rest of locations had a mean of shadowing standard deviation around 5.21 dB and a standard deviation of shadowing std of 1.14 dB.

6.5.3 Mountain or forest areas

Table 6.31 shows the shadowing values in forest areas.

Table 6.31 Mean and standard deviation of shadowing std in forest areas

Scenario	Mean of shadowing std [dB]			Std of shadowing std [dB]		
	2G	3G	WLAN	2G	3G	WLAN
France, Boissiere forest	N/A	4.24	N/A	N/A	0	N/A
France, forest area	N/A	5.49	N/A	N/A	0.43	N/A
France, Valmy	N/A	5.47	3.74	N/A	1.67	2.33
Romania, Busteni mountain area	N/A	6.81	10.18	N/A	2.18	1.85
Spain, Collserola (hilly/mountain area)	N/A	7.21	N/A	N/A	0.32	N/A
Spain, Can Coll hilly area	N/A	6.44	3.57	N/A	1.39	2.91
Spain, Garraf natural reservation (mountain area)	N/A	7.48	4.54	N/A	3.13	0.70
Spain, Montseny natural reservation (mountain area)	4.00	4.50	N/A	3.10	2.09	N/A
Mean	**4.00**	**5.96**	**5.51**	**3.10**	**1.40**	**1.95**

The only measure of 2G signal in mountain was obtained in Montseny natural reservation (4.00 dB) and it had a standard deviation of shadowing std of 3.10 dB. For 3G signal, the mean of shadowing standard deviation values goes from 4.24 dB in Boissiere to 6.81 dB in Busteni mountain area. The standard deviations of shadowing std of these measurements were 0 dB in Boissiere and 2.18 dB for Busteni. At this last location the WLAN signal had a mean of shadowing standard deviation of 10.18 dB with a standard deviation of shadowing std of 1.85 dB. In the rest of towns the value of mean of shadowing standard deviation was around 4 dB and a standard deviation of shadowing std of around 1.95 dB.

6.5.4 Suburban (various areas)

The results of suburban areas are shown in Table 6.32.

Table 6.32 Mean and standard deviation of shadowing std in suburban areas

Scenario	Mean of shadowing std [dB]			Std of shadowing std [dB]		
	2G	3G	WLAN	2G	3G	WLAN
Finland, Rovaniemi (railways station area plus via train)	N/A	6.54	7.53	N/A	3.34	3.02

Finland, Kaukajärvi district	N/A	7.20	18.55	N/A	2.48	0.31
France, Elne town	N/A	5.10	10.21	N/A	0.64	0.68
France, Carcassone castle area	N/A	6.68	6.13	N/A	1.10	1.38
France, Disneyland park area	4.83	N/A	8.49	2.54	N/A	1.19
Spain, UAB university campus between hills	5.22	7.33	6.03	2.20	1.97	1.18
France, Limours town	2.91	N/A	7.93	1.67	N/A	3.25
Mean	**4.32**	**6.57**	**9.27**	**2.14**	**1.91**	**1.57**

From all the cities mentioned in Table 6.32 Disneyland park area and Barcelona university campus measurements had a mean of shadowing standard deviation in 2G signal of around 5 dB and a standard deviation of shadowing std over 2 dB while Limours had a mean of shadowing standard deviation of 2.91 dB and 1.67 dB standard deviation of shadowing std. The 3G signal measurements had an average of mean of shadowing standard deviation around 6.57 dB and an average of standard deviation of shadowing std of 1.91 dB. The highest value of WLAN mean of shadowing standard deviation was in Kaukajärvi and it was 18.55 dB with a standard deviation of shadowing std of 0.31 dB. The WLAN values had an average of mean of shadowing standard deviation of 9.27 dB and a standard deviation of shadowing std of 1.57 dB.

6.5.5 Densely urban areas or downtowns

Table 6.33 shows the results collected in densely urban areas.

Table 6.33 Mean and standard deviation of shadowing std in densely urban areas

Scenario	**Mean of shadowing std [dB]**			**Std of shadowing std [dB]**		
	2G	3G	WLAN	2G	3G	WLAN
Belgium, Brussels	N/A	7.23	7.78	N/A	3.21	1.62
Germany, Munich downtown	N/A	6.86	7.17	N/A	1.60	2.08
Romania, Bucharest downtown	8.19	7.54	8.80	2.63	2.31	1.14
Spain, Barcelona downtown	2.75	6.60	N/A	1.43	2.25	N/A
Mean	**5.47**	**7.06**	**7.92**	**2.03**	**2.34**	**1.61**

The values of mean of shadowing standard deviation of 2G signals in densely urban areas were 8.19 dB in Bucharest and 2.75 dB in Barcelona. The standard deviations of shadowing standard deviation of these locations were 2.63 dB in Bucharest and 1.43 dB in Barcelona downtown. The 3G signal had an average mean of shadowing standard deviation of 7.06 dB and 2.34 dB standard deviation of shadowing std. The measurements of WLAN signal had a mean of shadowing standard deviation around 7.92 dB and a standard deviation of shadowing std of 1.61 dB.

6.5.6 Lake areas

The results of lake areas are shown in Table 6.34.

Table 6.34 Mean and standard deviation of shadowing std in lake areas

Scenario	Mean of shadowing std [dB]			Std of shadowing std [dB]		
	2G	3G	WLAN	2G	3G	WLAN
Finland, Tampere around a lake	4.89	6.69	8.30	1.29	2.34	1.56
Germany, Starnberg, lake area	N/A	6.50	4.81	N/A	1.87	2.70
Mean	**4.89**	**6.60**	**6.56**	**1.29**	**2.12**	**2.13**

The mean of shadowing standard deviation of Tampere lake area for 2G signal was 4.89 dB and a standard deviation of shadowing std of 1.29 dB. The mean of shadowing standard deviation of 3G signal was around 6.60 dB and 2.12 dB of standard deviation of shadowing std. The mean of shadowing standard deviation of WLAN signal were 8.30 dB in Tampere and 4.81 dB in Starnberg lake area which make an average of 6.58 dB. The average of standard deviation of shadowing std of these two lake areas was 2.13 dB.

6.5.7 Urban various other scenarios

Table 6.35 shows the results of shadowing statistics in urban areas.

Table 6.35 Mean and standard deviation of shadowing std in urban areas

Scenario	Mean of shadowing std [dB]			Std of shadowing std [dB]		
	2G	3G	WLAN	2G	3G	WLAN
Finland, Tampere	9.88	7.78	6.06	2.28	2.26	0.72
France, Montpellier	N/A	6.94	6.95	N/A	1.93	1.45
France, Narbonne	N/A	5.98	7.05	N/A	1.18	1.22
France, Perpignan	N/A	5.35	4.75	N/A	0.08	1.16
Romania, Bucharest residential area	8.54	9.01	5.42	2.42	6.04	1.16
Spain, Sant Cugat	5.57	N/A	8.51	2.36	N/A	0.69
Mean	**8.00**	**7.01**	**6.46**	**2.35**	**2.30**	**1.07**

The minimum value of mean of shadowing standard deviation of 2G signal measured in suburban area was in Sant Cugat (5.57 dB) and the maximum was measured in Tampere (9.88 dB). The standard deviations of shadowing std were 2.36 dB in Sant Cugat and 2.28 dB in Tamere. The average mean of shadowing standard deviation of all the suburban areas was 8.00 dB and the average standard deviation of shadowing std 2.35 dB. Respecting the 3G signal, the average mean of shadowing standard deviation was 7.01 dB and its standard deviation of shadowing std 2.30 dB. The WLAN signal had a mean of shadowing standard deviation value around 6.46 dB and a standard deviation of shadowing std of 1.07 dB.

6.5.8 Comparison between the different terrains

The highest mean of shadowing standard deviation in most of the cases were in densely and urban terrains.

As we saw in the previous tables the highest values of mean of shadowing standard deviation of 2G signal were in densely urban (5.47 dB) and urban areas (8 dB), whereas the minimum mean of shadowing standard deviation was in airport areas (2.85 dB). The standard deviations of shadowing std in these terrains were 2.03 dB in densely urban and 2.35 dB in urban areas. These high values of mean of shadowing standard deviation occurred due to the high height and density of buildings in these terrains which hide the receiver during the propagation of signal. The low mean of shadowing standard deviation in airport areas was because the measurements were taken in a small area near the BSs.

For 3G signal, the highest values of mean of shadowing standard deviation were collected in beach areas (7.61 dB), densely urban (7.06 dB) and urban areas (7.01 dB). The standard deviations of shadowing std of these locations were 1.43 dB, 2.34 dB and 2.30 dB for seaside, densely urban and urban, respectively. The lowest mean of shadowing standard deviation values were collected in airport areas (2.36 dB) and its standard deviation of shadowing std was 1.10 dB.

The mean of shadowing standard deviation values of 3G signal would be higher than 2G signal because of the location of BSs and Node Bs and the operating frequencies. 3G networks use higher frequencies so these waves will suffer more reflections and will produce a higher mean shadowing standard deviation. The path losses will be also higher in 3G networks than in 2G networks due to the same reason.

The higher WLAN mean of shadowing standard deviation values were in airport areas (10.72 dB), suburban areas (9.27 dB) and densely urban areas (7.92 dB). The standard deviations of shadowing std of these values were 1.10 dB in airport areas, 1.57 dB in suburban areas and 1.61 dB in densely urban areas. The lowest mean of shadowing standard deviation occurred in seaside (5.21 dB) and mountains areas (5.51 dB).

WLAN signal has the smaller wavelength of the analyzed signals. This small wavelength will suffer shadowing even with small objects in the radio propagation path.

6.6 Power maps and emitter position estimation

In Figure 6.4, 6.5, 6.6, 6.7, 6.8, 6.9 and 6.10 show the power maps and the emitter position estimation in different terrains.

6.6.1 Airport areas

Figure 6.4 shows an example of the received power and the estimated position of one AP in Helsinki airport.

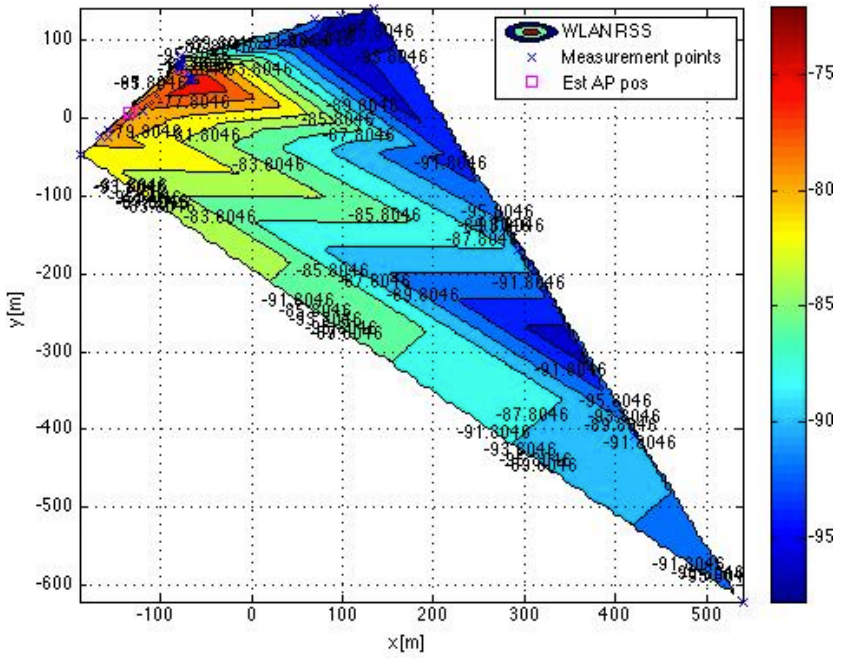

Figure 6.4 Power map of WLAN signal in Helsinki airport

In the top left side of the plot we can observe an area with high received power values (red color) where is the estimated AP position. The received power of this AP varies depending on the propagation direction. In the right side of the plot we can see some areas where the received level decrease rapidly. In these blue color areas there could be obstacles such as pillars of the building that impede the propagation of the WLAN signal.

6.6.2 Seaside or beach areas

The Figure 6.5 shows the power map of 3G signal in Argeles sur mer. In the figure below we can see that the estimated Node B position, on the right side of the plot, was in the area with the highest received power values. We can see that the 3G signal did not propagate equally in all the directions. In the direction of the bottom side of the plot the signal decrease rapidly while in the direction of the top side of the plot the signal was reduced gradually. We could say that in this last direction is an open area such as sea or a park.

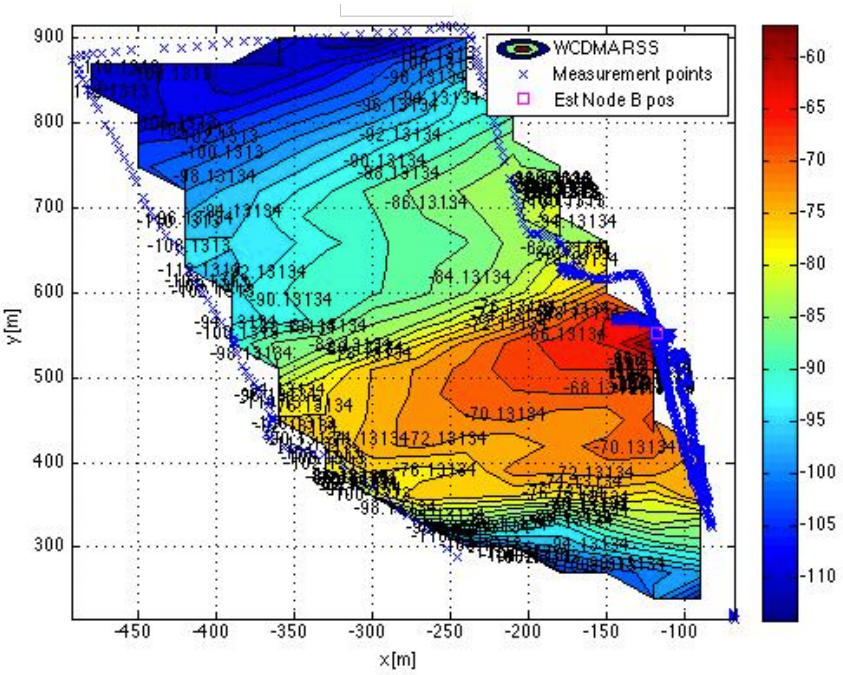

Figure 6.5 Power map of 3G signal in Argeles sur mer

6.6.3 Mountain or forest areas

Figure 6.6 shows the power map of the 3G signal in Can Coll hilly area.

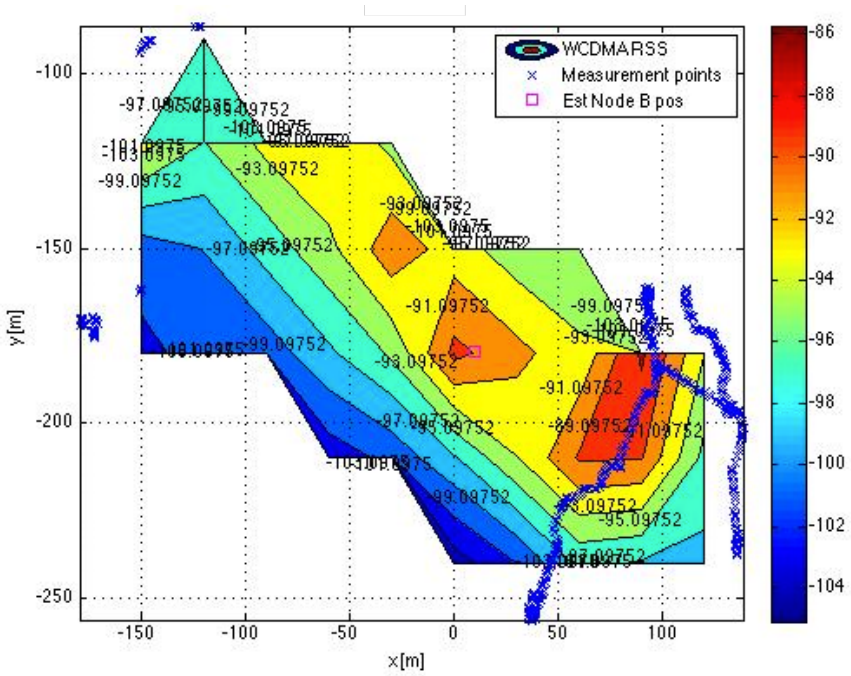

Figure 6.6 Power map of 3G signal in Can Coll hilly area

In the figure above we can see that the estimated position of the Node B is in a small red area in the centre of the plot. In this terrain the received power decreases in a distance of

few meters in one direction and how the received power remains constant in other direction. The explanation of this situation is that the yellow area is a clear of obstacles area while the sides of this area is probably an area covered by vegetation. In this yellow area there are two red areas apart from the BS coverage area where the received power increase. These areas could be due to the amplification of the 3G signal by reflection produced by some elements such as rocks.

6.6.4 Suburban (various areas)

Figure 6.7 show the power map of 2G signal in Disneyland park area.

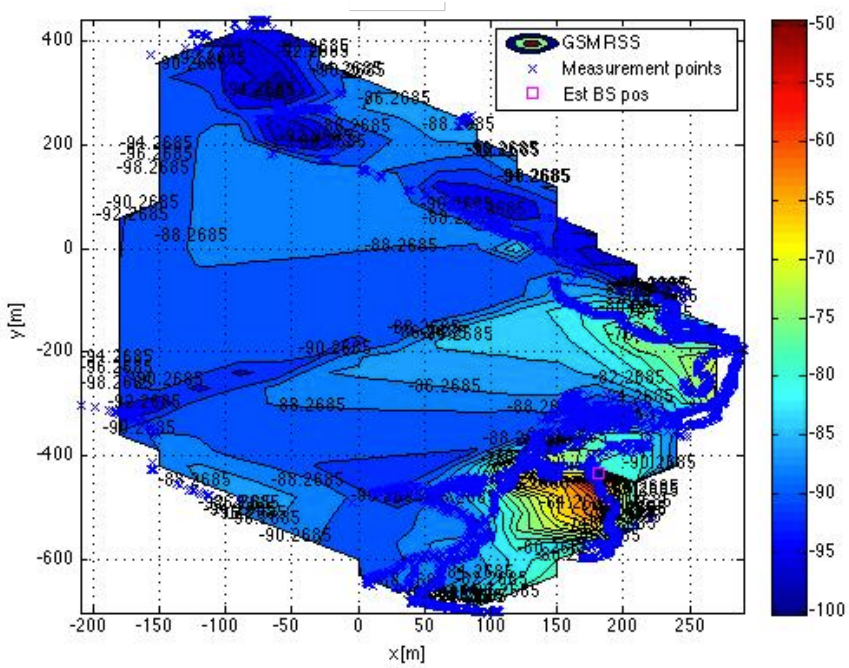

Figure 6.7 Power map of 2G signal in Disneyland park area

Here we can observe that there are two small areas where the received power had high values and the rest of the area where the received power had very low values. In one of these small areas is the estimated location of the BS. The second small area could be the coverage area of other BS or an area where the 2G signal of the first BS was heard due to reflections in the terrain. On the left side of the first small area we could say that there is a building that shadow the signal to the rest of the terrain.

6.6.5 Densely urban areas or downtowns

Figure 6.8 show the power map of 3G signal in Barcelona downtown. The main characteristic of the measurements of Figure 6.8 is that there are areas with very different received power. The red area on the top of the plot is the estimated position of the Node B. Near the Node B the received signal had high power but around this area the received power changes randomly. In the bottom left side of the plot we can see that

there are four areas where the received power was extremely low. In these zones the received power is shadowed by some obstacles such as buildings or walls. These shadowed areas are very common in densely urban areas due to the high density of buildings and obstacles in the terrain.

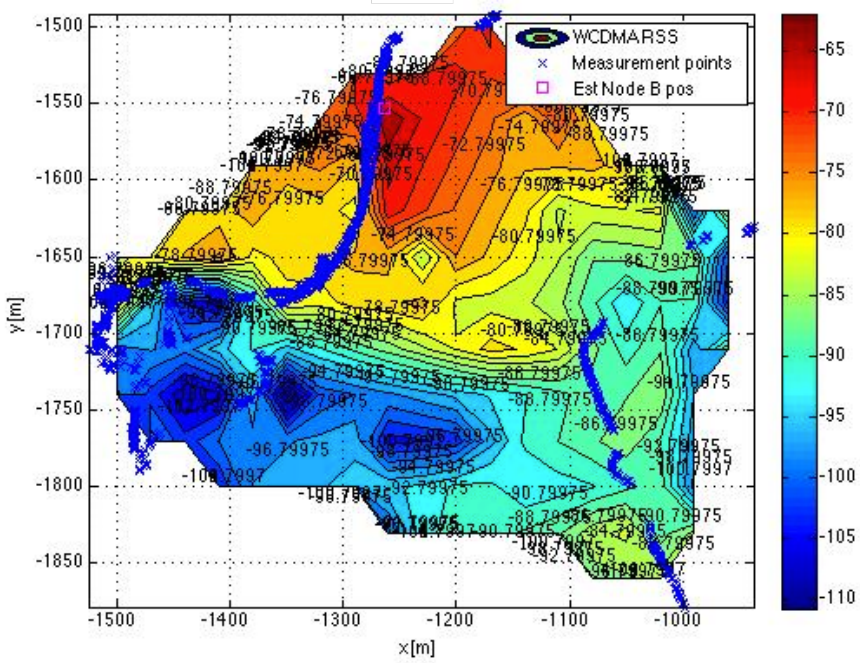

Figure 6.8 Power map of 3G signal in Barcelona downtown

6.6.6 Lake areas

Figure 6.9 shows the results of Tampere lake area.

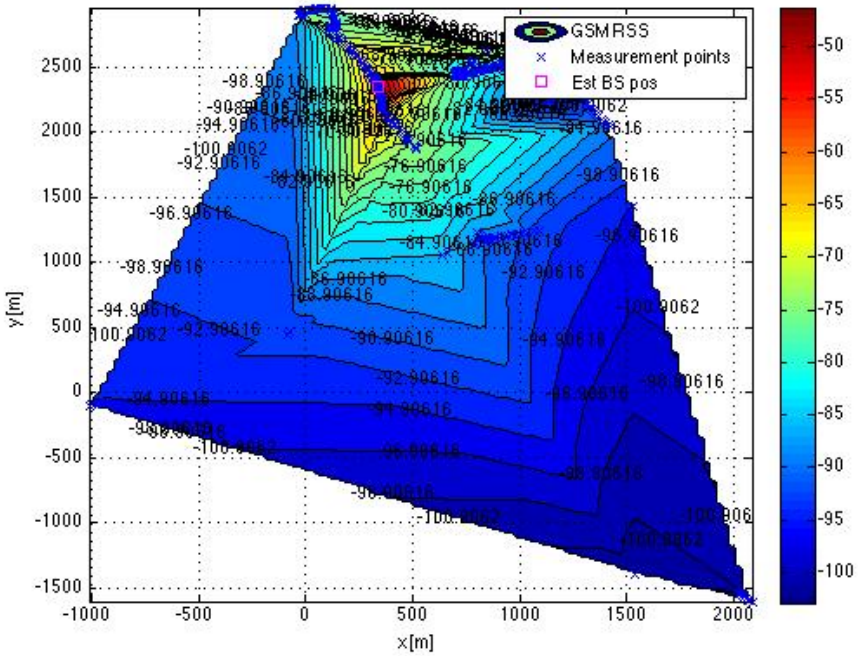

Figure 6.9 Power map of 2G signal in Tampere lake area

In Figure 6.9 we can see that the estimated BS position is exactly in the small red area on the top of the plot. If we move far away of this area, the received power decreases constantly in all directions. This way of propagation of signal is due to the open area around the Node B. The absence of obstacles causes free space propagation.

6.6.7 Urban various other scenarios

Figure 6.10 shows the power map of 2G signal in Sant Cugat.

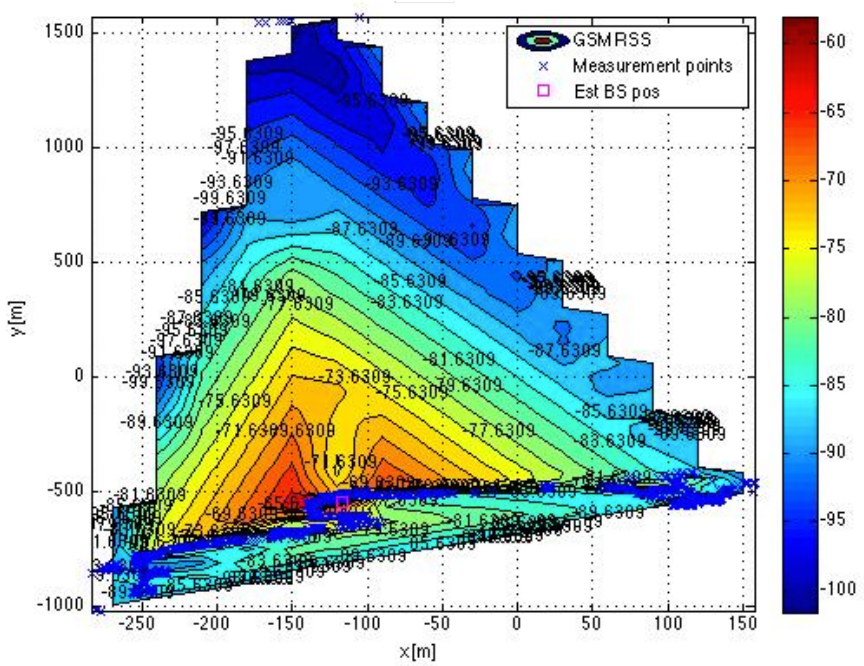

Figure 6.10 Power map of 2G signal in Sant Cugat

In Figure 6.10 we can see that the estimated position of the BS is in a small red area on the bottom side of the plot where the received power had high values. Around this area the received power decrease in equal manner in all directions. In the top side of the BS is a small reduction of the received power that could be due to a small object such as a tree but some meter farther the received power is the same as the surrounding areas. This could happen due to the multipath propagation of the signal.

6.7 Voronoi tesselation areas

In this section we also investigated the density of the emitters in cellular and WLAN scenarios. For this purpose, we first estimated the position of the transmitters via the weighted centroid approach [15], and we then built the Voronoi diagrams of all the heard transmitters. Tables 6.36, 6.37, 6,38, 6.39, 6.40, 6.41 and 6.42 show the mean and median of Voronoi tesselateration areas in different terrains. Median values of around 1 mm^2 have been considered as 0.

6.7.1 Airport areas

Table 6.36 shows the mean and median values of Voronoi tesselation areas in airport areas.

Table 6.36 Mean and median of Voronoi areas in airport areas

Scenario	Mean and median of Voronoi areas in Km^2					
	2G		3G		WLAN	
	mean	median	mean	median	mean	median
Finland, Helsinki airport	61.2116	1.2755	N/A	N/A	0.0291	0.0010
France, Paris airport	0.7002×10^{-3}	0.0913×10^{-3}	N/A	N/A	0.1427×10^{-3}	0.0129×10^{-3}
Germany, Munich airport	N/A	N/A	N/A	N/A	0.2810×10^{-4}	0.1635×10^{-4}
Hungary, Budapest airport	N/A	N/A	N/A	N/A	N/A	N/A
Finland, Tampere airport	0.8484×10^{-3}	0.8484×10^{-3}	N/A	N/A	N/A	N/A
Mean	**20.40**	**0.43**	**N/A**	**N/A**	$\mathbf{9.76\times10^{-3}}$	$\mathbf{3.43\times10^{-4}}$

As is shown in the table above the biggest Voronoi areas of 2G signal were found in Helsinki airport (61.21 Km^2) while in the other airports the values of Voronoi areas were much smaller. For 3G signal there were not data to create Voronoi areas. The WLAN signal had a smaller Voronoi area. The mean of this area for all the airports was 9760 m^2 and the median 343 m^2.

Figure 6.11 shows an example of the Voronoi diagram for the Node Bs heard in Paris airport. The x and y axis are in meters, in local coordinates.

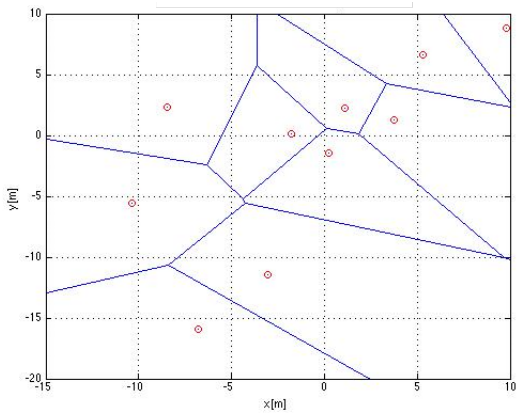

Figure 6.11 Voronoi areas for Node B position in Paris airport

6.7.2 Seaside or beach areas

Table 6.37 shows the results for seaside terrain.

Table 6.37 Mean and median of Voronoi areas in beach areas

Scenario	Mean and median of Voronoi areas in Km^2					
	2G		3G		WLAN	
	mean	median	mean	median	mean	median
Denmark, Sletterstrand (sea region)	N/A	N/A	1.2618×10^{-3}	0.1983×10^{-3}	0.0001×10^{-3}	0
France, Argeles sur Mer, downtown	N/A	N/A	N/A	N/A	0.2434	0.0103
France, Cerbere sea resort	N/A	N/A	N/A	N/A	0.5994×10^{-3}	0.0133×10^{-3}
France, Collioure sea resort	N/A	N/A	53.6637	53.6637	0.0163	0.0040
Spain, Montgat beach area	N/A	N/A	0.0078	0.0095	0.1440	0.0014
Spain, Castelldefelts, beach area	N/A	N/A	N/A	N/A	0.2974×10^{-6}	0.2974×10^{-6}
Spain, Caldes d'Estrac, beach area	N/A	N/A	N/A	N/A	0.1203×10^{-3}	0.0731×10^{-3}
Mean	**N/A**	**N/A**	**17.89**	**17.89**	**0.06**	$\mathbf{2.63\times10^{-3}}$

In Table 6.37 we can observe that there were no values for 2G signal. There was a big difference between Collioure sea resort Vornonoi area and the rest of the seaside locations. The value of Voronoi areas in Collioure sea resort was 53.66 Km^2 while in the rest of the beach towns the Voronoi areas were between 198.3 m^2 and 9500 m^2. Regarding WLAN signal, the average of all the beach areas was 60000 m^2 and its median 2630 m^2.

Figure 6.12 is an example of the Voronoi diagram for the APs heard in seaside terrain.

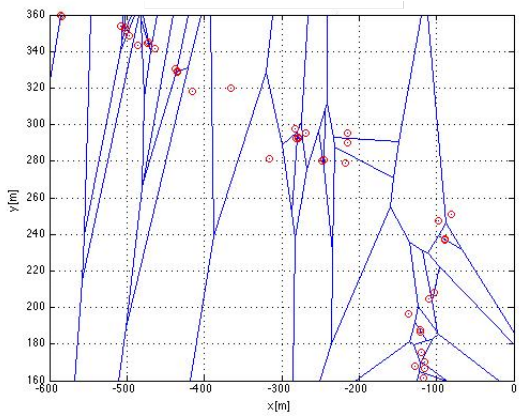

Figure 6.12 Voronoi areas for AP position in Collioure sea resort

6.7.3 Mountain or forest areas

Table 6.38 shows the values of Voronoi areas in forest areas.

Table 6.38 Mean and median of Voronoi areas in mountain areas

Scenario	Mean and median of Voronoi areas in Km^2					
	2G		3G		WLAN	
	mean	median	mean	median	mean	median
France, Boissiere forest	N/A	N/A	N/A	N/A	N/A	N/A
France, forest area	N/A	N/A	N/A	N/A	N/A	N/A
France, Valmy	N/A	N/A	N/A	N/A	0.3714×10^{-3}	0.3714×10^{-3}
Romania, Busteni mountain area	N/A	N/A	N/A	N/A	0.8139×10^{-4}	0.8139×10^{-4}
Spain, Collserola (hilly/mountain area)	N/A	N/A	N/A	N/A	N/A	N/A
Spain, Can Coll hilly area	N/A	N/A	2.3467	1.3936	2.1144	0
Spain, Garraf natural reservation (mountain area)	N/A	N/A	56.2677	32.3500	0.1226	0.0005
Spain, Montseny natural reservation (mountain area)	N/A	N/A	0.4773	0.4773	N/A	N/A
Mean	**N/A**	**N/A**	**19.70**	**11.41**	**0.56**	**3.18×10^{-4}**

As we can see in Table 6.38 the only available data were 3G and WLAN signals. The mean of the Voronoi areas of 3G signal and forest terrain was 19.70 Km^2 and the median of this value 11.41 Km^2. The widest Voronoi areas were found in Garraf mountain area and it had a mean value of 56.27 Km^2. For WLAN signal the Voronoi areas were much more smaller than for cellular signals. The size of the Voronoi areas varied on each mountain location but the average of all locations Voronoi areas was 0.56 Km^2 and its median 318 m^2.

The Voronoi diagram for Node Bs heard in Can Coll is illustrated in Figure 6.13.

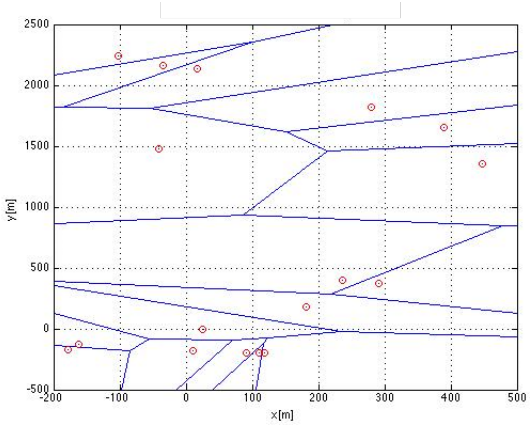

Figure 6.13 Voronoi areas for Node B position in Can Coll

6.7.4 Suburban (various areas)

Table 6.39 shows the results measured in suburban areas.

Table 6.39 Mean and median of Voronoi areas in suburban areas

Scenario	Mean and median of voronoi areas in Km^2					
	2G		3G		WLAN	
	mean	median	mean	median	mean	median
Finland, Rovaniemi (railways station area plus via train)	N/A	N/A	112.7695	7.1185	0.0159	0.0001
Finland, Kaukajärvi district	N/A	N/A	8.2866	3.8423	N/A	N/A
France, Elne town	N/A	N/A	N/A	N/A	0.0054	0.0003
France, Carcassone castle area	N/A	N/A	0.0259	0.0056	0.0017	0.0002
France, Disneyland park area	0.0274	0.0116	N/A	N/A	0.3169	0.0033
Spain, UAB university campus between hills	0.1999	0.0494	0.0465	0.0283	0.0727	0.0001
France, Limours town	18.7150	7.2691	N/A	N/A	0.0103	0
Mean	**6.3141**	**2.4434**	**30.2821**	**2.7487**	**0.0705**	**0.0008**

The maximum mean of Voronoi areas of 2G signal was measured in Limours town. The value of this area was 18.72 Km^2 and its median 7.27 Km^2. The rest of suburban locations had mean and median values lower than 1 Km^2. Regarding 3G signal, the average of Voronoi areas of different suburban terrains was 30.28 Km^2 and its median was 2.75 Km^2. The Voronoi areas of WLAN signal, as in the previous terrains, was smaller than in cellular signals. The mean Voronoi area of this type of signal was 70500 m^2 and the median 800 m^2.

Figure 6.14 shows the Voronoi diagram for the Node Bs heard in UAB university campus.

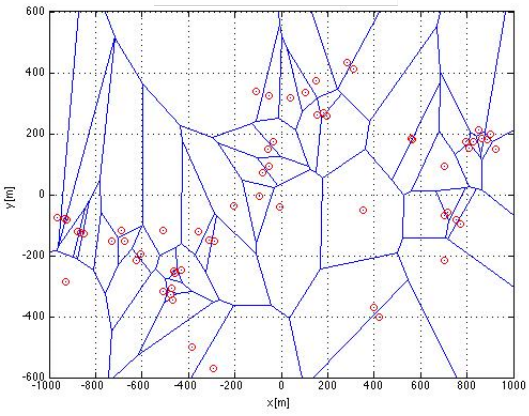

Figure 6.14 Voronoi areas for Node B in UAB university campus

6.7.5 Densely urban areas or downtowns

The mean and median values of Voronoi areas in densely urban areas are shown in Table 6.40.

Table 6.40 Mean and median of Voronoi areas in downtowns

Scenario	Mean and median of voronoi areas in Km^2					
	2G		3G		WLAN	
	mean	median	mean	median	mean	median
Belgium, Brussels	N/A	N/A	0.0477	0.0179	0.0181	0.0013
Germany, Munich downtown	N/A	N/A	4.7998	0.3178	0.0024	0.0002
Romania, Bucharest downtown	2.7331	0.1426	0.0920	0.0336	0.0069	0.0010
Spain, Barcelona downtown	0.0001	0.0001	0.4846	0.0340	N/A	N/A
Mean	**2.7332**	**0.0714**	**1.3560**	**0.1008**	**9.13×10^{-3}**	**8.33×10^{-4}**

In Table 6.40 we can see that the Voronoi areas in densely urban areas had smaller size than in the previous terrains. The averages of the mean and median values of Voronoi areas in 2G signal were 2.73 Km^2 and 71400 m^2. The 3G signal had smaller Voronoi areas than 2G signal. The average value of Voronoi areas of 3G signal was 1.36 Km^2 and its median value 0.10 Km^2. The WLAN Voronoi areas are extremely small in densely urban areas. The average value of these small areas was 9139 m^2 and the median value was 833 m^2.

Figure 6.15 shows an example of the Voronoi diagram for the APs heard in densely urban terrains.

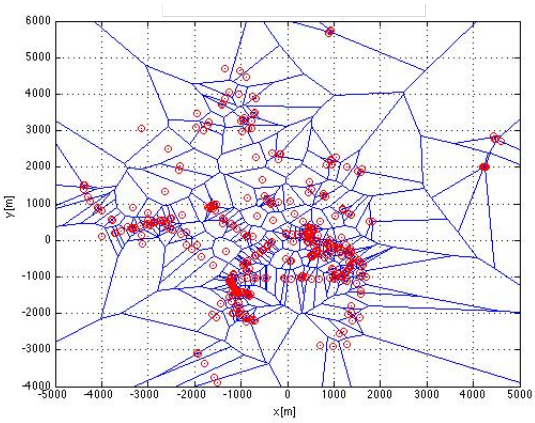

Figure 6.15 Voronoi areas for APs in Barcelona downtown

6.7.6 Lake areas

The mean and median of Voronoi areas are collected in Table 6.41.

Table 6.41 Mean and median of Voronoi areas in lake areas

Scenario	Mean and median of Voronoi areas in Km^2					
	2G		3G		WLAN	
	mean	median	mean	median	mean	median
Finland, Tampere around a lake	3.6521	0.1866	15.8350	0.9957	1.0089	0.0045
Germany, Starnberg lake area	N/A	N/A	29.4128	3.6644	3.8575	0
Mean	**3.6521**	**0.1866**	**22.6239**	**2.3301**	**2.4332**	**0.0045**

The mean and median Voronoi areas of 2G signal was only calculated for Tampere lake area. In this location the mean and median of Voronoi areas were 3.65 Km^2 and 0.19 Km^2. 3G signal had wider Voronoi areas than 2G signal. The value of mean and median of Voronoi areas of 3G signal were 22.62 Km^2 and 2.33 Km^2. The mean Voronoi areas of WLAN signal and lake areas was 2.43 Km^2 and its median 4500 m^2.

An example of the Voronoi diagram for the BSs heard in lake areas is given in Figure 6.16.

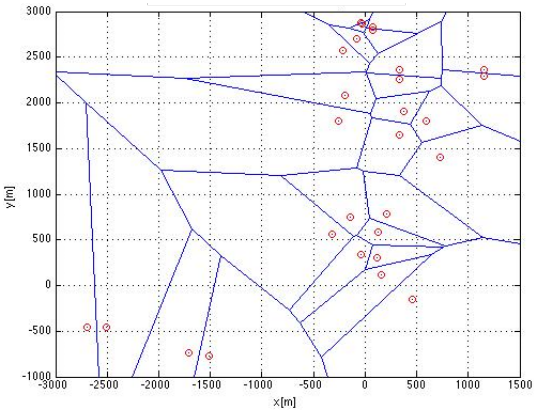

Figure 6.16 Voronoi areas for BS in Tampere lake area

6.7.7 Urban various other scenarios

The mean and median values of Voronoi areas are given in Table 6.42.

Table 6.42 Mean and median of Voronoi areas in urban areas

Scenario	Mean and median of Voronoi areas in Km^2					
	2G		3G		WLAN	
	mean	median	mean	median	mean	median
Finland, Tampere	4.7928	0.4596	28.4807	0.2901	0.0482	0.0023
France, Montpellier	N/A	N/A	7.7983	0.2315	0.3724	0.0018
France, Narbonne	N/A	N/A	0.9967	0.6659	0.0253	0.0002
France, Perpignan	N/A	N/A	N/A	N/A	N/A	N/A
Romania, Bucharest residential area	1.0357	0.3365	9.3976	0.3304	5.3342	0.0331

Spain, Sant Cugat	0.4799	0.0543	N/A	N/A	0.0197	0.0010
Mean	**2.1028**	**0.2835**	**11.6683**	**0.3795**	**1.1600**	**0.0077**

In table 6.42 we can observe that the average of the mean and median of Voronoi areas for 2G signal in urban areas were 2.10 Km^2 and 0.28 Km^2 respectively. These values are higher in 3G signals and they were 11.67 Km^2 and 0.38 Km^2. For WLAN signal the average mean and median of Voronoi areas for all the urban locations were 1.16 Km^2 and 7700 m^2.

An example of the Voronoi diagram for the BSs heard in urban areas is shown in Figure 6.17.

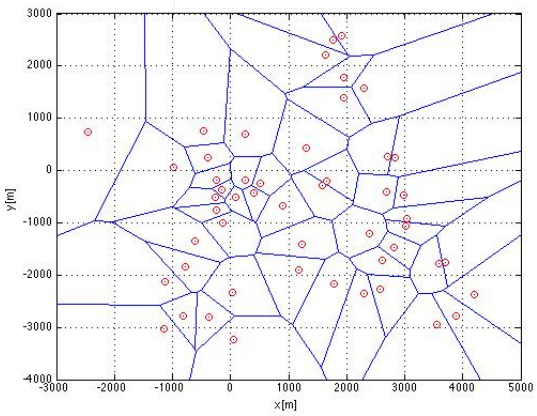

Figure 6.17 Voronoi areas for BS in Bucharest residential area

6.7.8 Comparison between the different terrains

We saw that for 2G signal, the wider Voronoi areas were measured in airport areas and the smaller Voronoi areas in densely urban and urban areas. A smaller Voronoi area means a more dense infrastructure, and it is normal to have denser BS and Node B infrastructure in urban areas than in suburban and rural areas. The covered areas had an average of 20.40 Km^2 in airport terrain and 2.73 Km^2 and 2.10 Km^2 in densely urban and urban areas.

Regarding 3G signal, the biggest Voronoi areas were in forest (19.70 Km^2), lake (22.62 Km^2) and suburban areas (30.28 Km^2). Moreover, the smaller areas were in densely urban area and they had a value of 1.36 Km^2.

The highest Voronoi areas of WLAN signal was in lake areas with a value of 2.43 Km^2 while the smallest Voronoi area of this signal were in airport (9760 m^2) and densely urban areas (9130 m^2). This shows that the WLAN infrastructure in airports is typically very dense.

If we compare all the terrains we can see clearly that the coverage area of WLAN signal is much more smaller than cellular signals coverage area or cells. This difference of cells is due to the emitted power by the BSs, Node Bs and APs and the operating frequency of each system. WLAN has the highest operating frequency so this will cause higher path losses and therefore a smaller coverage area.

The differences of the Voronoi areas between urban and rural terrains are huge in all the signals. In general rural and suburban areas support the propagation of signal more that urban terrains and produce higher coverage areas.

7. CONCLUSIONS AND FUTURE WORKS

In this thesis, we analysed the RSS fluctuations in different environments, using 2G, 3G and WLAN signals. The main objective was to create a simulator to convert .xml files into Matlab variables and to analyse these variables in terms of signal availability, location of the emitters in seven different terrains, RSS fluctuations, shadowing statistics and path-loss parameters. To achieve this goal we used the measured received signal strength values and one-slope path loss model. Our results can form the basis of further developments of RSS-based positioning algorithms, which take into account the terrain type. One of the multiple advantages of RSS-based positioning methods using 2G, 3G and WLAN signals is that the entire infrastructure is already deployed. One of the challenges when trying to implement probabilistic approaches for RSS-based positioning methods is to choose a path-loss model that match to the environment where the measurement takes place.

For future implementations, one could create new models which use a different path-loss modeling or several path-loss models, distinguished, for example, based on terrain type parameters. With a new model we could develop the Matlab simulator to work in all the environments and get even more accurate results. Also, the positioning phase was out the scope of this thesis, but could be further implemented to extend the results obtained so far.

Another option would be to combine different positioning parameters, in addition to RSS, to achieve a more detailed location. We could use other data such as Time of Arrival (TOA), Time Difference of Arrival (TDOA) or Timing Advance (TA) values to increase the precision of the current model. However, such additional information is harder to obtain than RSS and currently, there are no measurements of these parameters available in the research group where this thesis was made.

In conclusion, our findings on the path-loss models are very important in terms of giving better insight on the path-loss parameters and shadowing levels, as well as on the current availability of cellular and WLAN signals for positioning purposes.

REFERENCES

[1] Rusu-Casandra & A., Lohan, E. S. Contributions to the characterization of the indoor GPS propagation channel. In Proc. of the International Multidisciplinary Scientific GeoConference SGEM, Jun 2013, Bulgaria.

[2] Melikov, A., Cellular Networks-Positioning, Performance Analysis and Reliability. Rijeka, Croatia. 2011. InTech. 404 p.

[3] Korhonen, J. Introduction to 3G Mobile Communications. Norwood, Massachusetts USA. 2001. Artech House, Inc. 559 p.

[4] Esposito, C., Cotroneo, D. & Ficco, M. Calibrating RSS based Indoor Positioning systems. IEEE International conference on Wireless and Mobile Computing, Networking and Communications WIMOB, October 2009.

[5] Xu, J., Wang, J. & Ma, L., A novel WLAN Indoor Positioning Algorithm based on positioning Characteristic Extraction. 4th International Conference on Genetic and Evolutionary Compting. 2010.

[6] Zhang, Z., Wan, G., Jiang, M. & Yang, G. Research on An adjacent Correction Positioning Algorithm Based on RSSI-Distance Measurement. 8th International Conference on Fuzzy Systems and Knowledge Discovery FSKD. 2011

[7] Fang. S.H. Lin T.S. & Lee, K.C. A novel Algorithm for Multipath Fingerprinting in Indoor WLAN Environments. IEEE Transactions on Wireless Communications, Vol. 7, No. 9. September 2008.

[8] Blaunstein, N. Radio Propagation in Cellular Networks. Norwood, Massachusetts USA. 2000. Artech House, Inc. 386 p.

[9] Zhu, S., Ghazaany T. S., Jones, S. M. R., Abd-Alhammed R. A., Noras J. M., Van Buren, T., Wilson, J., Sugget T. & Marker S. Probability Distribution of Rician K-Factor in Urban, Suburban and Rural Areas using Real –World Captured Data. IEEE Transactions on Antennas and Propagation, Vol. 62, No. 7. July 2007.

[10] Rama Rao, T., Balanchander, D., Nanda Kiran, A. & Oscar, S. RF propagation Measurements in Forest & Plantation Environments for Wireless Sensor Networks. Dept. of telecommunications Engineering, SRM University, Chennai, India. Report. pp. 308-313.

[11] GSM 05.08. Digital Cellular Telecommunications system (Phase 2+); Radio Subsystem Link Control. Valbonne, France. 1996. European Telecommunication Standard Institute. 39 p.

[12] Update of TS 25.225 concerning measurements definitions, ranges and mappings. Siemens. Internal memorandum. 20 p.

[13] IEEE 802.11. Part 11: Wireless LAN Medium Access Control (MAC) and Physical layer (PHY) Specifications, New York, New York USA. 2012. The Institute of Electrical and Electronics Engineers, Inc. 2695 p.

[14] Roos, T., Myllyäki, P., Tirri, H., Misikangas, P. & Sievänen, J. A Probabilistic Approach to WLAN User Location Estimation. International Journal of Wireless Information Networks Vol. 3 (2002). pp.155.

[15] Talvitie, J., Lohan, E.S. & Renfors, M., The Effect of Coverage Gaps and Measurement Inaccuracies in Fingerprinting based Indoor Localization, in Proc. of IEEE ICL-GNSS conference, Jun 2014, Helsinki, Finland

[16] Talvitie J. & Lohan E.S., Modeling Received Signal Strength Measurements for Cellular Network Based Positioning. In Proc. of IEEE ICL-GNSS (2013), Italy.

[17] Zhang, J. Salmi, J. Analysis of Kurtosis-based LOS/NLOS Identification Using Indoor MIMO channel measurements. IEEE Transactions on Vehicular Technology, vol. 62, issue 6, (2013). pp. 2871-2874.

[18] Lohan E. S., K. Koski, J. Talvitie, L. Ukkonen, WLAN and RFID propagation channels for hybrid indoor positioning, in Proc. of IEEE ICL-GNSS conference, Jun 2014, Helsinki, Finland

[19] Nurminen, H., Talvitie J., Ali-Löytty, S., Lohan E.S., Piché, R. & Renfors M. Statistical path loss parameter estimation and positioning using RSS measurements. Journal of Global Positioning Systems Vol.12, No. 1(2013). pp. 13-27.

[20] Shrestha, S. Talvitie J. & Lohan E.S., Deconvolution-based indoor localization with WLAN signals and unknown access point locations. In Proc. of IEEE ICL-GNSS, Jun 2013, Italy.

[21] Amine Amid & Cherkaoui S. Wireless Technology Agnostic Real-time Localization in Urban Areas. 4th IEEE Workshop on Wireless and Internet Services (2011).

[22] Lu, H., Zhang, S., Dong, Y. & Lin X. A Wi-fi/GPS Integrated System for Urban Vehicle Positioning. 13th International IEEE Annual Conference on Intelligent Transportation Systems ITSC, September 2010, Portugal.

[23] Brida, P., Cepel, P. & Duha, J. The Accuracy of RSS Positioning in GSM Networks.

[24] Cheung, K. W., So, H. C., Ma, W. K. & Chan, Y.T. Received Signal Strength Based Mobile Positioning via Constrained Weighted Least Squares.

[25] Gundlegård, D. The smartphone as Enabler for Road Traffic Information Based on Cellular Network Signalling. In Proc. of 16th International IEEE Annual Conference on Intelligent Transportation Systems ITSC, October 2013, Netherlands.

[26] Wed, B.L. 2014. Why GSM networks still matter. [WWW]. [accessed on 10.07.2014]. Available at: http://conversations.nokia.com/2013/05/22/why-gsm-networks-still-matter/

[27] Schiller, J. Mobile Communications. Second Edition. Great Britain. 2003. Pearson Education Limited. 492 p.

[28] GSM 05.08. Digital Cellular Telecommunications system (Phase 2+); Radio Transmission and reception. Valbonne, France. 1996. European Telecommunication Standard stitute. 48 p.

[29] Aas Pedersen, Ø. Detecting Wireless Identity Spoofs in Urban Settings, Based on Received Signal Strength Measurements. 2010. Norwegian University of Science and Technology. Department of Telematics. 120 p.

[30] Li, K., Bigham, J. Bodanese, E. L. & Torkarchuk. Location Estimation In Large Indoor Buildings Using Hybrid Networks. United Kongdom.

[31] Holma H., Toskala A.WCDMA for UMTS. Third Edition. England. 2004. John Wiley & sons Ltd. 450 p.

[32] 3GPP TS.25.401. Universal Mobile telecommunication system (UMTS); UTRAN overall description. Valbonne, France. 1999. European Telecommunication Standard stitute. 37 p.

[33] Gast, M., 802.11 Wireless Networks The Definitive Guide. 2005. California, USA. O'Reilly. 626 p.

[34] Sendra, S., Garcia, M., Turro, C. & Lloret, J. WLAN IEEE 802.11a/b/g/n Indoor Coverage and Interference Performance Study. International Journal on Advances in Networks and Services, Vol. 4, No 1 & 2. 2011.

[35] Borenovic, M. N. & Neskovic A.M. Comparative analysis of RSSI, SNR and Noise Level Parameters Applicability for WLAN Positioning Purposes. IEEE. 2009

[36] Mazuelas, S., Bahillo, A., Lorenzo, R. M., Fernandez, P., Lago, F. A., Garcia, E., Blas, J. & Abril, E. J. Robust Indoor Positioning Provided by Real-Time Values in Unmodified WLAN Networks. IEEE Journal of Selected Topics in Signal processing, Vol. 3, No. 5. October 2009.

[37] Bardwell, J. The Truth About 802.11 Signal and Noise Metrics. 2004. Connect 802. 28 p.

[38] Robitzsch S., Murphy, L. & Fitzpatrick. An Analysis of the Received Signal Strength Accuracy in 802.11a Networks Using Atheros Chipsets: A Solution Towardsa Self Configuration. Broadband Wireless Access Workshop.

[39] Stallings, W. Wireless Communications and Networks. Second Edition. New York USA. 2005. Pearson Education, Inc.

[40] Zhang, J. Radio Channel Characteristics. 2013. Tampere, Finland. Tampere University of Technology. Lecture handouts. 83 p.

[41] Bianchi, C. & Meloni, A. Natural and man made terrestrial electromagnetic noise: an outlook. Annals of geophysics. Vol 50 (2007). pp. 442

[42] Ram, S. Satellites: Unintentional and Intentional Interference. Panel Discussion on Radio Frequency Interference and Space Sustainability, Washington DC USA, 2013. Secure World Foundation. pp. 3-4.

[43] Bergel, I. Fishler, E. & Messe, H. Narrowband Interference Mitigation in Impusle Radio. IEEE Transactions on Communications, Vol. 53. No. 8. August 2005.

[44] Landron, O., Feuerstein, M. J. & Rappaport, T.S. A comparison of the Theoretical and the Empirical Reflection Coefficient for Typical Exterior Wall Sufaces in a Mobile Radio Environment. IEEE Transaction on Antennas and Propagation. Vol 44, No. 3. March 1996.

[45] Ishimaru, A. Wave Propagation and Scattering in Random Media and Rough Surfaces. In Proc. IEEE Vol. 79. No. 10. October 1991.

[46] Glenn, A.B. & Lieberman, G. Effect of Propagation Fading and Antenna Fluctuations on Communication Systems in Jamming Environment. IRE Transactions on Communication Systems. March 1962.

[47] Liberti, J. C. & Rappaport, T. S. Statistics of Shadowing in Indoor Radio Channels At 900 and 1900 MHz. Military Communication Conference MILCOM ´92, Communications Fusing Command, Control and Intelligence. IEEE. 1992.

[48] Rakesh, N & Srivatsa, S.K. A Study on Path Loss Analysis for GSM Mobile Networks for Urban, Rural and Suburban Regions of Karnataka State. International Journal of Distributed and Parallel systems (IJDPS) Vol. 4 (2013). pp.55.

[49] Ranvier, S. Path loss models. Helsinki, Finland. 2004. Helsinki University of Technology. Lecture handouts. 36 p.

[50] Shabbir, N. Sadiq, M. T., Kashif, H. & Ullah, R. Comparison of Radio Propagation Models for Long Term Evolution (LTE) Network. International Journal of Next-Generation Networks Vol. 3 No. 3 (2011). pp. 28-29.

[51] Chebil, J., Lwas, A.K., Islam, R. & Zyoyud A. Adjustment of Lee path Loss Model for Suburban Area in Kuala Lumpur-Malaysa. International Conference on Telecommunications Technology and Applications Vol. 4 (2011). pp. 253.

[52] Lott, M. & Forkel, I. A Multi-Wall-and-Floor Model for Indoor Radio Propagation.

APPENDIX A: Measurements maps

This Appendix shows the measurement maps of all available data measurements used in this thesis. The red crosses represent the points were measurements were done and the background image is the map of the measurement area.

1. Airport areas

Figure A.1 Helsinki airport map, Finland

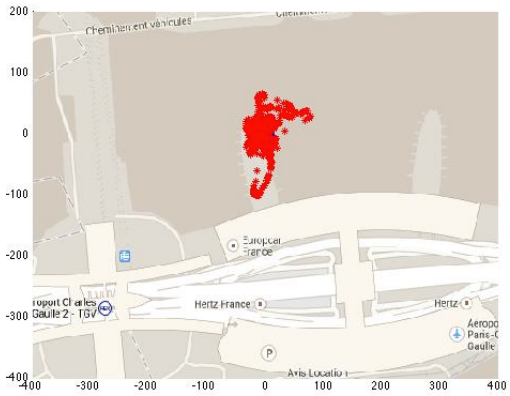

Figure A.2 Paris airport map, France

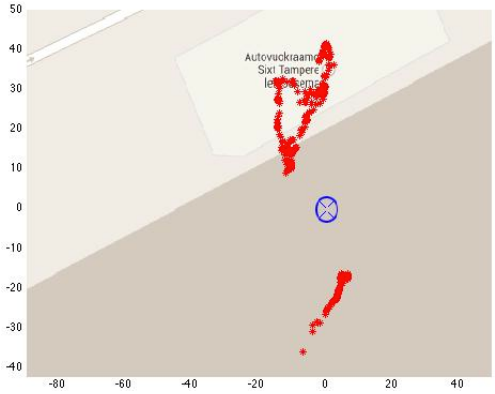

Figure A.3 Tampere airport map, Finland

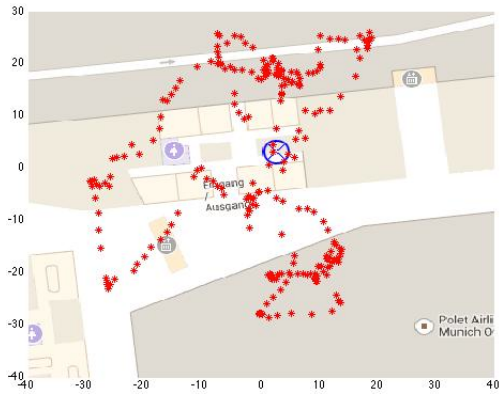

Figure A.4 Munich airport map, Germany

2. Seaside or beach areas

Figure A.5 Sletterstrand and surroundings map, Denmark

Figure A.6 Argeles sur mer map, France

Figure A.7 Cerbere sea resort map, France

Figure A.8 Collioure sea resort map, France

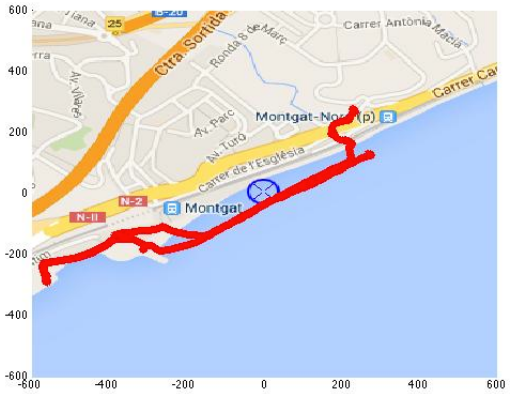

Figure A.9 Montgat beach area map, Spain

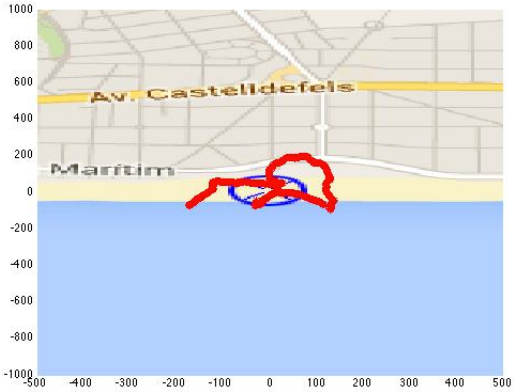

Figure A.10 Castelldefels beach area map, Spain

Figure A.11 Caldes d'Estrac beach area map, Spain

3. Mountain or forest areas

Figure A.12 Boissiere map, France

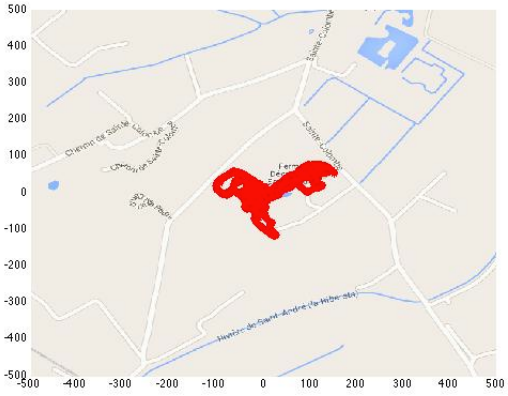

Figure A.13 Forest area map, France

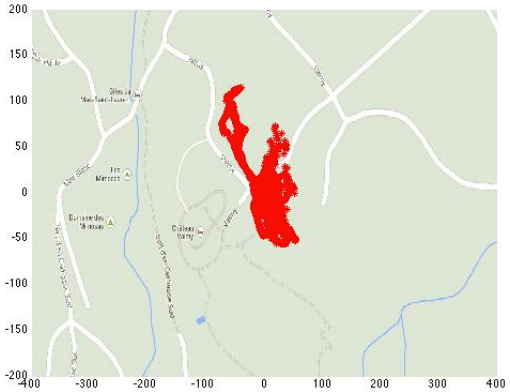

Figure A.14 Valmy map, France

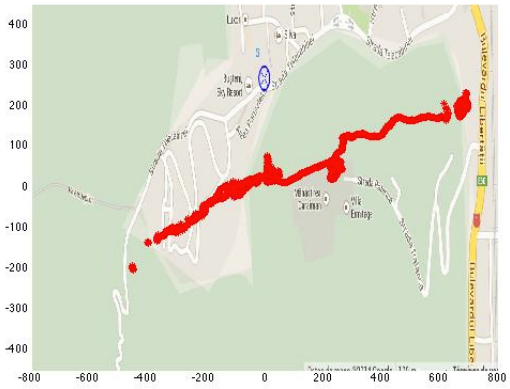

Figure A.15 Busteni mountain area, Romania

Figure A.16 Collserola mountain area map, Spain

Figure A.17 Can Coll hily area map, Spain

FigurA.18 Garraf natural reservation map, Spain

Figure A.19 Montseny natural reservation map, Spain

4. Suburban (various areas)

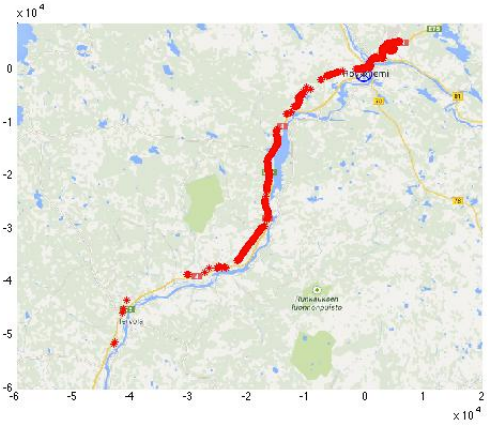

Figure A.20 Rovaniemi map, Finland

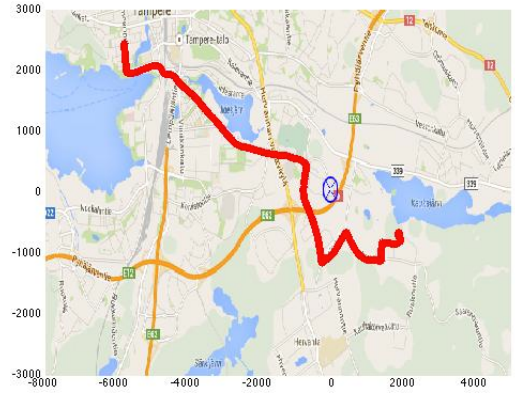

Figure A.21 Kaukajärvi map, Finland

Figure A.22 Elne map, France

Figure A.23 Carcassone castle area map, France

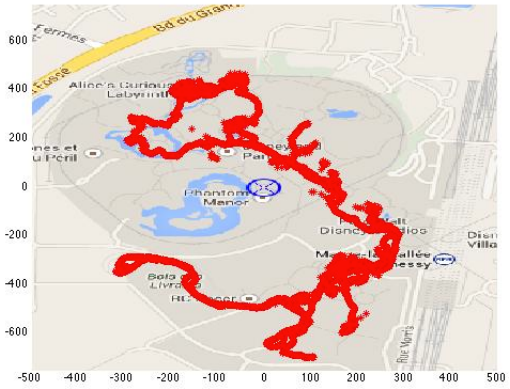

Figure A.24 Disneyland park area map, France

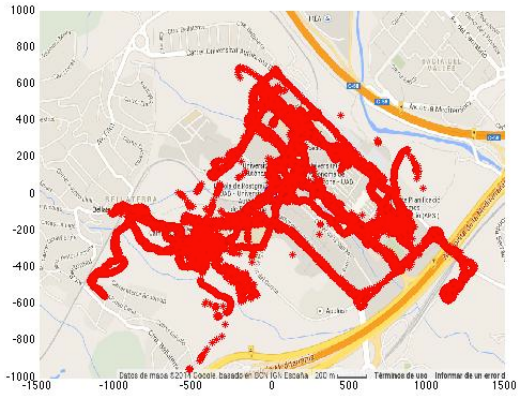

Figure A.25 Barcelona university campus map, Spain

Figure A.26 Limours map, France

5. Densely urban areas or downtowns

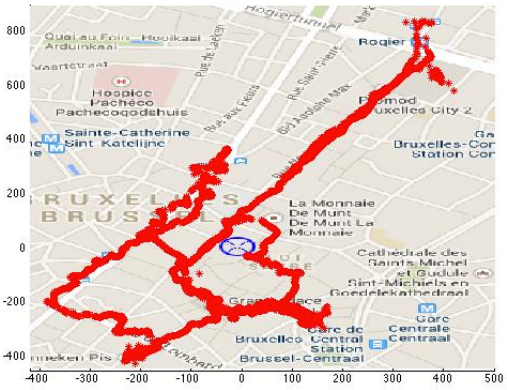

Figure A.27 Brussels downtown map, Belgium

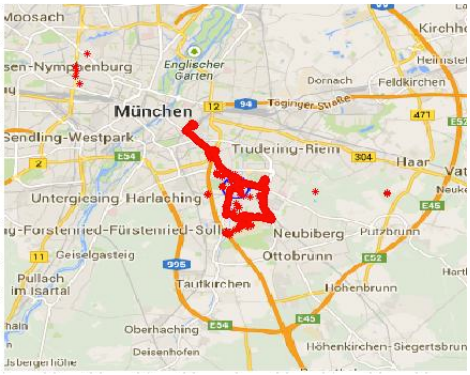

Figure A.28 Munich downtown map, Germany

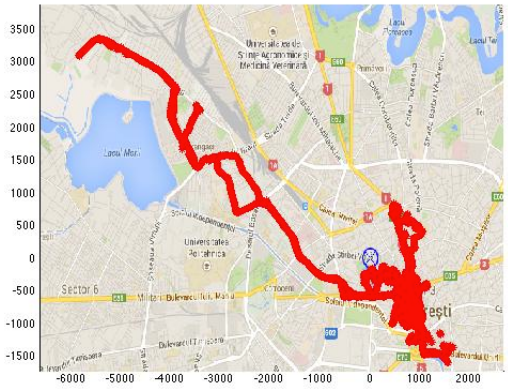

Figure A.29 Bucharest downtown map, Romania

Figure A.30 Barcelona downtown map, Spain

6. Lake areas

Figure A.31 Tampere lake area map, Finland

Figure A.32 Starnberg lake area map, Germany

7. Urban other various scenarios

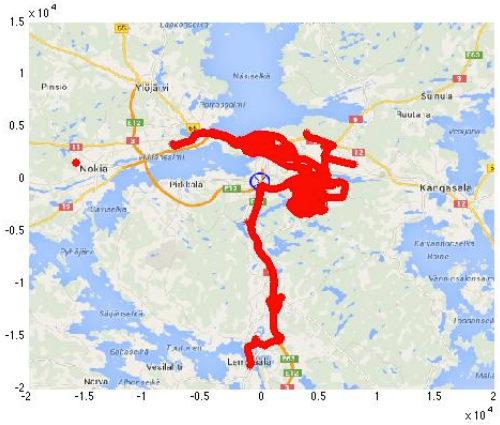

Figure A.33 Tampere map, Finland

Figure A.34 Montpellier map, France

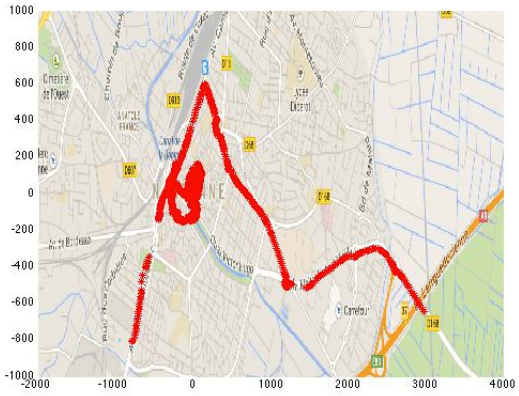

Figure A.35 Narbonne map, France

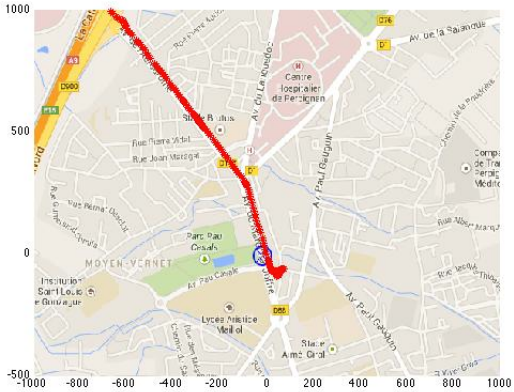

Figure A.36 Perpignan map, France

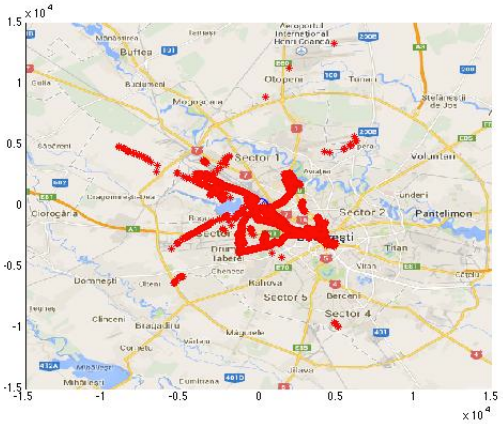

Figure A.37 Bucharest map, Romania

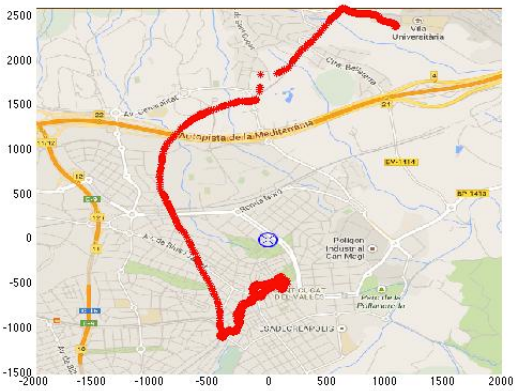

Figure A.38 Sant Cugat map, Spain